การศึกษากระบวนการกระตุ้นผิวโดยไม่ใช้ดีบุกสำหรับการชุบนิกเกิลโดยไม่ใช้ไฟฟ้าบนโฟมโพลียูริเทนและความเป็นไปได้สำหรับการเตรียมตัวเร่งปฏิกิริยา

นายจรัสพล สิทธิคุณ

วิทยานิพนธ์นี้เป็นส่วนหนึ่งของการศึกษาตามหลักสูตรปริญญาวิศวกรรมศาสตรมหาบัณฑิต
สาขาวิชาวิศวกรรมเคมี ภาควิชาวิศวกรรมเคมี
คณะวิศวกรรมศาสตร์ จุฬาลงกรณ์มหาวิทยาลัย
ปีการศึกษา 2554

ลิขสิทธิ์ของจุฬาลงกรณ์มหาวิทยาลัย
บทคัดย่อและแฟ้มข้อมูลฉบับเต็มของวิทยานิพนธ์ตั้งแต่ปีการศึกษา 2554 ที่ให้บริการในคลังปัญญาจุฬาฯ (CUIR)
เป็นแฟ้มข้อมูลของนิสิตเจ้าของวิทยานิพนธ์ที่ส่งผ่านทางบัณฑิตวิทยาลัย
The abstract and full text of theses from the academic year 2011 in Chulalongkorn University Intellectual Repository(CUIR)
are the thesis authors' files submitted through the Graduate School.

STUDY OF A TIN-FREE ACTIVATION PROCESS FOR ELECTROLESS NICKEL DEPOSITION ON POLYURETHANE FOAM AND FEASIBILITY FOR CATALYST PREPARATION

Mr. Jaratpon Sitthikun

A Thesis Submitted in Partial Fulfillment of the Requirements
for the Degree of Master of Engineering Program in Chemical Engineering
Department of Chemical Engineering
Faculty of Engineering
Chulalongkorn University
Academic Year 2011
Copyright of Chulalongkorn University

Thesis Title	STUDY OF A TIN-FREE ACTIVATION PROCESS FOR ELECTROLESS NICKEL DEPOSITION ON POLYURETHANE FOAM AND FEASIBILITY FOR CATALYST PREPARATION
By	Mr. Jaratpon Sitthikun
Field of Study	Chemical Engineering
Thesis Advisor	Associate Professor Joongjai Panpranot, Ph.D.
Thesis Co-advisor	Yuttanant Boonyongmaneerat, Ph.D.

Accepted by the Faculty of Engineering, Chulalongkorn University in Partial Fulfillment of the Requirements for the Master's Degree

…….. Dean of the Faculty of Engineering

(Associate Professor Boonsom Lerdhirunwong, Dr.Ing.)

THESIS COMMITTEE

…….... Chairman

(Associate Professor Artiwan Shotipruk, Ph.D)

…….... Thesis Advisor

(Associate Professor Joongjai Panpranot, Ph.D.)

……...… Thesis Co-advisor

(Yuttanant Boonyongmaneerat, Ph.D.)

……...… Examiner

(Assistant Professor Suphot Phatanasri, Ph.D.)

……...…… External Examiner

(Assistant Professor Okorn Mekasuwandamrong, Ph.D.)

จรัสพล สิทธิคุณ : การศึกษากระบวนการกระตุ้นผิวโดยไม่ใช้ดีบุกสำหรับการชุบนิกเกิลโดยไม่ใช้ไฟฟ้าบนโฟมโพลียูริเทนและความเป็นไปได้สำหรับการเตรียมตัวเร่งปฏิกิริยา (STUDY OF A TIN-FREE ACTIVATION PROCESS FOR ELECTROLESS NICKEL DEPOSITION ON POLYURETHANE FOAM AND FEASIBILITY FOR CATALYST PREPARATION) อ. ที่ปรึกษาวิทยานิพนธ์หลัก : รศ.ดร.จูงใจ ปั้นประณต, อ. ที่ปรึกษาวิทยานิพนธ์ร่วม : อ.ดร. ยุทธนันท์ บุญยงมณีรัตน์ 98 หน้า.

วิทยานิพนธ์นี้ศึกษากระบวนการกระตุ้นผิวโดยไม่ใช้ดีบุกสำหรับการชุบนิกเกิลโดยไม่ใช้ไฟฟ้าบนตัวรองรับโฟมโพลียูริเทน โดยศึกษาผลของความเข้มข้นของกรดไฮโดรคลอริก (2-6 โมลาร์) ความเข้มข้นของแพลเลเดียมคลอไรด์ (0.2-1.8 กรัม/ลิตร) และชนิดของตัวรีดิวซ์ (โซเดียมไฮโปฟอสไฟต์และไฮดราซีน) ที่มีต่อสมบัติของพื้นผิวที่ถูกกระตุ้นและการพอกพูนของนิกเกิลโดยการวิเคราะห์ด้วยเทคนิคกล้องจุลทรรศน์อิเล็กตรอนแบบส่องกราด เอ็กซเรย์สเปกโตรสโกปีแบบกระจายพลังงาน เอ็กซ์เรย์โฟโตอิเล็กตรอนสเปกโทรสโกปี เครื่องทดสอบแรงกด พบว่าเมื่อปริมาณความเข้มข้นของแพลเลเดียมคลอไรด์ เพิ่มขึ้นปริมาณการพอกพูนของนิกเกิลเพิ่มขึ้นและการพอกพูนสม่ำเสมอมากขึ้น สัณฐานวิทยาและสมบัติเชิงกลของนิกเกิลบนตัวรองรับโฟมโพลียูริเทนที่เตรียมด้วยการชุบโดยไม่ใช้ไฟฟ้าที่มีการกระตุ้นผิวโดยไม่ใช้ดีบุกเหมือนกับของตัวอย่างที่มีการกระตุ้นผิวโดยใช้ดีบุก นอกจากนี้ยังพบว่าการกระตุ้นผิวโดยไม่ใช้ดีบุกไม่ทำให้น้ำยาชุบเสียและสามารถนำมาใช้ใหม่ได้ เมื่อศึกษาคุณลักษณะและสมบัติของตัวเร่งปฏิกิริยาแพลเลเดียมบนไทเทเนียมไดออกไซด์ที่เตรียมโดยวิธีการพอกพูนโดยไม่ใช้ไฟฟ้าที่มีการกระตุ้นผิวโดยใช้ดีบุกและไม่ใช้ดีบุกพบว่าขนาดอนุภาคและสัณฐานวิทยาของแพลเลเดียมบนไทเทเนียมไดออกไซด์ขึ้นกับการกระตุ้นผิวโดยการกระตุ้นผิวโดยไม่ใช้ดีบุกจะได้ขนาดอนุภาคแพลเลเดียมที่ใหญ่กว่าการกระตุ้นผิวโดยใช้ดีบุก การทดสอบประสิทธิภาพของตัวเร่งปฏิกิริยาในปฏิกิริยาไฮโดรจิเนชันจาก 3-เฮกไซด์-1-ออลไปเป็น ซิส-เฮกซีน-1-ออล พบว่า Pd/TiO_2 ไม่ใช้ดีบุก ดีกว่า Pd/TiO_2 ดีบุก และดีกว่าตัวเร่งปฏิกิริยาที่เตรียมโดยวิธีการเคลือบฝัง คาดว่าการเตรียมโดยวิธีการพอกพูนโดยไม่ใช้ไฟฟ้าทำให้เกิดความบกพร่องบนพื้นผิวของตัวเร่งปฏิกิริยาน้อยกว่าวิธีการเคลือบฝัง

ภาควิชา วิศวกรรมเคมี ลายมือชื่อนิสิต .....

สาขาวิชา วิศวกรรมเคมี ลายมือชื่อ อ.ที่ปรึกษาวิทยานิพนธ์หลัก .....

ปีการศึกษา 2554 ลายมือชื่อ อ.ที่ปรึกษาวิทยานิพนธ์ร่วม .....

5370404021 : MAJOR CHEMICAL ENGINEERING
KEYWORDS : TIN-FREE ACTIVATION / ELECTROLESS NICKEL / CATALYST PREPARATION / TITANIA SUPPORTED PALLADIUM CATALYST/ CIS-3-HEXYNE-1 OL

JARATPON SITTHIKUN: STUDY OF A TIN-FREE ACTIVATION PROCESS FOR ELECTROLESS NICKEL DEPOSITION ON POLYURETHANE FOAM AND FEASIBILITY FOR CATALYST PREPARATION. ADVISOR: ASSOC. PROF. JOONGJAI PANPRANOT Ph.D, CO-ADVISOR: YUTTANANT BOONYONGMANEERAT, Ph.D. 98 pp.

A tin-free activation process has been studied for electroless nickel plating on polyurethane (PU) foam. The effect of HCl concentration (2-6 molar), $PdCl_2$ concentration (0.2-1.8 g/l), and the type of reducing agents (sodium hypophosphite and hydrazine) on the properties of the activated surface and the deposition of Ni were investigated by SEM, EDX, XPS, and Instron. More uniform coating and higher amount of Ni deposit were obtained with higher amount of $PdCl_2$ during activation. The morphology and mechanical properties of the Ni/PU foam prepared by electroless deposition with and without $SnCl_2$ activation were similar. In addition, for the non-$SnCl_2$ activation, the nickel electroless bath was not decomposed and can be reused. The characteristics and catalytic properties of Pd/TiO_2 catalysts prepared by electroless deposition method with and without $SnCl_2$ activation were investigated. The particle size and morphology Pd particles dispersed on TiO_2 powder were significantly dependent on the activation process. The non-Sn activation resulted in much larger Pd particle/cluster size than those of the electroless $SnCl_2$. The catalyst performances in the liquid-phase hydrogenation of 3-hexyne-1-ol to cis-hexene-1-ol were improved in the order: Pd/TiO_2 non-Sn > Pd/TiO_2 Sn > Pd/TiO_2 impregnation. It is suggested that electroless deposition resulted in lower surface imperfections of the Pd/TiO_2 catalysts than the conventional impregnation technique.

Department Chemical Engineering Student's Signature .....
Field of Study Chemical Engineering Advisor's Signature .....
Academic Year 2011 Co-advisor's Signature .....

ACKNOWLEDGEMENTS

The author would like to express my greatest sincere and deepest appreciation to Associate Professor Joongjai Panpranot, and co-advisor, Dr. Yuttanant Boonyongmaneerat from Metallurgy and Materials Science Research Institute, Chulalongkorn University, for their invaluable suggestions, support, guidance, and useful discussion throughout this thesis. In addition, the author would also be grateful to thank to Associate Professor Dr. Artiwan Shotipruk, as a chairman, and Assistant Professor Dr. Suphot Phatanasri, Assistant Professor Dr. Okorn Mekasuwandamrong, as the members of the thesis committee for their kind cooperation.

Most of all, the author would like to thank all members of the Center of Excellence on Catalysis and Catalytic Reaction Engineering, Department of Chemical Engineering, Faculty of Engineering, Chulalongkorn University for their assistance and friendly support.

Moreover, the author wishes to thank the members of the Metallurgy and Materials Science Research Institute, Chulalongkorn University for friendship and their kind assistance.

Finally, the author would like to express my highest gratitude to my parents who always pay attention for all times and encouragement. The most success of graduation is devoted to my parents.

CONTENTS

Page

Page

LIST OF TABLES

TABLE **Page**

LIST OF FIGURES

FIGURE **Page**

FIGURE **Page**

CHAPTER I

INTRODUCTION

1.1 Introduction

Electroless plating deposition is an autocatalytic oxidation-reduction reaction which metal ions are reduced and deposited as metal atoms [1]. This technique can be applied to both metallic and non-metallic substrates that has been pretreated and activated. The advantages of this process are its simplicity, low cost, and fast process. It can be prepared on any shape and there is a good metal to non-metallic substrate adhesion [2].

The conventional electroless plating deposition of non-metallic surface involves 3 steps: pretreatment, activation, and plating. The activation is the key to the subsequent successful electroless metal deposition [3]. The conventional activation process includes two-step method using sensitization solution of $SnCl_2$ and then activation solution of $PdCl_2$, or one-step method using a mixture of $SnCl_2$ and $PdCl_2$ [4]. However, these methods involve numerous problems such as the use of highly toxic tin and the uncontrollable process which results in the waste of Pd and the failure of plating [5]. Moreover from the study of Keuler et al., (2000), the excess of $SnCl_2$ in activation process can form impurities on the activated Pd surface and can be harmful to the electroless plating bath.

Electroless nickel plating is a widely used technique in industries which offers uniform deposition of nickel that exhibits good corrosion and wear resistance, decent electrical and thermal conductivity, and good solderability [6]. Polyurethane (PU) foams are porous materials available in a wide range of thermal and physical mechanical properties. PU foams have high energy absorption capacity and are particularly useful for, among many, shock absorbance, acoustic and thermal insulating applications, and filtering applications [7].

In the present work, a tin free activation process has been investigated for electroless nickel plating on PU foam. The use of hydrochloric acid (HCl) for chemically roughening the PU surface was explored as a route to enhance mechanical adhesion between the deposited metal and the PU foam. The effects of HCl concentration, $PdCl_2$ concentration, and the type of reducing agents on the electroless nickel plating on PU foam were examined in terms of both the morphology of Ni deposited and the deposition rate on PU foam. Particularly, sodium hypophosphite and hydrazine were investigated as potential Sn replacement for reduction of Pd.

In addition, the developed Sn-free activation for electroless Ni plating was employed for preparation of Pd/TiO_2 catalyst particles. The catalyst properties were compared to those from the conventional $SnCl_2$ activated/electroless deposition method. To the best of our knowledge, Pd/TiO_2 synthesized by Sn-free activated electroless plating deposition has never been reported so far. It is thus the aims of this thesis to synthesize Pd/TiO_2 by electroless plating technique and investigate their characteristics and catalytic properties in the liquid phase selective hydrogenation of 3-hexyne-1-ol.

1.2 Objectives

The objectives of this present work are to develop a tin free activation process for electroless nickel plating on PU foam and preparation of Pd/TiO_2 catalysts by electroless plating method.

1.3 Scope of work

Part I

1. Preparation of nickel on polyurethane foam (Ni/PU foam) with 1 g/l of palladium and tin (II) chloride using the conventional activation process for electroless plating deposition
2. Preparation of nickel on polyurethane foam (Ni/PU foam) with 0.2-1.8 g/l of palladium in activation process by Sn-free activated process for electroless plating deposition using two different reducing agents (sodium hypophosphite and hydrazine). The HCl concentration used for pretreatment of PU foam was varied from 2M-6M. The deposition time was varied from 10 min to 120 min
3. Characterization of nickel on polyurethane foam using several techniques such as scanning electron microscope (SEM), energy dispersive X-ray spectrometer (EDX), X-ray photoelectron spectroscopy (XPS), and Universal testing machine (Shimadzu)

Part II

1. Preparation of TiO_2-supported Pd catalysts (1-5 wt% Pd) by a Sn-free and conventional electroless deposition method.
2. Characterization of the titania-supported palladium catalysts using several techniques such as X-ray diffraction (XRD), scanning electron microscope (SEM), energy dispersive X-ray spectrometer (EDX), X-ray photoelectron spectroscopy (XPS), transmission electron microscopy (TEM), and CO-pulse chemisorptions.
3. Reaction study of titania-support palladium catalysts in liquid-phase hydrogenation of 3-hexyne-1-ol using stirring batch reactor (stainless steel autoclave 50 ml).

1.4 Research methodology

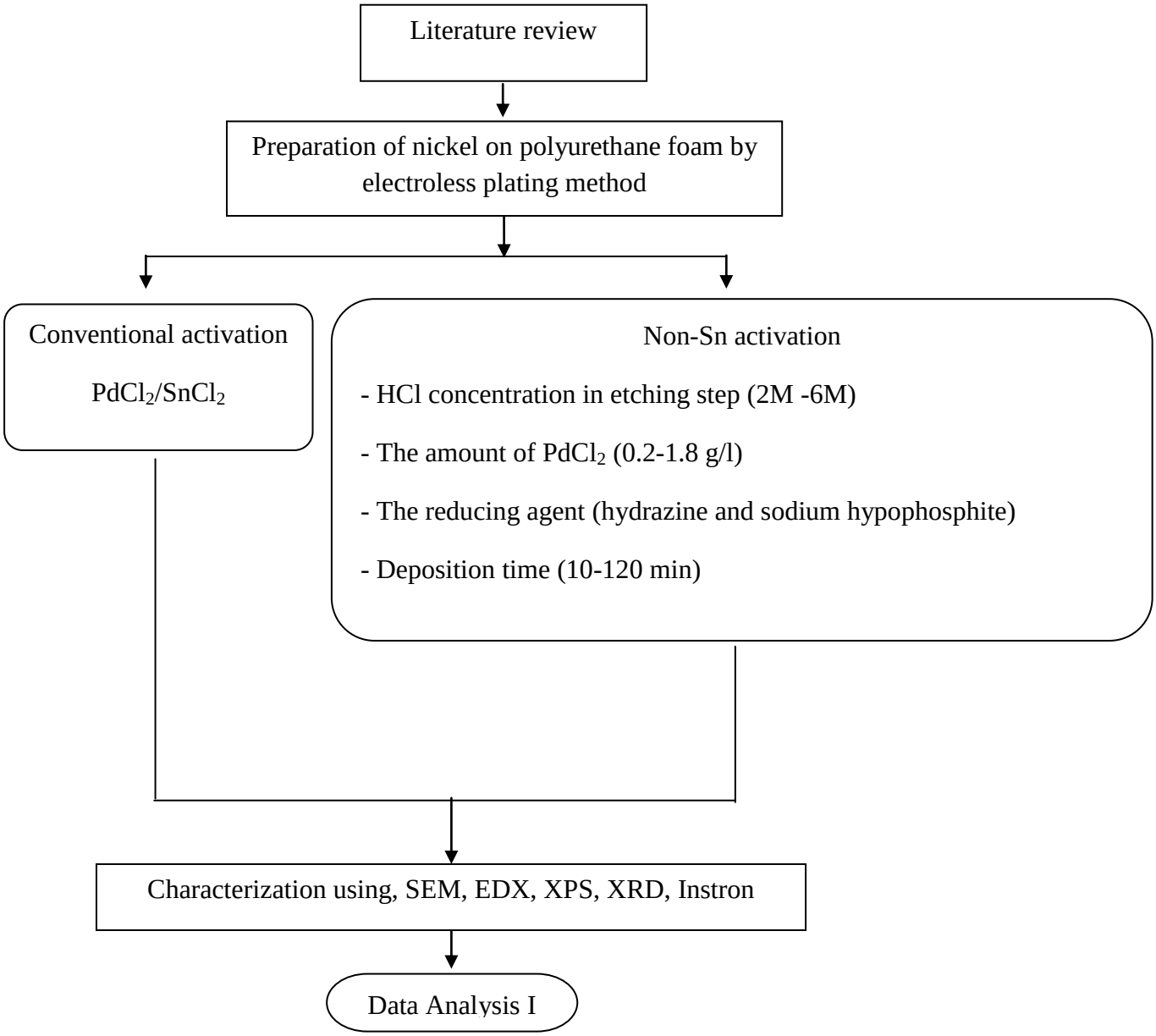

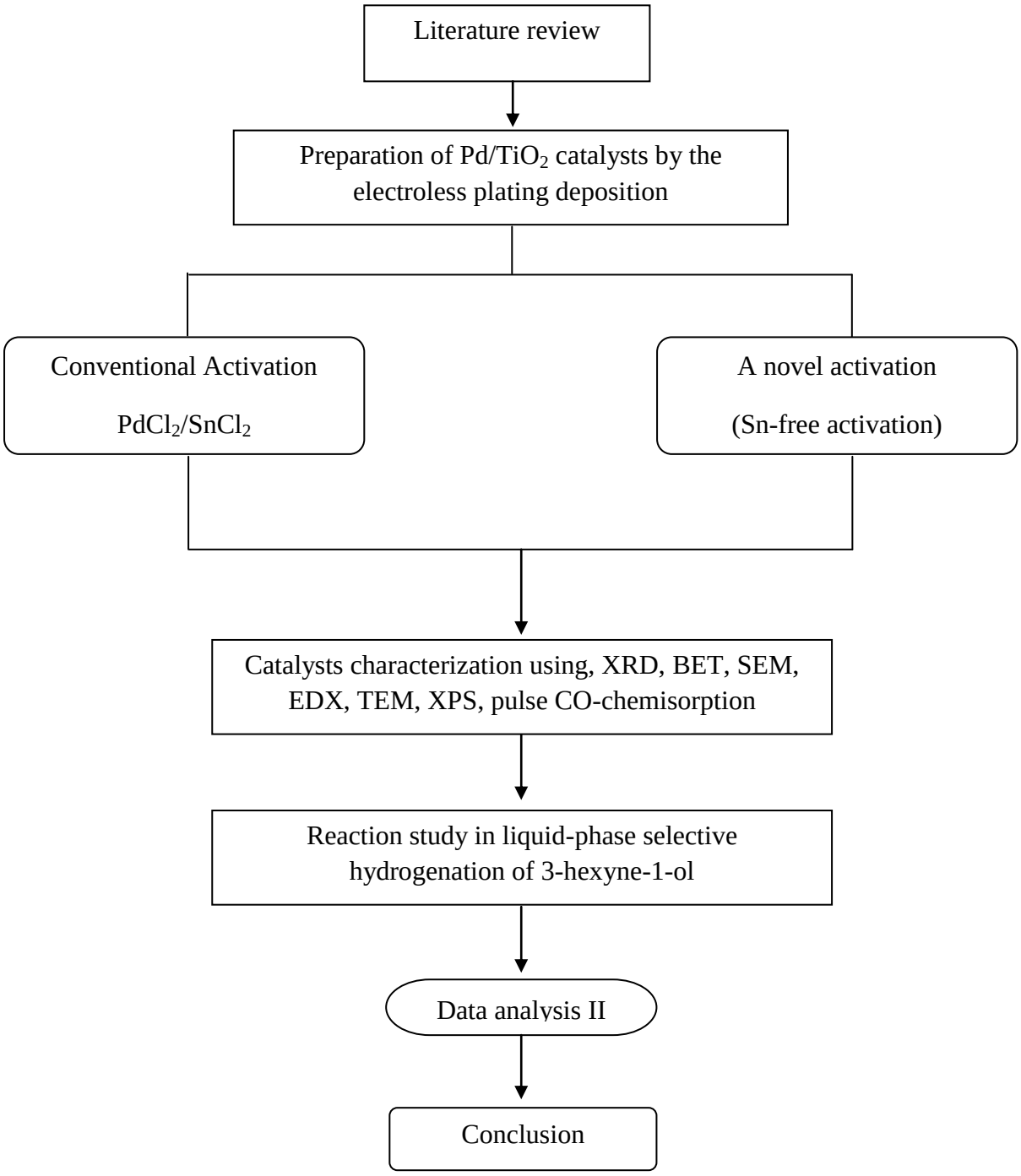
Literature review
Preparation of Pd/TiO2 catalysts by the electroless plating deposition
Conventional Activation
PdCl2/SnCl2
A novel activation
(Sn-free activation)
Catalysts characterization using, XRD, BET, SEM, EDX, TEM, XPS, pulse CO-chemisorption
Reaction study in liquid-phase selective hydrogenation of 3-hexyne-1-ol
Data analysis II
Conclusion

CHAPTER II

BACKGROUND AND LITERATURE REVIEW

2.1 Electroless plating deposition

Electroless deposition is a process of depositing coating with the aid of a chemical reducing agent in solution without the application of external electrical power. It is therefore applicable to non-conducting substrates. Electroless deposition is a process which occurs on a suitably-prepared/catalyzed surface only, and does not occur in the bulk of the electroless solution. This technique has been applied widely to glass, silicon and ceramic substrate that used mainly in the electronics industry. Which the conventional electroless plating deposition of non-metallic surface involves 3 steps: pretreatment, activation, and plating. The activation is the key to the subsequent successful electroless metal deposition.

Electroless deposition as we know today has involved in many applications, for examples, in corrosion prevention and electronics [8]. Electroless deposits are very uniform in thickness all over the part shape and size. This process offers distinct advantages when plating irregularly shaped objects, holes, recesses, internal surfaces, valves or threaded parts. Distinct advantages of electroless plating are: [9]

- There is uniformity of the deposits, even on complex shapes.
- The technique is quick, simple and inexpensive
- There is good metal to non-conductive surface adhesion
- It can be applied onto any material that has been properly pretreated
- It does not required external electric source
- No complex filtration is required

The main disadvantages are: [10].

- Thickness control is difficult and costly losses might occur due to the decomposition of the plating solution

- The deposition rates are typically lower than electrolytic deposition rates.
- Deposition of separate metal layers and subsequent alloying has also proven to be very difficult.
- Lifetime of chemical plating bath is limited.

2.1.1 Substrate pretreatment

The substrate needs to be cleaned before the electroless deposition. For electroless plating on non-conducting surface (plastics and ceramics), the surface needs to be activated previous to plating. The difference between metallic surface and nonmetallic surfaces is the nature of the bond between substrate and coating. While adhesion to metal is of an atomic nature, the adhesion to organic and inorganic substrates is only mechanical. The basis for obtaining adhesion to these materials is to develop the right topography on the surface using chemical or mechanical treatment.

The substrate pretreatment steps generally include roughening by chemical attack, activation with a catalytic metal, and then electroless plating. The composition of the chemical etching depends on the nature of the substrate. Some typical etch applications are shown in table 2.1.

Table 2.1 The substrate pretreatment for non-metallic surface [11].

Substrate	Methods
Alumina Ceramics	dip clean with alkaline cleaner Rinse And etching in hydrofluoric acid (50 percent) solution. for 5 min at room temperature
Barium and Zirconium Titanates	Dip clean with alkaline cleaner Rinse And etching in fluoboric acid (48 percent) for 10 min at

	room temperature
Glass and Ceramlcs	dip clean with detergent Rinse Etching with hydrofluoric acid (40 percent) and Ammonium fluoride 18 g/L

After the etching of nonmetallic surfaces which lack of catalytic properties, the surface was required activating treatments for the conventional activation process is done by seeding the surface with a catalytically active metal.

There are two conventional methods for catalyzing the surface to be plated [12]. Both process employ palladium and tin. In the older process, the substrate is first placed in a sensitization solution of $SnCl_2$ and then activation solution of $PdCl_2$, or for the exchange process using a mixture of $SnCl_2$ and $PdCl_2$ in one-step method. Palladium ions are reduced and Pd nuclei are deposited on the substrate. The two step process deposits more metal than the one-step method does and there is a higher Pd content in the deposit. This is favorable for preparing high purity deposition [1].

2.1.2 Activation process of electroless plating

In the activation process is to employ the palladium as a catalyst metal sites on the substrate to introduce oxidation of a reducing agent in electroless plating solution. Pd ion (2+) ions reduction is the most important step of this process. The hydrazine and sodium hypophosphite were selected to reduce Pd ion (2+) to Pd (0) metal which the Pd ion (2+) reduction reaction by sodium hypophosphite was written as follows:

$$Pd^{2+} + 2H_2PO_2^- + 2H_2O \rightarrow Pd^0 + 2H_2PO_3^- + H_2 + 2H^+$$

The Pd ion (2+) reduction reaction by hydrazine was written as follows: [13]

$$2Pd^{2+} + N_2H_4 + 4OH^- \rightarrow 2Pd^0 + N_2 + 4H_2O$$

2.1.3 Electroless plating solution

An electroless solution typically consists of: [8]

- A source of metal ions that needs to be deposited
- A reducing agent such as hypophosphite for nickel deposition
- A pH regulator, buffer
- A stabilizer that forms a complex with the metal ions and allows for a slower metal release from the solution.
- Oxygen gas dissolved in the solution, which is invariably present, may also undergo reduction, and which can influence deposition uniformity due to non-planar diffusion

In this work the nickel plating baths was reduce with sodium hypophosphite as a reducing agent. The Ni ion (2+) reduction reaction by sodium hypophosphite was written as follows: [14]

$$Ni^{2+} + 2H_2PO_2^- + 2H_2O \rightarrow Ni^0 + 2H_2PO_3^- + H_2 + 2H^+$$

Figure 2.1 Electroless nickel plating solution [15].

2.2 Polyurethane foams

Polyurethane (PU) is polymer making up of a chain of organic units with joined urethane links. Polyurethane polymers are formed by combining two bi- or higher functional monomers.

Polyurethane (PU) foams are porous materials available in a wide range of thermal and physical mechanical properties. PU foams have high energy absorption capacity, low water adsorption, and are particularly useful for, among many, shock absorbance, acoustic and thermal insulating applications, and filtering applications [16]. A number of researchers indicated that the density of PU foam is an important affect on mechanical properties of PU foam. PU foam with higher polymer density generally retains their original properties and gives better support, durability and comfort [17].

2.3 Titanium dioxide

Titanium dioxide is a ceramic membrane within thermally stable (mp 1855 ºC) due to highly stable electronic bonding, and very resistant to chemical attack. Titanium dioxide is normally in three crystalline forms: Rutile, Anatase, and Brookite. Which anatase forms have the most stable at low temperature and normally shows a higher photoactivity than other types. These properties make them much interest as supports for metal deposit for application in catalysts for selective hydrogenation reaction [18].

2.4 Liquid-phase selective hydrogenation of alkynes

For several years, the selective hydrogenation of unsaturated hydrocarbons has been of major interest to the industry. The selective hydrogenation of alkynes to alkenes is an area of catalysis that has been active for over 100 years and yet our understanding is not complete. Selective hydrogenation of alkynes is an addition of hydrogen to a carbon-carbon triple bond in order to produce only alkenes product.

The overall effect of such an addition is the reductive removal of the triple bond functional group.

The catalysts most commonly used for selective hydrogenation reactions are nickel, platinum, and palladium. Palladium shows high activity but only limited selectivity and long-term stability for hydrogenation of unsaturated hydrocarbon. In this respect, the nature of support controls molecular access to the active site. The support may be as different as titania [19], [20], [21], [22], carbon [23], silica [24], ZrO_2-TiO_2 [25] in order to obtain higher activity and selectivity.

2.5 Electroless nickel plating deposition on non-metallic surface.

The electroless nickel plating on non-metallic surface has been wildly used in many applications because the method provides a uniform coating of materials. The high performance products with wear resistance and corrosion resistance were produced. In 2003, Yutaka T., et. al [26]. and Xuejiao Tang, et. al [5] studied the process of electroless nickel deposition onto ABS substrate. Qiuyu Z., et. al [27] synthesized nickel plating on hollow glass microsphere by electroless deposition. With this method a uniform and continuous deposit layer were obtained.

L. Laima, et. al [28], synthesized nickel coating on tungsten carbide (WC) composite powders without conventional sensitization step. The supports (WC powders) were pretreated (activation) by immersion into an aqueous solution of 30 mL/L hydrofluoric acid, 20 mL/L nitric acid, and 3 g/L ammonium fluoride. The process was reinforced with an ultrasonic wave for 20–30 min at room temperature. After the pretreatment, the WC powders were cleaned in deionized water for three times. The results shown the novel activation method was found to be effective for electroless nickel plating. Smooth, dense, and uniformly distributed Ni coatings were obtained on the WC powders.

A number of researchers [5, 26, 29-32] have studied electroless nickel plating on non-metallic substrate. Nickel electroless deposition can be plate on many non-

metallic substrates such as ABS [5], [26], hollow glass [27], polystyrene, [4], PET [29], ceramic membrane [30], [31], [32]. From the literature review, nickel plating on non-metallic substrate can occur when suitable pretreatment method has been employed which increase a performance for electroless plating deposition.

2.6 Sn-free activation process in electroless plating deposition

The conventional activation process (Sn) involves numerous problems such as the use of highly toxic tin and the uncontrollable process which results in the waste of Pd and the failure of plating [5]. The electroless plating process was modified by replacing the conventional activation (Sn-free activation processes). Table 2.2 shows the studies reporting Sn-free activation process for electroless plating deposition.

Table 2.2 Sn-free activation process for electroless plating deposition

Ref.	Substrates	Metal deposited	Sn-free activation processes
M. Charbonnier, et. al. [34] 2002.	Glass surface	Nickel	The glass surface was first coated by plasma polymerization with an ultra-thin carbon film capable of accepting nitrogen containing groups by plasma treatment.
M. Charbonnier, et. al. [3] 2006.	Poly (etherimide)	Nickel	There are the different 3 steps of the Sn-free activation process: i) The surface treatment of polymers by plasma was performed under ammonia, oxygen, argon or hydrogen atmosphere or using various organic precursors in a radio-frequency (RF) reactor (RIE 80 model from Plasma Technology, England) working at 13.56 MHz, ii) The functionalized surfaces was performed either by dipping the samples for 1 min in a dilute aqueous $PdCl_2$ solution (0.1 g l−1) and by rinsing them in water for 30 s, iii) The chemical reduction of Pd(+2) ions was performed with sodium

			hypophosphite solutions either at 85 °C (working temperature of the Ni plating baths)
Hongbin Dai, et. al. [35] 2006.	Mica powder	Ni-P	This activation process involves only one-step using the Pd(II)–APTHS activator, without an etching or sensitization process. APTES was dissolved in a solution of ethanol–water under stirring to finally obtain ethanol/water/APTES in the volume ratio of (95/4/1), and then 0.25 g/l of $PdCl_2$ was dissolved in this mixture solution, stirred magnetically for 20 min, and the obtained activation solution was aged at room temperature for 24 h. The activator of the obtained solution with the method is a complex of Pd(II) ion with APTHS (Pd(II)–APTHS).
Dan Song, et. al. [4] 2009.	PS microspheres	Nickel	A novel activation process was performed by 1 g PS microspheres were dispersed into 50 mL deionized water with ultrasonic vibration and 2mL $PdCl_2$ solution was added, then the pH value was adjusted to 6.5 by sodium hydroxide. Subsequently, yellowsponge- like precipitation of $(Pd(OH)_2$@PS) appeared at once. Then the precipitation was reduced with an excess of Hydrazine (1 mL) with ultrasonic vibration, and the activated microspheres (Pd@PS) were gained by filtration and washing.
Xuejiao Tang, et. al. [36] 2011.	ABS plastic	Nickel	The first step, etching procedure was employed to make the ABS foil surfaces rough and hydrophilic. The etching was performed by dipping the foils in a mixed solution of 1:4 hydrogen peroxide (H_2O_2; 30%) and sulfuric acid (H_2SO_4; 98%) at room temperature. The etching time on ABS was chosen as the most optimal at 5 min. After rinsing, the etched foils were dipped into 1% acetic acid solution containing 15 g/L Chitosan (CTS) for 5 min at room temperature, and were then dried at 60 °C for 15 min. These foils were denoted as ABS–CTS.

2.7 Preparation of supported metal catalysts by electroless plating deposition

Nowadays electroless plating deposition is a novel method which can be used for preparation of catalysts. In 1995, Sun-Hua KO, et al. [37] studied nickel catalysts prepared by electroless deposition for selective hydrogenation of 1-α-pinene and Sun-Hua, et al. [38] investigated the bimetallic catalysts consisting of Ni-P on aluminum oxide for the same hydrogenation reaction. The results show that the catalysts which prepared by electroless plating has very high selectivity for hydrogenation of 1-α-pinene to cis-pinane. From these works, they concluded that the important procedure by which the catalysts were prepared involved four steps: etching, sensitization, activation, and plating deposition.

In 2010, the electroless plating deposition was used to prepare carbon supported platinum catalysts. Sriring, N., et al. [39] synthesized. Pt/C catalysts were used for proton exchange membrane fuel cell (PEMFC). The Pt/C catalyst has a good dispersion and the efficiency of the catalyst is closely the commercial electrodes. The catalysts can also be used in methanol oxidation reaction as reported by Mustain,W.E., et al. [40].

The electroless plating deposition interest for synthesis received considerable of bimetallic catalysts. This method can replace the conventional method (co-impregnation). Schaal, M., et al. [41] studied bimetallic catalyst prepared by electroless plating deposition which the silver was the pre-existing metal (catalysis) for the plating step. The pre-existing metal (catalysis) was an important step for electroless plating deposition. Schaal, M., et al. [42] synthesized bimetallic catalyst (Cu-Pd/SiO_2) using palladium as a catalyst for pre-existing step. These bimetallic catalysts show the good activity and selectivity for the hydrogenation of 3,4-epoxy-1-butene. Not only silver and palladium were used in the pre-existing metal (catalysis) for the plating step but also platinum was used from the studies of Schaal, M.T., et al. [43]. Schaal, M.T., et al. [43] synthezied bimetallic catalysts Ag-Pt/SiO_2. It started with pre-existing Pt/SiO_2 by electroless plating and silver was deposited onto the

Pt/SiO_2 catalysts. The results indicated that silver deposition did not suddenly occur on the support but it deposited essentially limited to the Pt surface.

Reblli, L., et al. [44]. And Reblli, L., et al. [45] prepared a series of bimetallic catalysts $Au\text{-}Pd/SiO_2$, $Ag\text{-}Pd/SiO_2$ and $Cu\text{-}Pd/SiO_2$. Hydrazine was used as reducing agent for Au and Ag. Dimethylamineborane (DMAB) was used as reducing agents for Cu. The primary monometallic catalysts deposition of 1.85 wt% Pd/SiO_2 after the primary step the deposition of Au and Ag were carried out at room temperature, while electroless plating deposition of Cu was carried out at 40 ^oC. The results show deposition of Ag and Cu were selective to Pd sites, although the deposition of Au could not be identified on all the Pd sites.

In 2011, the electroless plating deposition technique was applied to prepare ternary alloy catalysts ($CO\text{-}Ni\text{-}P/Pd\text{-}TiO_2$) in the studied of Rakap,M., et. al. [46]. The ternary alloy catalysts were prepared by electroless deposition of Pd/TiO_2, which Pd acted as a catalytically active surface for deposition of alloy. Sodium hypophosphite was used as the reducing agent and the bath was maintained at 75 ^oC. The ternary alloy catalysts prepared by electroless deposition were stable enough to be isolated as solid materials. They were redispersible and reusable as an active catalyst in the hydrolysis of ammonia-borane.

CHAPTER III

EXPERIMENTAL

This chapter reports the experimental procedure used in this research. This chapter can be divided into six sections. First, the section 3.1 explains the conventional $SnCl_2$ activation process for electroless plating deposition. Details of the Sn-free activation process for electroless plating are shown in section 3.2. The electroless nickel plating on polyurethane form is explained in section 3.3. The preparation of Pd/TiO_2 by electroless plating deposition is shown in section 3.4. The reaction study in the liquid-phase selective hydrogenation of 3-hexyne-1-ol hydrogenation is explained in section 3.5. Finally, in section 3.6, the various techniques used for catalyst characterization are shown.

3.1 The conventional $SnCl_2$ activation process for electroless plating deposition.

There are two types of activation process for electroless plating deposition used in this research. The first one is the conventional $SnCl_2$ activation process and the second type is the Sn-free activation process for electroless plating deposition.

In the conventional ($SnCl_2$) activation process the support (polyurethane foam) was treated with 30% sodium hydroxide (NaOH) at 60^{o}C for 10 min, in which high surface roughness with some cracks were observed over the surface. After etching with sodium hydroxide, the support was activated by a mixture of $PdCl_2$ and $SnCl_2$ at room temperature for 10 min**.** Then, it was rinsed and dried subsequently.

3.2 The Sn-free activation process for electroless plating deposition

The polyurethane (PU) foam samples (1x1x1 cm^3) was cleaned in distilled water and dip in acetone for 5 min at room temperature, and then cleaned in distilled water again. After cleaning, etching was performed on PU foams by dripping in

hydrochloric acid solutions (2M, 4M, 6M) for 1 hr. After etching, the samples were cleaned in distilled water and dip in acetone for 5 min, filtered to remove excess acetone, and then dried. Subsequently, the PU foams were immersed in a solution of palladium chloride ($PdCl_2$: (0.2, 1, 1.8) g/l, HCl: 2 g/l) at 40 ^oC for 10 min with ultrasonic vibration. Then it was rinsed and reduced in a reducing agent (sodium hypophosphite or hydrazine) at 40 ^oC for 2 min. The color of the solution turned to black, as the formation of Pd nanoparticles was obtained [29].

3.3 The electroless nickel plating on PU foam

Nickel deposition was achieved by dipping the activated PU foam into an electroless nickel plating bath (300 ml for each sample) for 1 hr at 85^oC. The bath was maintained at pH of 9.8 ± 2.0 to ensure a high cation exchange. The chemicals used for electroless plating deposition are shown in table 3.1

Table 3.1 The chemicals used for electroless nickel plating deposition.

Chemicals	Supplier
Sodium hypophosphite	Carlo Erba
tri- Sodium citrate dihydrate	Carlo Erba
Ammonium Sulphate	Carlo Erba
Nickel (II) Sulphate	Carlo Erba

3.4 The preparation of Pd/TiO_2 by electroless plating deposition.

In this experiment, electroless plating deposition was used for loading palladium on to commercial a titania support (Fluka). Palladium chloride was used as Pd precursor. There are two steps for palladium electroless plating deposition. The first step is the activation of titania support and then plating palladium on the activated support.

The support (titanium dioxide) was etched in hydrochloric acid solution (14%) for 15 min, and then cleaned in distilled water. After etching and cleaning, the support was immersed in a mixture solution of palladium chloride and tin (II) chloride for 20 min with ultrasonic vibration, then cleaning two times with distilled water, precipitated to remove excess distilled water, and then dried at 110 ^{o}C for 24 hr. The activated TiO_2 was turned to a gray powder.

For the next step, palladium was plating on TiO_2 by dipping the activated TiO_2 into an electroless palladium plating bath (100 ml for each sample) for 1 hr at 50^{o}C with ultrasonic vibration. The bath was maintained at pH of 9.8 ± 2.0 to ensure a high cation exchange. The chemicals used for palladium electroless plating deposition are shown in table 3.2 After electroless plating, the catalyst was cleaned with distilled water for two times and then it was dried at 110 ^{o}C for 24 hr.

Table 3.2 The chemicals used for palladium electroless plating deposition.

Chemicals	Supplier
Palladium (II) chloride (99.999%)	Aldrich
Tin (II) chloride dihydrate	Fluka
Sodium hypophosphite	Carlo Erba
Hydrochloric acid 37%	Carlo Erba
Ammonia hydroxide 28%	Aldrich
Ammonia chloride	Carlo Erba

3.5 The Reaction study in liquid-phase selective hydrogenation of 3-hexyne-1-ol

In this research, the liquid-phase hydrogenation of 3-hexyne-1-ol was used to study the properties of catalysts. Ethanol was used as organic solvent for 3-hexyne-1-ol. The reaction conditions were similar to those of ref. [47]

3.5.1 Chemical and Reagents

The chemicals and reagents which used in this reaction are shown in table 3.3

Table 3.3 The chemicals and regents used in the liquid-phase selective hydrogenation of 3-hexyne-1-ol

Chemicals and Reagents	Supplier
High purity hydrogen (99.99 vol %)	Thai Industrial gases limited
3-hexyne-1-ol	Aldrich
Ethanol	EMSURE

3.5.2 Instrument and Apparatus

The main instruments and apparatus are described as the follows:

The autoclave reactor

The autoclave has size 50 ml which made from stainless steel was used as reactor. Hot plate stirred is used to stir with magnetic bar to guarantee that the reactant and catalyst were well mixed which can neglect the mass transfer effect.

Gas chromatograph

A gas chromatograph (Shimadzu GC-2014) equipped with flame ionization detector (FID) was used to analyze the reactant and product. The operating conditions for GC and detector are shown in table 3.4

Table 3.4 Operating condition for gas chromatograph

Gas Chromatograph	Shimadzu GC-2014
Detector	FID
Packed column	Rtx®-5
Carrier gas	Helium (99.99vol.%)
Make-up gas	Air (99.99vol.%)
Column Temperature	70 ^{o}C
Injector Temperature	250 ^{o}C
Detector Temperature	310 ^{o}C

The schematic drawing of equipment used for the liquid phase hydrogenation of 3-hexyne-1-ol is shown in Figure 3.1

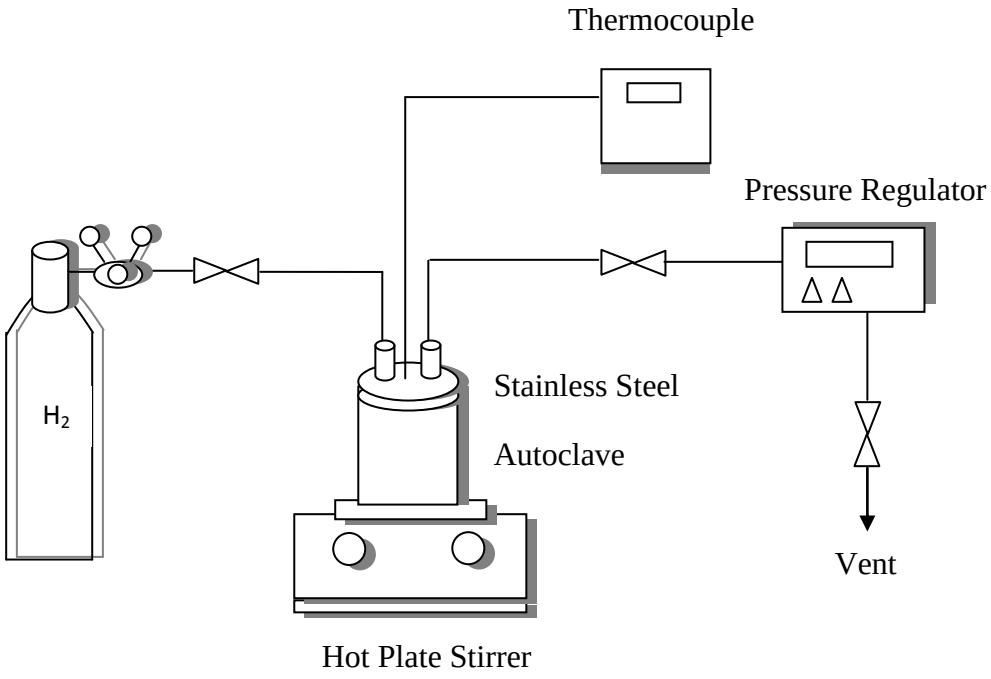

Figure 3.1 A schematic of liquid phase hydrogenation system

3.5.3 Liquid – phase hydrogenation procedure

The reaction studies of liquid-phase hydrogenation of 3-hexyne-1-ol in ethanol are explained in detail below which consisted of two steps of reaction.

1. Reduction step

Approximately 0.3 gram of palladium on titania catalyst was located into the glass tube. Then the catalyst was reduced by hydrogen gas at the volumetric flow rate of 50 ml/min at 40 degree Celsius for 2 hours.

2. Reaction step

0.2 ml of 3-hexyne-1-ol, 9.8 ml of ethyl alcohol and 10 mg of catalyst were mixed in the autoclave reactor. Subsequently, hydrogen was purged to remove

remained air in the reactor. Afterwards, the hydrogen gas was vent out of the reactor and heat up to 40 ^{o}C for 30 min. The liquid phase hydrogenation reaction was carried out under hydrogen atmosphere at 2 bars for 10-60 min. The reaction was started with a stirring magnetic stirrer. After the reaction, the vent valve was opened to releases hydrogen gas. The product was analyzed by gas chromatography.

3.6 Catalyst characterization

The catalysts were characterized by several techniques as follow:

3.6.1 X-ray Diffraction (XRD)

The bulk crystal structure and chemical phase composition were determined by diffraction of an X-ray beam as a function of the long fine focus. The XRD spectrum of the catalyst was measured by using a D8 Advance of Bruker AXS X-ray diffractometer and CuK_{α} radiation in the 2θ range of 20-80 degrees resolution 0.02^{o}. The crystallite size was calculated from Scherrer's equation.

3.6.2 Scanning Electron Microscopy (SEM)

Catalysts granule morphology and elemental distribution were obtained using a JEOL JSM-35F scanning electron microscope. The SEM was operated using the back scattering electron (BSE) mode at 20 kV at the Scienctific and Technological Researh Equipment Center, Chulalongkorn University (STREC)

3.6.3 X-ray Photoelectron Spectroscopy (XPS)

The XPS spectra, the binding energy and the composition on the surface layer of the catalysts were determined by using a Kratos Amicus X-ray photoelectron spectroscopy. The analyses were carried out with these following conditions: Mg Ka

X-ray source at current of 20 mA and 12 kV, 0.1 eV/step of resolution, and pass energy 75 eV and the operating pressure was approximately $1x10^{-6}$ Pa

3.6.4 Transmission Electron Microscopy (TEM)

The palladium nanoparticles, of titania supports, and prepared catalysts are investigate the structure, Pd particles size, and distribution of palladium on titania supported are observe using JEOL-JEM 200CX transmission electron microscope operated at 100 kV at National Metal and Materials Technology Center.

3.6.5 N_2 physisorption

The BET surface area of solid, pore volume, average pore size diameters and pore size distributions of catalyst were determined by physisorption of nitrogen (N_2) using a Micromeritics ASAP 2020.

3.6.6 CO-Pulse Chemisorption

The active sites and the relative percentages dispersion of palladium catalyst was determined by CO-pulse chemisorptions technique using Micromeritics ChemiSorb 2750 (pulse chemisorptions system)

Approximately 0.2 g of catalyst was filled in a glass tube, incorporated in a temperature-controlled oven and connected to a thermal conductivity detector (TCD). He was introduced into the reactor at the flow rate of 15 ml/min in order to remove remaining air. Prior to chemisorp, the sample were reduced in a H_2 flow rate at 50 ml/min with heated from room temperature to 40 ^{o}C and held at this temperature for 2 h. Carbon monoxide that was not adsorbed was measured using thermal conductivity detector. Pulsing was continued until no further carbon monoxide adsorption was observed. Calculation details of % metal dispersion are given in Appendix D.

3.6.7 Inductive coupled plasma optical emission spectrometer (ICP-OES)

ICP-OES is technique of quantitative measurement of the metals loading. It was determined using a Perkin Elmer Optima 2100DV AS93 PLUS inductive coupled plasma optical emission spectrometer. The catalysts samples were prepared in a solution containing 49% HF and 37% HCl with volume ratio 8:2 and were heated at 40 ^{o}C to increase the solubility.

CHAPTER IV

RESULTS AND DISCUSSION

The results and discussion in this chapter are divided into two parts. The first part describes about the characterization of nickel on polyurethane foam by using several techniques such as SEM, EDX, XPS, and Universal testing machine (Shimadzu). The parameters studied include the HCl concentration (2M-6M) used for pretreatment of PU foam, the amounts of palladium (0.2g/l-1.8g/l) in the activation process for nickel electroless plating, the reducing agents (sodium hypophosphite and hydrazine), and the electroless deposition time (10min-120min). The second part reports the catalytic properties of Pd/TiO_2 catalysts prepared by electroless deposition method with and without Sn activation (ED-1%Pd/TiO_2 Sn, and ED-1%Pd/TiO_2 non-Sn) in the liquid-phase selective hydrogenation of 3-hexyne-1-ol.The 1% Pd/TiO_2 prepared by the conventional incipient wetness impregnation method (IMP-1% Pd/TiO_2) was used for comparison purposes. In addition, several analytical techniques were employed for catalyst characterization such as, SEM, TEM-EDS, XPS, XRD, and CO-pulse chemisorption.

4.1 Characterization of the nickel on polyurethane foam

4.1.1 The effect of HCl concentration used for pretreatment of PU foam

SEM is an important tool for observing directly the surface texture and morphology of materials. The typical SEM images of PU foam before and after etching/activation are presented in Figure 4.1(a)-(f). The quality of the deposited metal layers, in the electroless deposition on non-metallic surface, is noted to be dependent on the adhesion between the Pd activation particles and the PU's surface. Electroless deposition also requires sufficient surface cleaning pre-treatment to increase the adhesion of Pd(+2) ions to the polymer surface [48].

In the conventional activation by $PdCl_2$ and $SnCl_2$ process, the surface was treated with 30% sodium hydroxide (NaOH) at 60^oC for 10 min. High surface roughness with some cracks were observed over the surface of PU foam after conventional activation as shown in Figure 4.1 (b). On the contrary, the tin-free activation did not result in an obvious surface roughness. Comparing to the original PU foam in Figure 4.1 (a), the surface morphology of the PU foam after etching with 4M HCl for 1 hr (Figure 4.1 (c) and the PU foam after etching and $PdCl_2$ activation (Figure 4.1 (e), were quite smooth and were not significantly different from the ones after etching.

There were no significantly differences in the morphologies of PU foam after etching/activation with different concentrations of hydrochloric acid as shown in Figure 4.1 (d)-(f). However, the use of HCl concentration $\geq$ 6 M resulted in partial destruction of the PU foam.

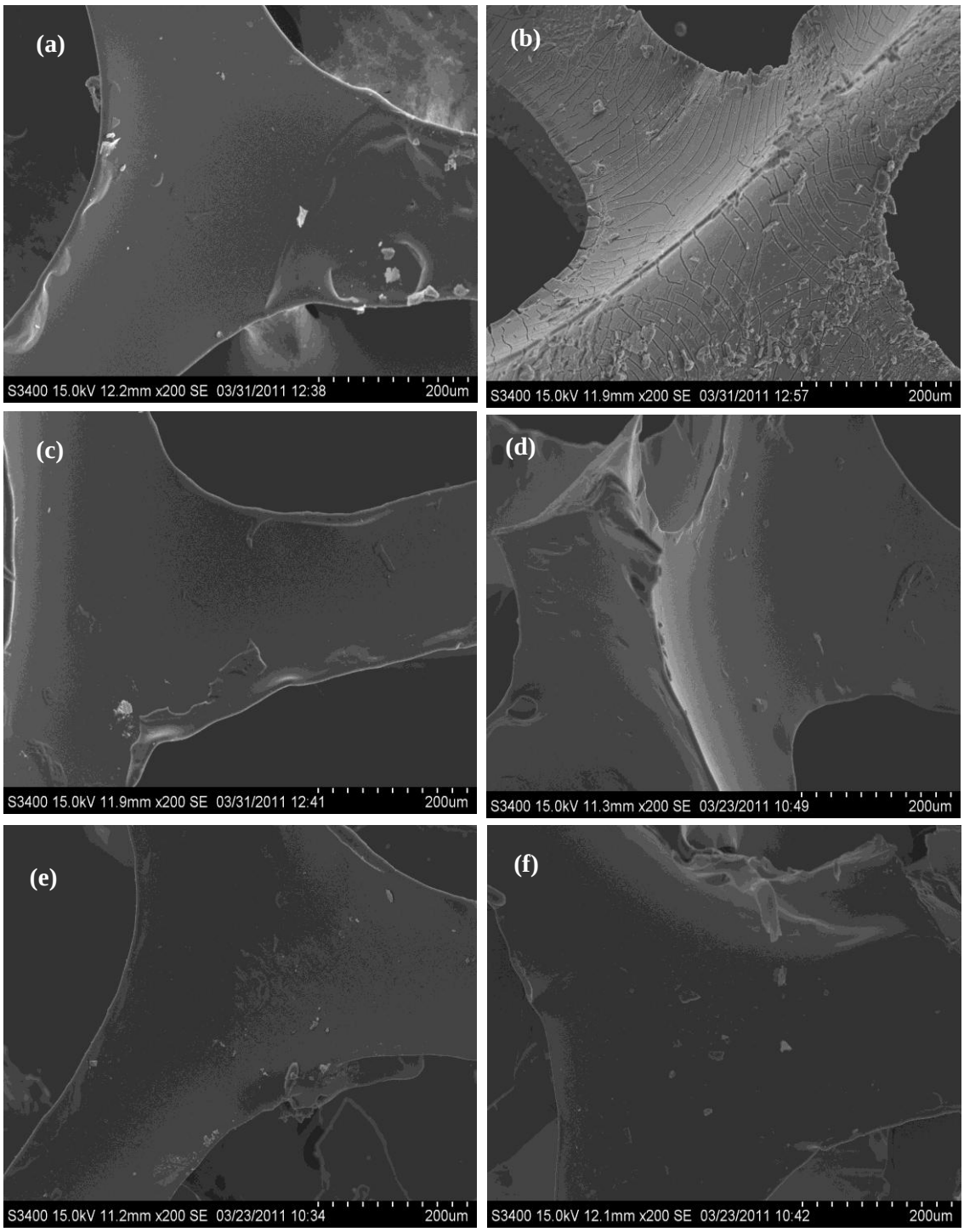

Figure 4.1 SEM micrographs of the top-layer morphology of PU foam, etching/activation: (a) PU foam; (b) PU foam + Pd-Sn; (c) PU foam + HCl 4M; (d) PU foam + HCl 2M /activation; (e) PU foam + HCl 4M /activation and (f) PU foam + HCl 6M /activation.

4.1.2 Effect of $PdCl_2$ concentration during the activating process on nickel plating

In the activation process is to employ the palladium as a catalyst metal sites on the substrate to introduce oxidation of a reducing agent in electroless plating solution. This process has a direct influence on the quality of plating layer so that the effect of $PdCl_2$ concentration (0.2 g/l-1.8 g/l) on nickel plating was investigated.

4.1.2.1 Scanning electron microscopy (SEM)

The SEM images of the PU foam after electroless nickel deposition prepared by etching with 4M HCl for 1 hr, activated by $PdCl_2$ solution, and reduced in sodium hypophosphite are shown in Figure 4.2 (a)-(f). It can be seen from Figure 4.2 that the three dimensional network of the PU foam microstructure was not much altered after electroless nickel plating. The nickel layer, however, was not clearly evident in the SEM images when the PU foam was prepared by etching with 4M HCl for 1 hr and activated by $PdCl_2$ 0.2g/l as shown in Figure 4.2 (a) and Figure 4.2 (b). Increasing the amount of $PdCl_2$ during activation to 1.0g/l and 1.8 g/l resulted in more uniformly coating of nickel layer on the surface as shown in Figure 4.2 (c) and Figure 4.2 (e), respectively.

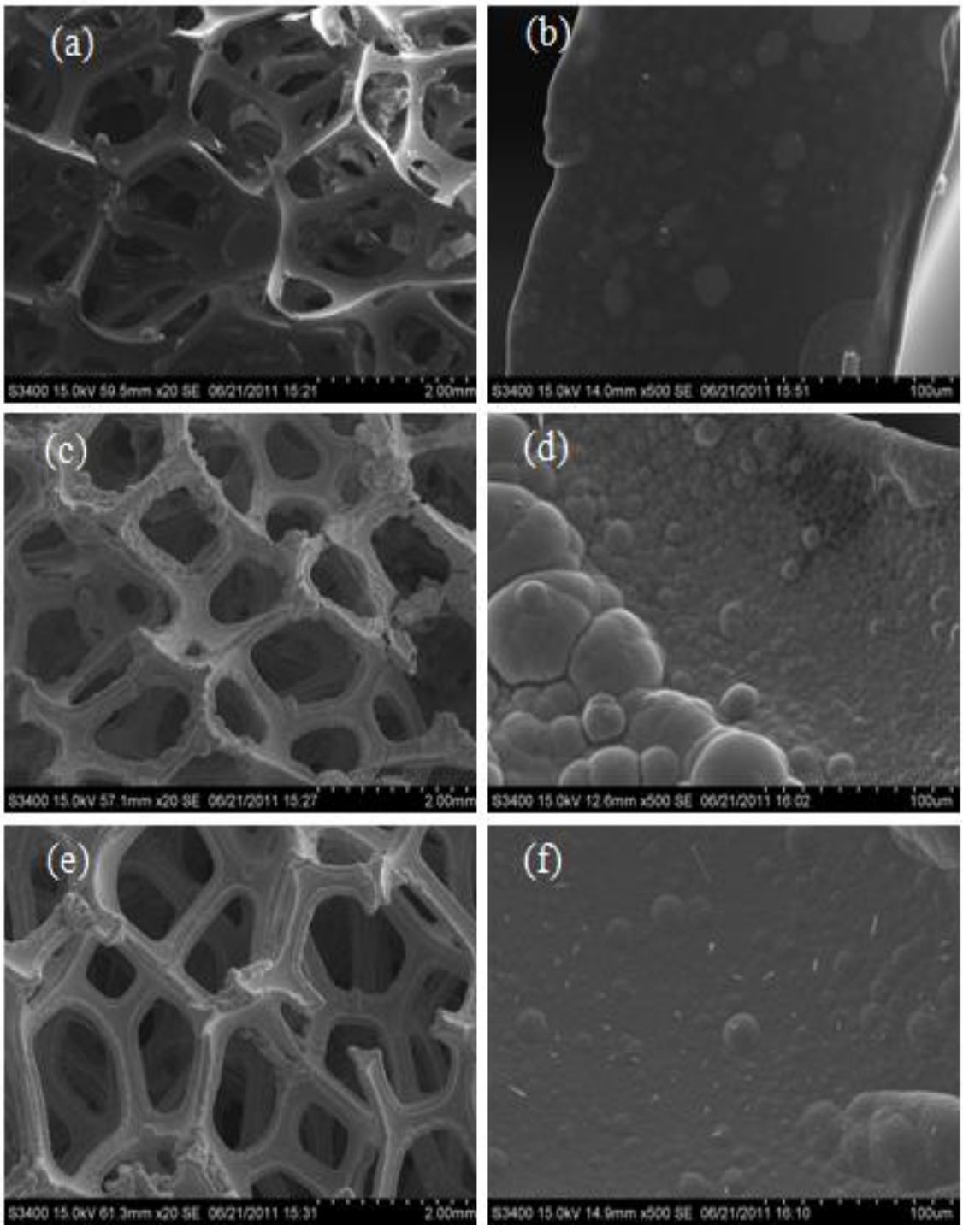

Figure 4.2 SEM micrographs of the surface morphologies of the electroless Ni deposit on PU foam: (a) Ni/PU activated $PdCl_2$ 0.2 g/l (x20); (b) Ni/PU activated $PdCl_2$ 0.2 g/l (x500); (c) Ni/PU activated $PdCl_2$ 1.0 g/l (x20); (d) Ni/PU activated $PdCl_2$ 1.0 g/l (x500); (e) Ni/PU activated $PdCl_2$ 1.8 g/l (x20); (f) Ni/PU activated $PdCl_2$ 1.8 g/l (x500).

4.1.2.2 Energy dispersive X-ray spectroscopy (EDX)

Figure 4.3 shows the EDX spectra of Ni, O, and C elements on the Ni/PU foam prepared with different amounts of $PdCl_2$ in the activating solution. It is clearly seen that the amount of Ni deposit increased with increasing amount of $PdCl_2$ in the activating solution. Therefore, a non-metallic substrate, such as PU foam has to be catalyzed during the activation process before electroless nickel plating can be performed. Pd is commercial used as a catalyst for electroless plating due to its high activity [3, 15]. The amount of $PdCl_2$ during activation 1.8 g/l resulted in the highest amount of coated nickel layer on the surface as shown by EDX results.

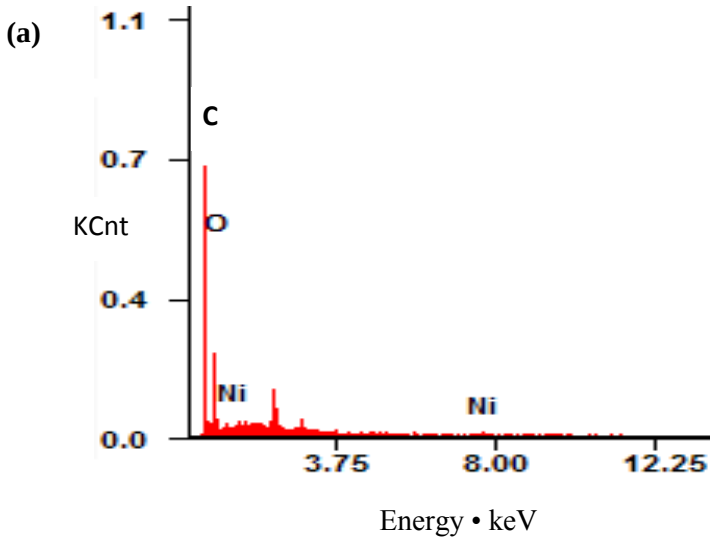

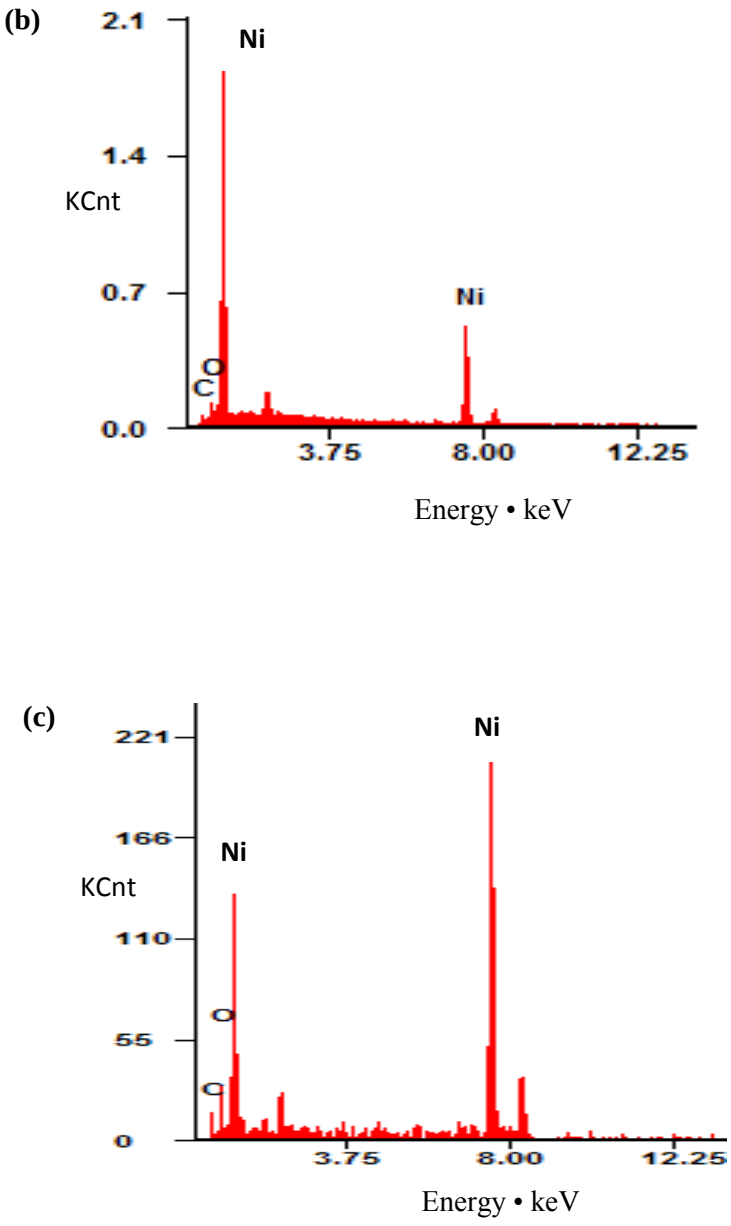

Figure 4.3 EDX spectra of the Ni/PU foam: (a) Ni/PU activated $PdCl_2$ 0.2 g/l; (b) Ni/PU activated $PdCl_2$ 1.0 g/l; (c) Ni/PU activated $PdCl_2$ 1.8 g/l.

4.1.3 Effect of reducing agent on nickel plating

4.1.3.1 The nickel deposition rate

The effect of reducing agent during the activation process on the nickel plating on PU foam was investigated. Reducing agent produce the reduction of Pd^{2+} ions to Pd^0 by the redox reaction, making the catalyst (Pd^0) active for initiation of plating reaction. Hydrazine and sodium hypophosphite were selected as the reducing agents for Pd during the activating process in order to demonstrate the effect of reducing agent on the plating efficiency. Here, the plating efficiency was evaluated by the deposition rate testing. The deposition rate was calculated by the following equation:

$$v= (m_2-m_1)/(m_1t)$$

Where m_1 and m_2 are the masses of the specimen before and after electroless plating procedure, respectively; t is the stabilizing time of electroless plating bath [49].

The effect of reducing agent on the deposition rate is shown in Figure 4.4. The results indicate that the use of hydrazine provided slower plating rate than sodium hypophosphite. Furthermore, both reducing agents appear to give optimum deposition rate near the early stage of plating, after which the plating gradually declined. The plating time deposition was optimized at 60 min. According to the experimental results, the deposition rate was low after 60-120 min. Moreover, it was found that the bath decomposed easily after plating for 60 min.

The electroless nickel deposition is known to have a principal problem of rapid bath decomposition. This results in increasing of the operating cost and generates hazardous waste [49]. It is demonstrated that $SnCl_2$ significantly improved the decomposition of nickel electroless bath. From the experimental results with two

samples (1x1x1 cm^3) in the electroless nickel baths, it was found that the nickel electroless bath decomposed after 49 min. On the other hand, using a non-Sn activation process, the nickel electroless bath was not decomposed and can be reused when nickel source components were added.

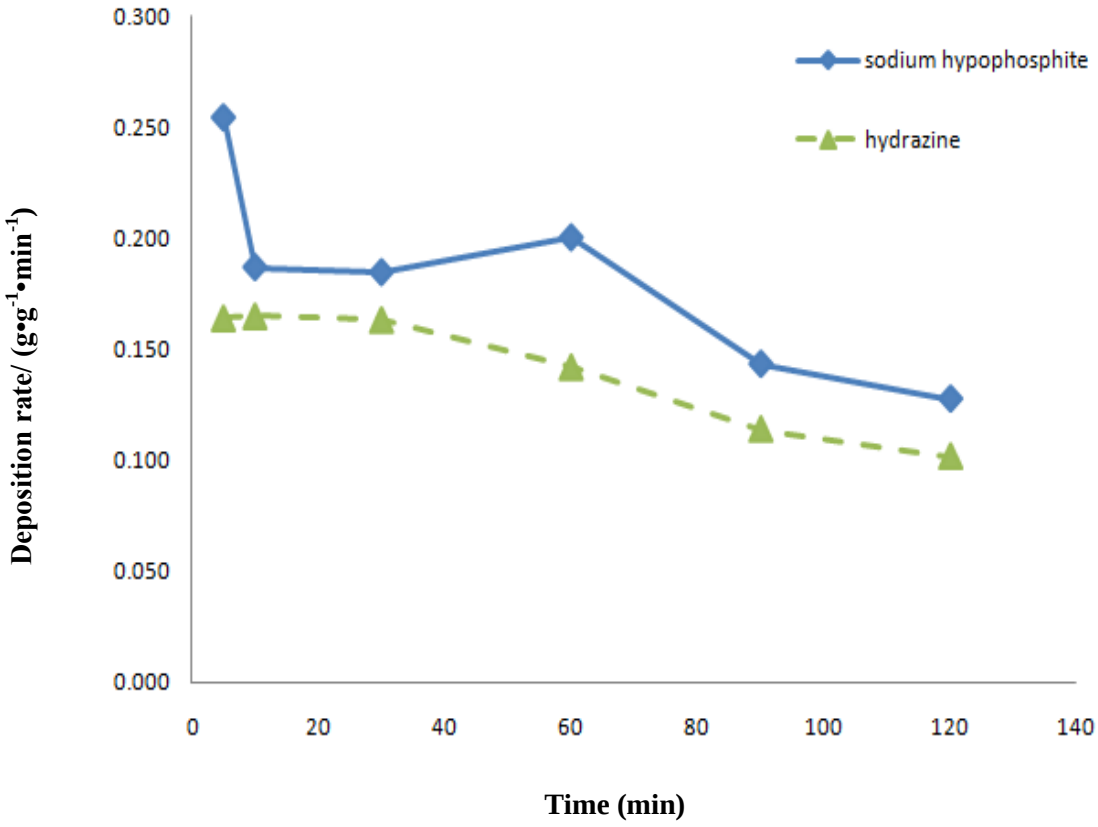

Figure 4.4 Effect of reducing agent on nickel electroless deposition rate

4.1.3.2 Scanning electron microscopy (SEM)

The SEM images of the PU foam after electroless nickel deposition prepared by etching with 4M HCl for 1 hr, activated by $PdCl_2$ solution 1.8 g/l and reduced in sodium hypophosphite and hydrazine are shown in Figure 4.5 (a)-(f). It can be seen from Figure 4.5 (a)-(c) that reduction in sodium hypophosphite, smooth and dense nickel plating layer were observed by optical observation. As shown in Figure 4.5 (d)-(f), reduction in hydrazine resulted in a not-so-smooth nickel deposition and poor dispersion on the surface. From these results, it can be concluded that the sodium hypophosphite is a better reducing agent than hydrazine for electroless nickel plating on PU foam.

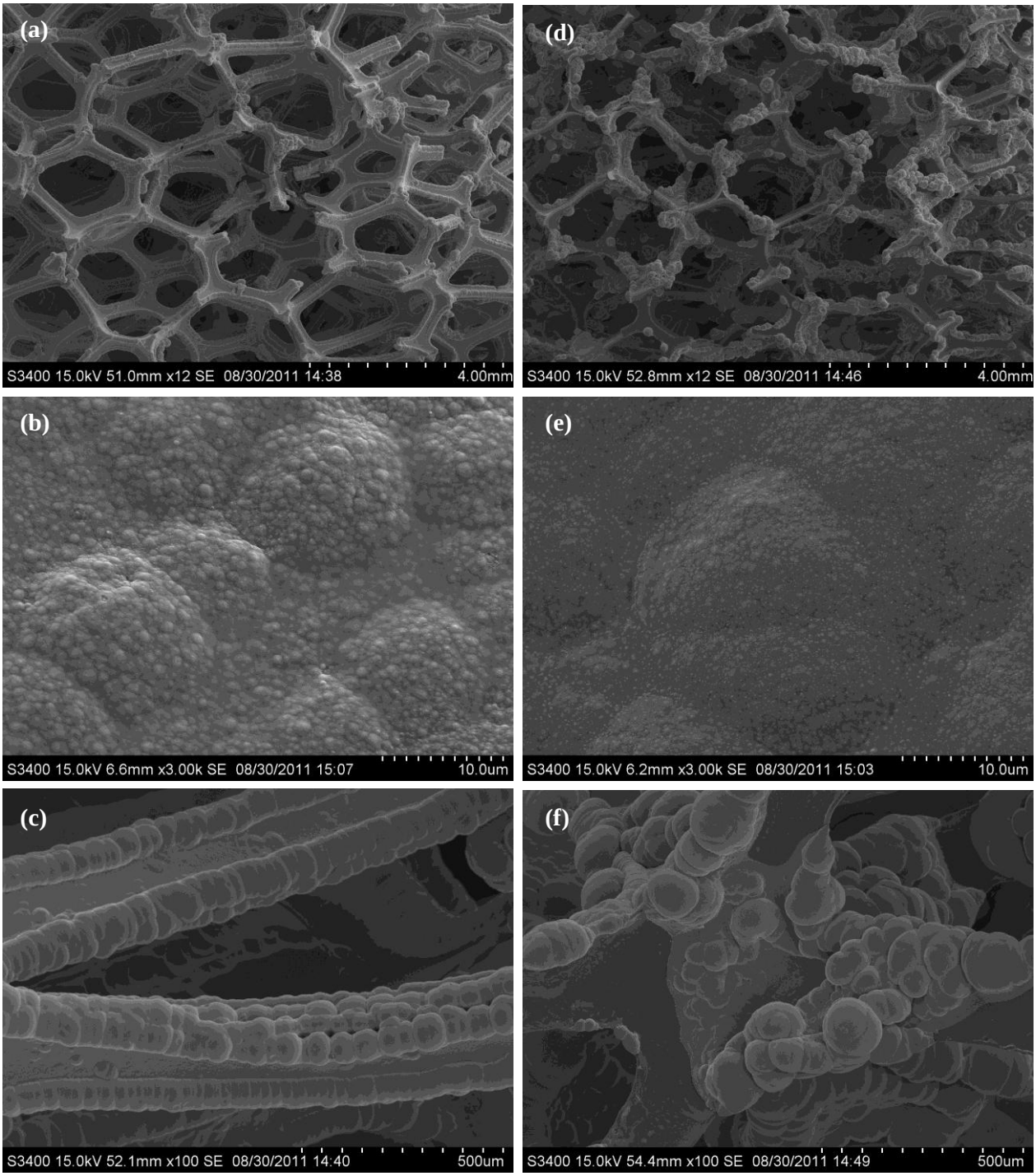

Figure 4.5 SEM micrographs of the surface morphologies of the electroless Ni deposit on PU foam, etching/activation in 4 M HCl/activation in $PdCl_2$ solution 1.8 g/l : (a) Ni/PU reduce with sodium hypophosphite (x4); (b) Ni/PU reduce with sodium hypophosphite (x10); (c) Ni/PU reduce with sodium hypophosphite (x500); (d) Ni/PU reduce with hydrazine (x4); (e) Ni/PU reduce with hydrazine (x10); (f) Ni/PU reduce with hydrazine (x400).

4.1.3.3 Compression test

The Ni/PU foam samples (1x1x1 cm^3 each) prepared by electroless nickel plating with different reducing agents (sodium hypophosphite and hydrazine) were performed using an Instron universal testing machine (SHIMADZU). Load cell 50 N, strain rate of 4×10^{-4}/ second and force-displacement curve were auto saved. Figure 4.6 shows typical stress-strain curves for Ni/PU foam reduced by hydrazine. The result shows stress (Mpa) was increased with increasing electroless deposition time. Figure 4.7 shows typical stress-strain curves for Ni/PU foam reduced with sodium hypophosphite. The results show a higher stress (Mpa) value than that of Ni/PU foam which was reduced by hydrazine with the same deposition time.

From Table 4.1 shows the density and modulus of the Ni/PU foam which can indicate the nickel plating efficiency. From the experimental results comparing the density of Ni/PU foam at the same plating time with different reducing agents, it was found that sodium hypophosphite > hydrazine. At 60 min, the density and modulus of Ni/PU foam reduced with conventional $SnCl_2$ were 0.133 $g•cm^{-3}$ and 0.069 Mpa, respectively. It was found that sodium hypophosphite is better reducing agent comparing to$SnCl_2$ and hydrazine for nickel electroless plating on PU foam.

These compression test results were found to be in good agreement with the nickel deposition rate and SEM micrographs that sodium hypophosphite is better reducing agent than hydrazine.

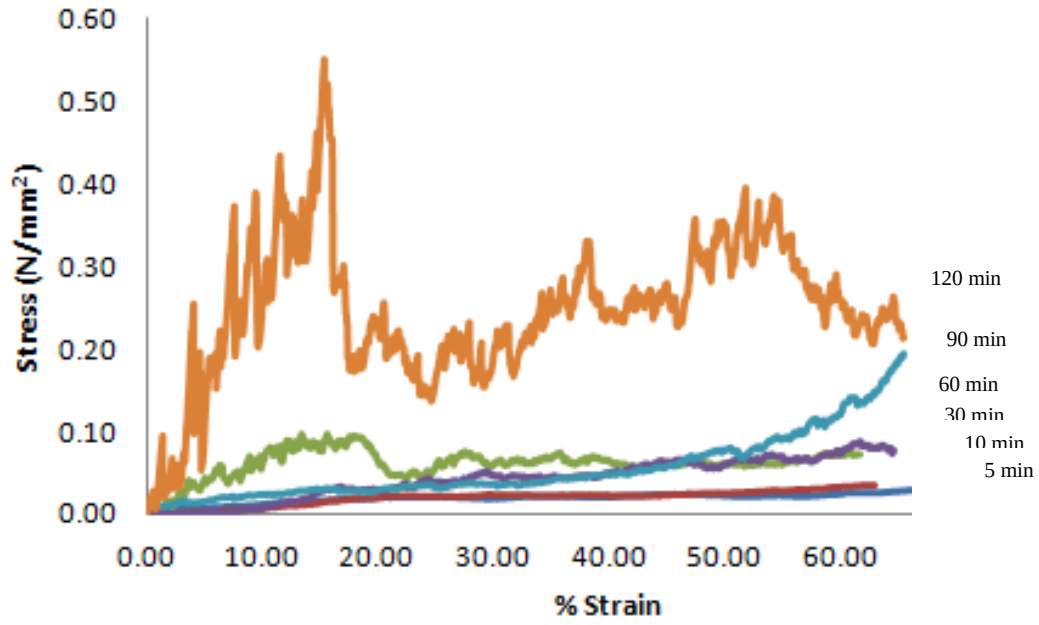

Figure 4.6 Stress-Strain curves for Ni/PU foam reduce with hydrazine

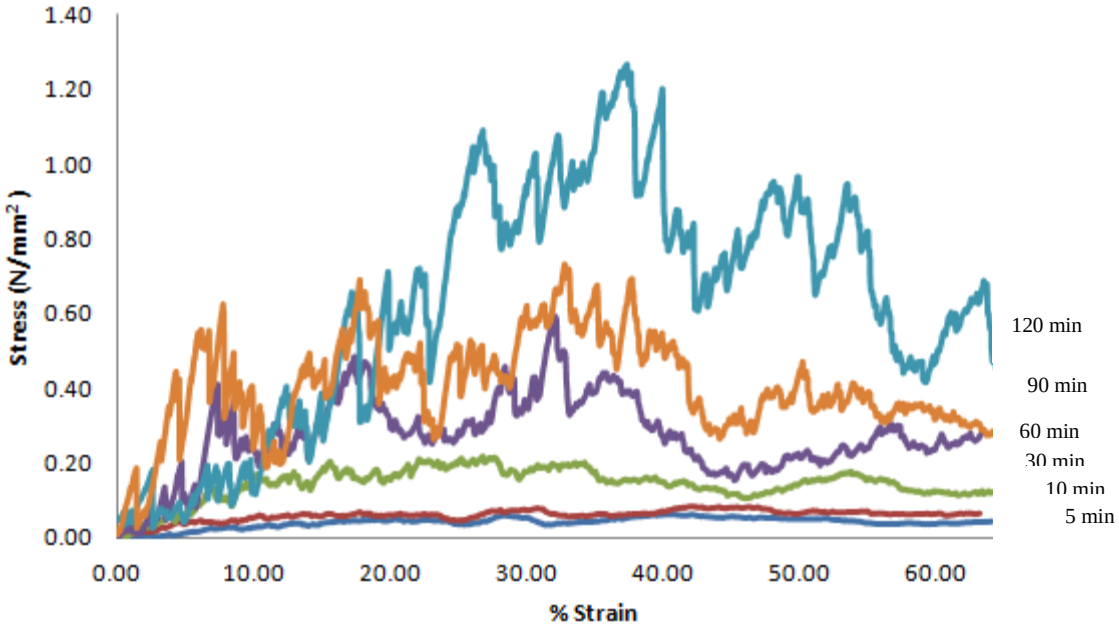

Figure 4.7 Stress-Strain curves for Ni/PU foam reduce with Sodium hypophosphite

Table 4.1 The properties of Ni/PU foams prepared with different reducing agents

	Reducing agent			
Plating time	**Sodium hypophosphite**		**hydrazine**	
(min)	**Density (g •cm^{-3})**	**Modulus (Mpa)**	**Density (g •cm^{-3})**	**Modulus (Mpa)**
5	**0.053**	**0.0027**	**0.053**	**0.0009**
10	**0.064**	**0.0038**	**0.059**	**0.0009**
30	**0.129**	**0.0109**	**0.112**	**0.0012**
60	**0.214**	**0.0215**	**0.179**	**0.0015**
60*	**0.113**	**0.0069**		
90	**0.236**	**0.0250**	**0.212**	**0.0017**
120	**0.268**	**0.0329**	**0.218**	**0.0214**

*** reduced in conventional ($SnCl_2$)**

4.1.4 X-ray Photoelectron Spectroscopy (XPS)

The XPS spectra, the binding energy, and the composition on the surface layer of the catalysts were determined by using a Kratos Amicus X-ray photoelectron spectrometer. The analyses were carried out with the following conditions: Mg K_α X-ray source at current of 20 mA and 12 kV, 0.1 eV steps of resolution, and pass energy 75 eV. The operating pressure was approximately $1x10^{-6}$ Pa.

The chemical states of nickel on the Ni/PU foam prepared by a tin-free activation electroless deposition are shown in Figure 4.8. The Ni 2p peak is always characterized by a complex shape due to the presence of multiplet splitting, shake-up and plasmon loss structures [50]. In the present work, the binding energy of Ni 2p was observed in the range of 856.9-862.6 eV and was attributed to Ni^{2+} ions according to the literature [52-53]. It is thus suggested nickel on the surface of Ni/PU foam surface is presented mostly in the form of nickel oxides.

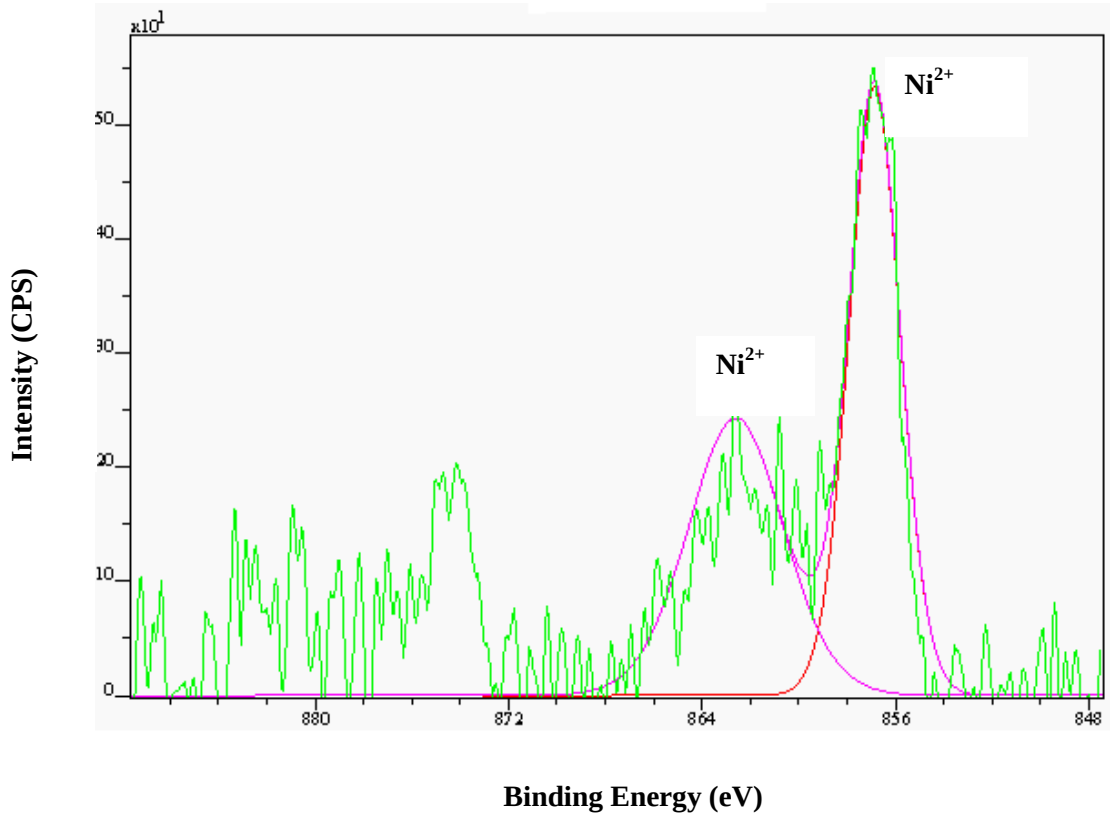

Figure 4.8 XPS spectra of Ni/PU +HCl 4M activated $PdCl_2$ 1.8 g/l using sodium hypophosphite as reducer

4.2 Characterization of the Palladium on Titanium dioxide

The second part of the Results and discussion reports the characteristics and catalytic properties of Pd/TiO_2 catalysts prepared by electroless deposition method with and without $SnCl_2$ activation. The same catalysts were also prepared by the conventional incipient wetness impregnation method (IMP Pd/TiO_2) for comparison purposes. All the catalysts were evaluated in the liquid-phase selective hydrogenation of 3-hexyne-1-ol. A commercial titania support was obtained from Fluka and used in all experiments.

4.2.1. Scanning Electron Microscopy (SEM)

The BET specific surface area and average pore size of the commercial titania support (Fluka) were 7.616 m^2/g and 1.51 nm, respectively. The original powder was white and the SEM micrograph of the titanium dioxide support is shown in Figure 4.9 (a). The TiO_2 morphology had a uniform particle size of 0.1-0.3 μm.

Figure 4.9 (b) shows the SEM image of titanium dioxide that was etched in hydrochloric acid solution (14%) for 15 min, and cleaned in distilled water. After etching and cleaning, the support was immersed in a mixture solution of palladium chloride and tin (II) chloride for 20 min with ultrasonic vibration, then cleaning two times with distilled water, precipitated to remove excess distilled water, and then dried at 110^oC for 24 hr. The TiO_2 activated in Pd/Sn solution were not significantly different from the corresponding TiO_2 before activated. However, the activated TiO_2 turned to gray color powder.

Figure 4.9 (c) shows the SEM micrographs of Pd/TiO_2 catalysts prepared by electroless Sn. There were no significantly differences in the morphology of Pd/TiO_2 support particles before and after electroless deposition probably because the SEM technique has low resolution in micro scale.

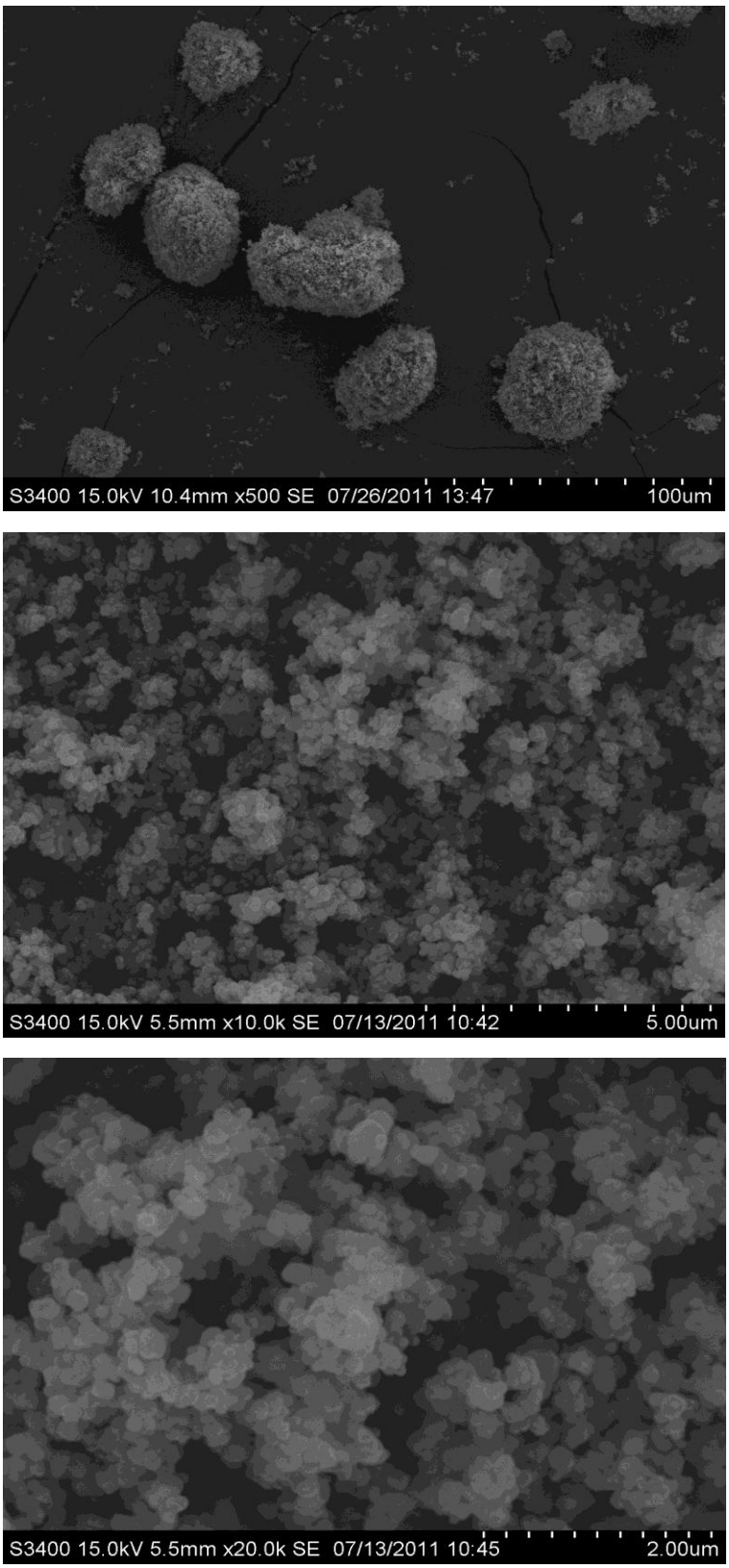
S3400 15.0kV 10.4mm x500 SE 07/26/2011 13:47
100um
S3400 15.0kV 5.5mm x10.0k SE 07/13/2011 10:42
5.00um
S3400 15.0kV 5.5mm x20.0k SE 07/13/2011 10:45
2.00um

(a)

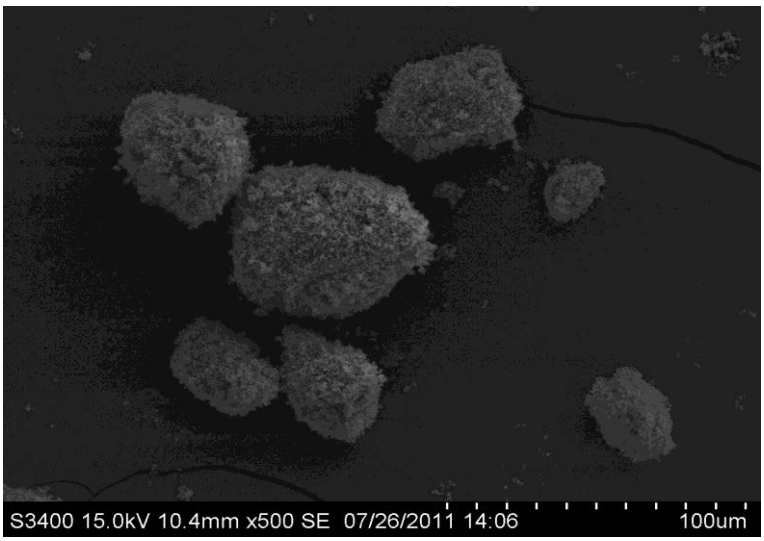
S3400 15.0kV 10.4mm x500 SE 07/26/2011 14:06
100um

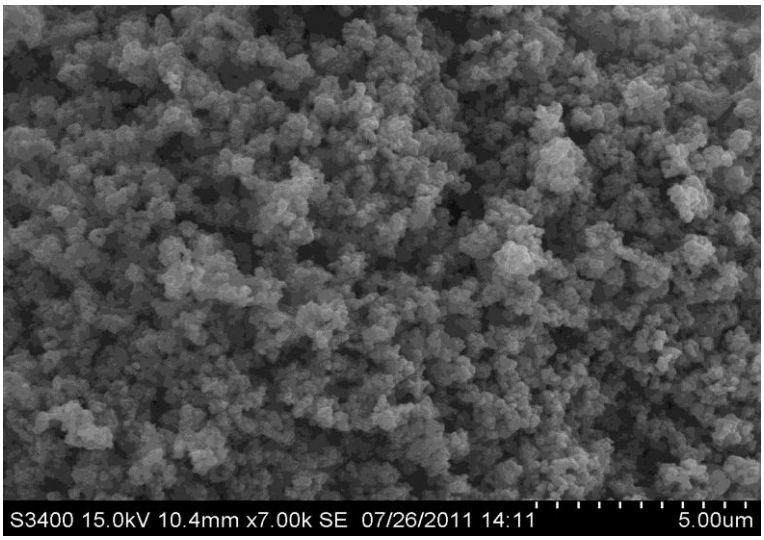
S3400 15.0kV 10.4mm x7.00k SE 07/26/2011 14:11
5.00um

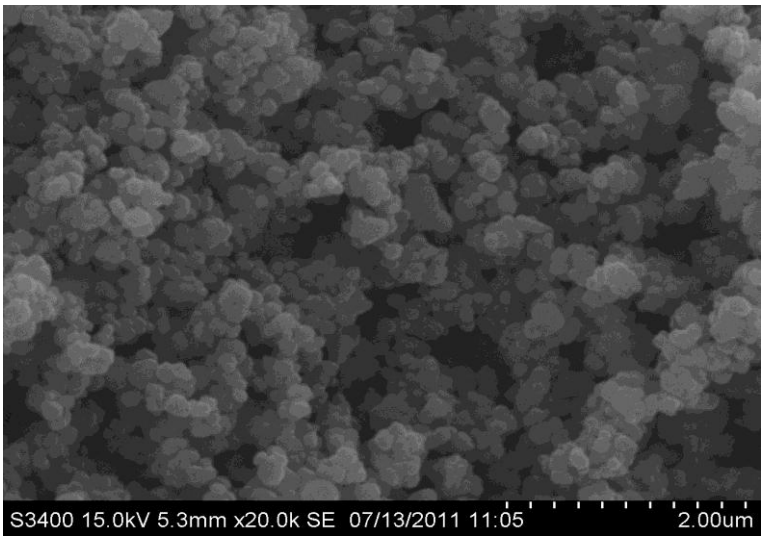
S3400 15.0kV 5.3mm x20.0k SE 07/13/2011 11:05
2.00um

(b)

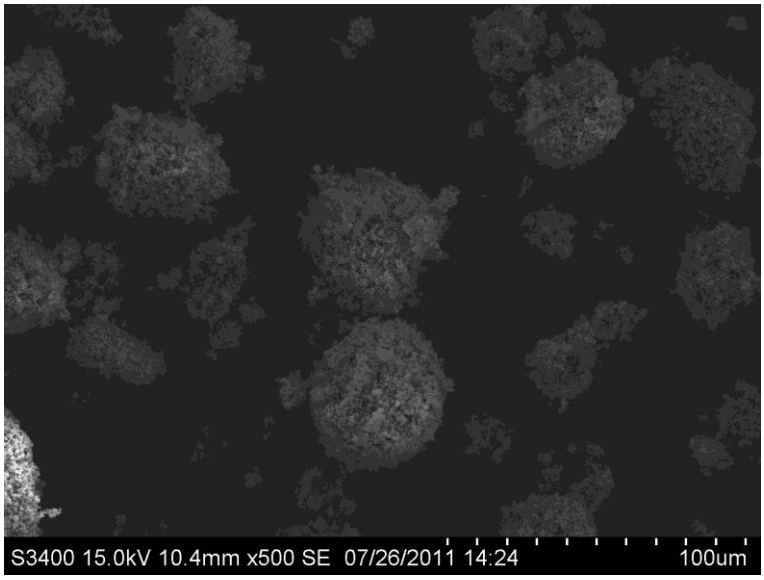

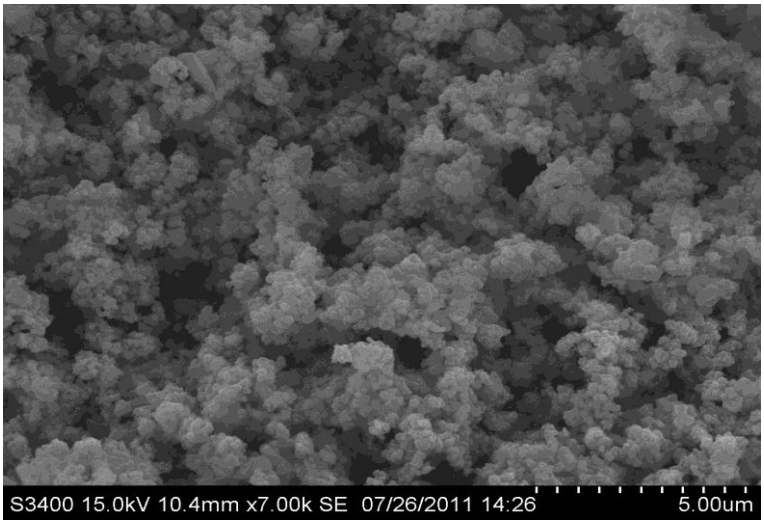

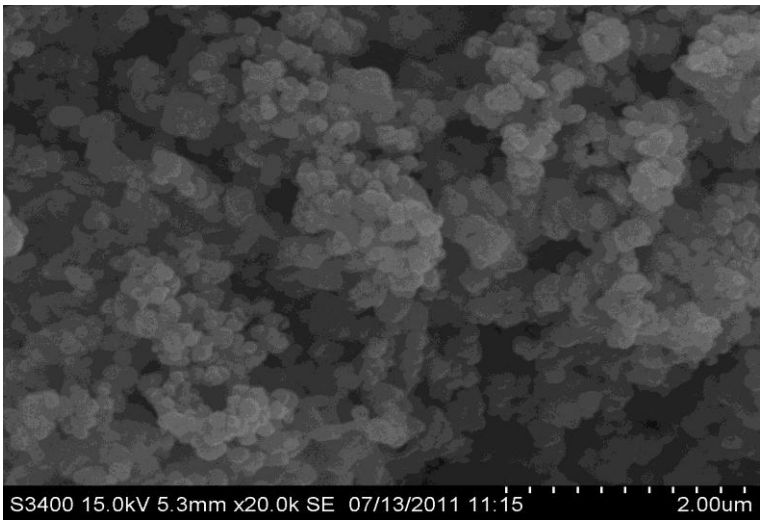

(c)

Figure 4.9 SEM Micrographs of (a) TiO_2, (b) TiO_2 after activated surface and (c) Pd/TiO_2 catalysts electroless

4.2.2 X-Ray Diffraction (XRD)

The XRD patterns of original TiO_2 support, TiO_2 after activated, and Pd/TiO_2 electroless Sn were collected at the 2θ degrees between 20º and 80ºandare shown in Figure 4.10. The titania support exhibited the XRD patterns of anatase TiO_2 crystalline structures. The peaks corresponding to anatase titania appeared at 25º (major), 37º, 48º, 55º, 62º, 71º and 75º 2θ. The peak intensity was decreased after activation process and after loading of Pd by electroless deposition.

The XRD peak corresponding to Pd^0 metal has been found at 2θ = 40º (major) [54]. However, due to the very low amount of Pd in the activation process, the Pd^0 peak was not detected from the diffraction pattern of the TiO_2 activated Sn sample.

Figure 4.11 shows the characteristic peaks of Pd/TiO_2 prepared by electroless deposition with Sn in activated process and non-Sn in activated process, respectively. The XRD patterns of Pd/TiO_2 prepared by electroless deposition with Sn in activation process and non-Sn in activation process were similar in which the Pd^0 metal peak was observed at 2θ = 40º. This result indicates that the Pd/TiO_2 catalysts prepared by electroless palladium deposition were in Pd metal form.

Furthermore, the oxidation state of Pd in all the Pd/TiO_2 catalysts prepared by electroless deposition was confirmed by XPS results.

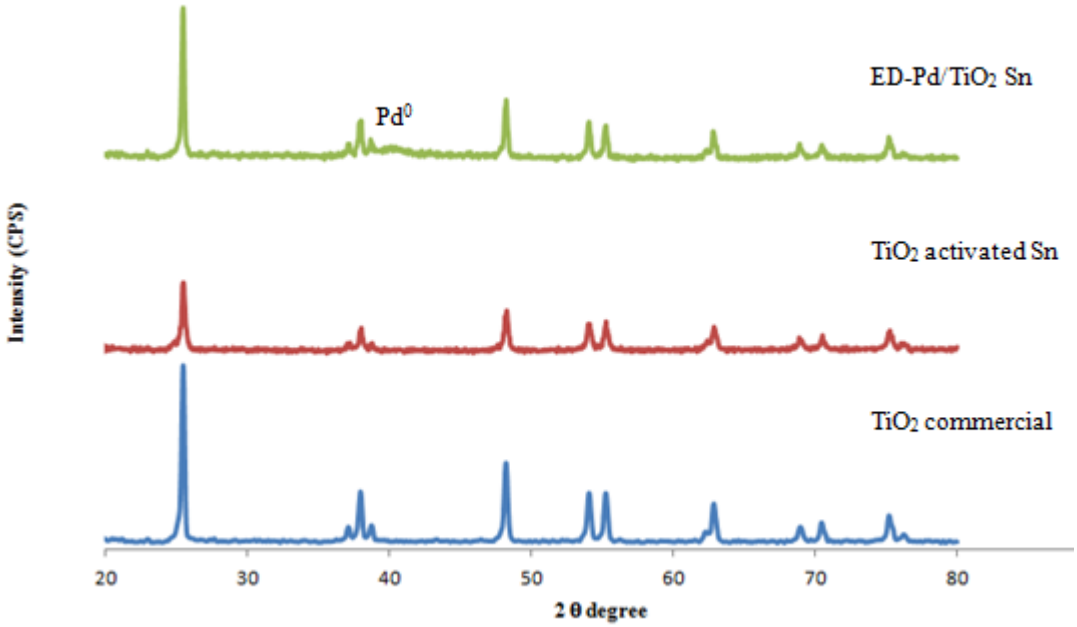

Figure 4.10 XRD patterns of the TiO_2, TiO_2 after activated and ED-Pd/TiO_2 Sn

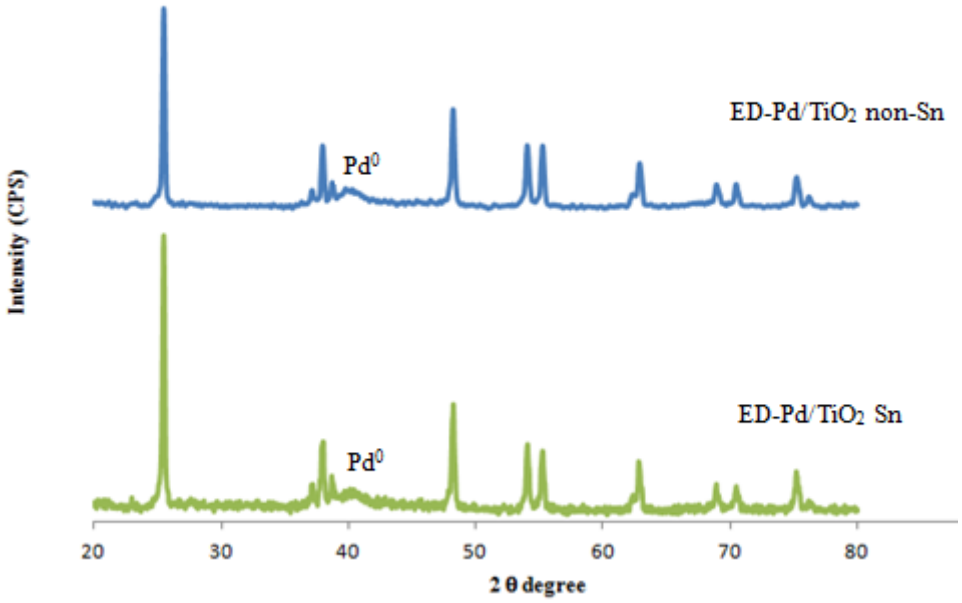

Figure 4.11 XRD patterns of ED-Pd/TiO_2 Sn and ED-Pd/TiO_2 non-Sn

4.2.3 X-ray Photoelectron Spectroscopy (XPS)

XPS is a useful technique to determine the binding energies and the composition of element on surface of the catalysts. The XPS results such as binding energies of TiO_2 activated Sn, ED-Pd/TiO_2 Sn, and ED-Pd/TiO_2 non-Sn are shown in Figure 4.12, Figure 4.13, and Figure 4.14, respectively. According to the literature, the XPS peaks of Pd $3d_{5/2}$ and Pd $3d_{3/2}$ at binding energy 335.01 eV and 340.40 eV are attributed to Pd metallic form [55-56].

Because of the very low amount of Pd in the activation process, the Pd metallic peaks were not clearly seen in Figure 4.12. On the other hand, in Figure 4.13 and Figure 4.14, the Pd $3d_{5/2}$ and Pd 3d3/2 at binding energy 335.01 eV and 340.40 eV were detected. It is indicated that the preparation of catalysts by electroless deposition with Sn and non-Sn activated processes resulted in metallic Pd. The XPS results were consistent to the XRD results.

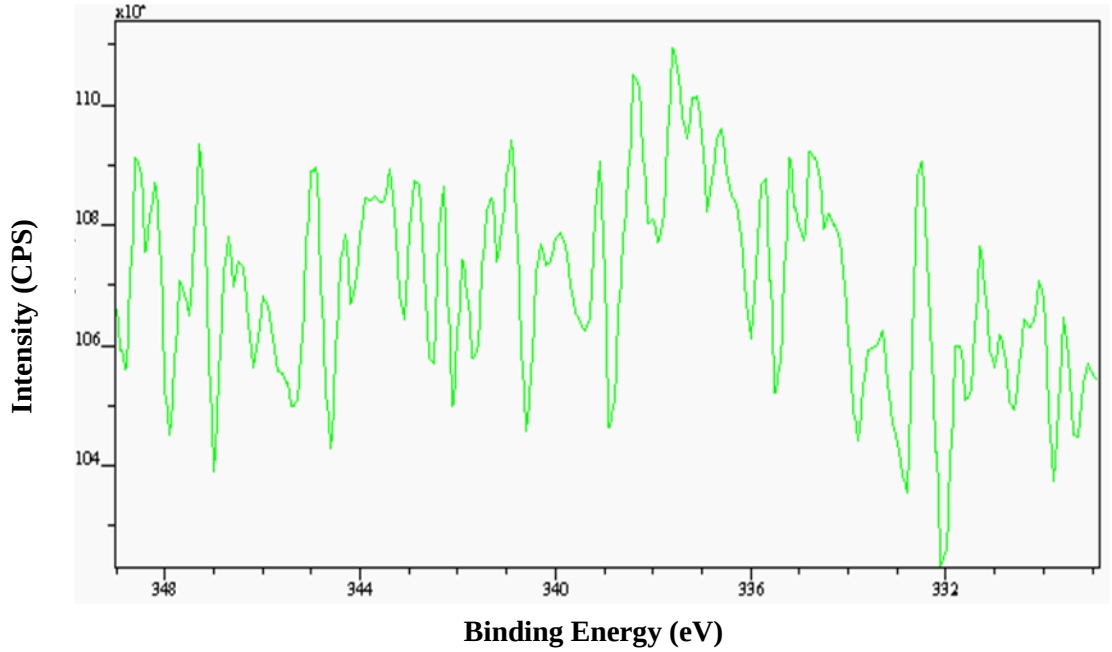

Figure 4.12 Binding energies of TiO_2 activated Sn

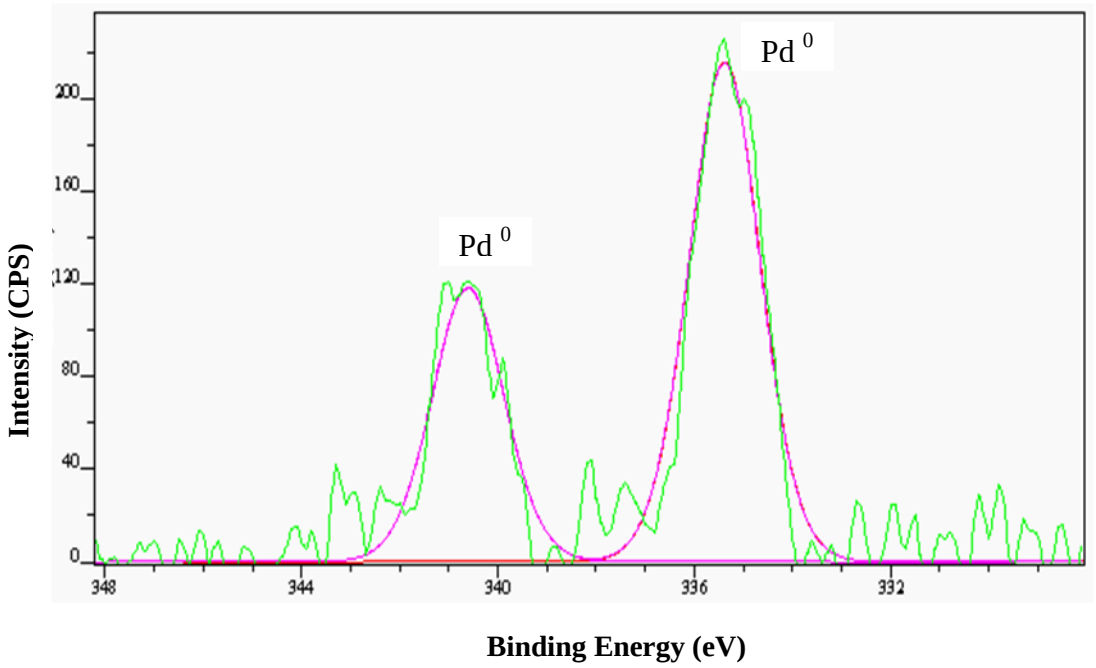

Figure 4.13 Binding energies of ED-Pd/TiO_2 Sn

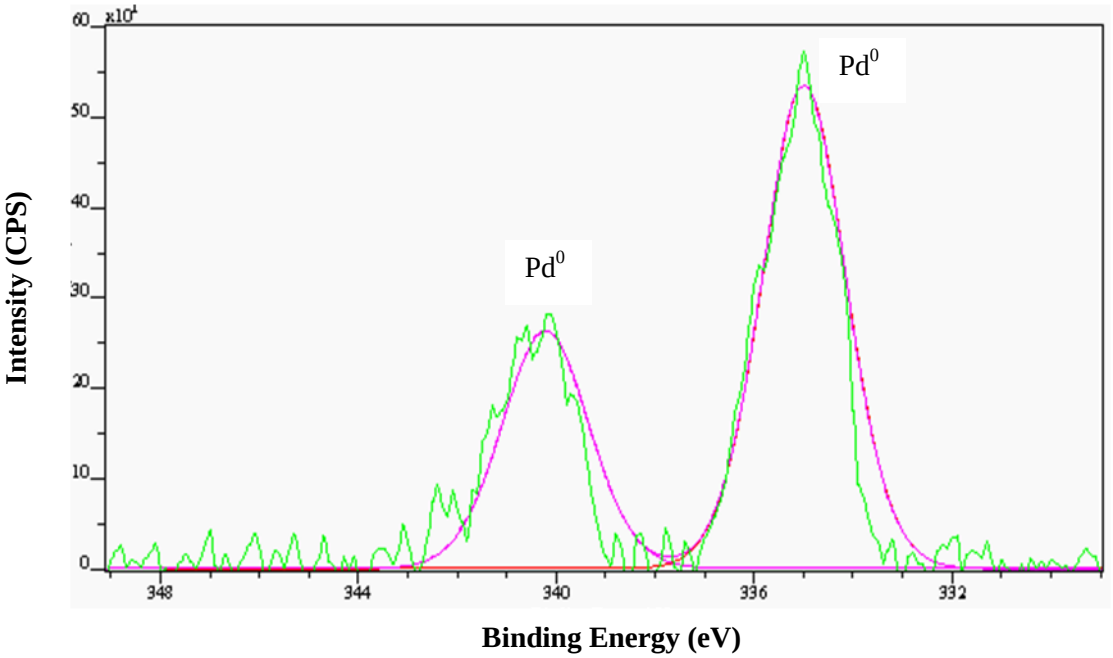

Figure 4.14 Binding energies of ED-Pd/TiO_2 non-Sn

4.2.4 Transmission Electron Microscopy (TEM)

TEM micrograph is a useful tool for measuring the size of palladium particle, crystallite size, and size of distribution of supported metals. The TEM micrograph is used for determination of micro-texture and microstructure of the Pd/TiO_2 catalysts in this study.

The TEM micrographs of the original commercial titanium dioxide support are shown in Figure 4.15. The average particle size of titanium dioxide measured from TEM images was found to be in the range of 100-150 nm.

Figure 4.16 shows the TEM micrographs of titanium dioxide after activated in Pd/Sn solution. Pd metal with average particle size 5 nm was observed on the titania support. Palladium is used to make the catalyst active for electroless plating deposition. Sn not only acts as the reducing agent for palladium ions to palladium metal as shown in the following redox reaction [57]

$$Pd^{2+} + Sn^{2+} \rightarrow Pd + Sn^{4+}$$

but it is also claimed to stabilize the palladium metals via a strong Sn^{4+} adsorption [57].

Figure 4.17 shows the TEM micrographs of Pd/TiO_2 prepared by electroless plating in palladium plating bath for 1 hr at $50^{o}C$ with ultrasonic vibration. From the TEM images, Pd particles having average particle sizes of 2-5 nm were observed with a good Pd dispersion on the titania support.

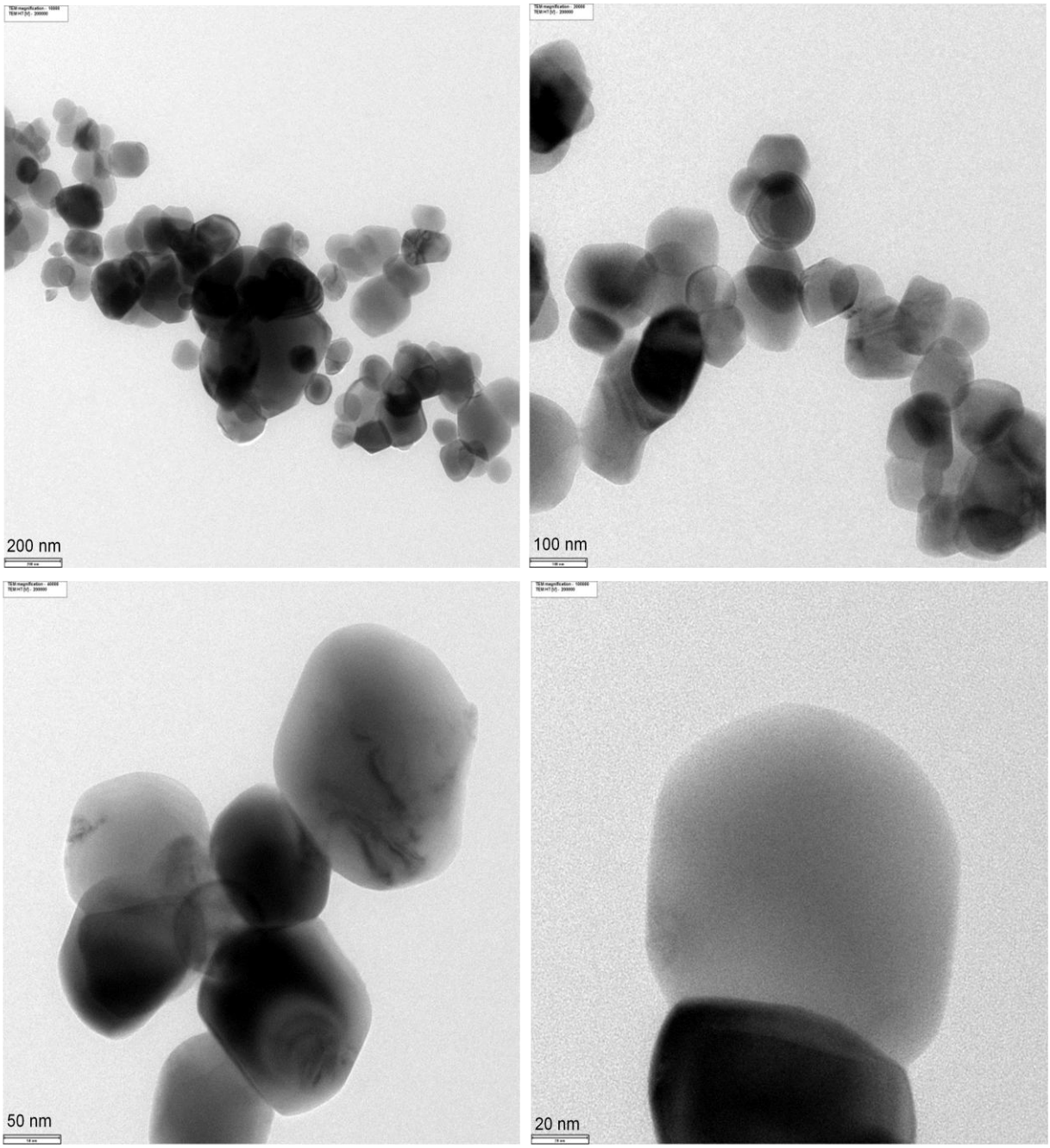

Figure 4.15 TEM micrographs of titanium dioxide support (commercial Fluka)

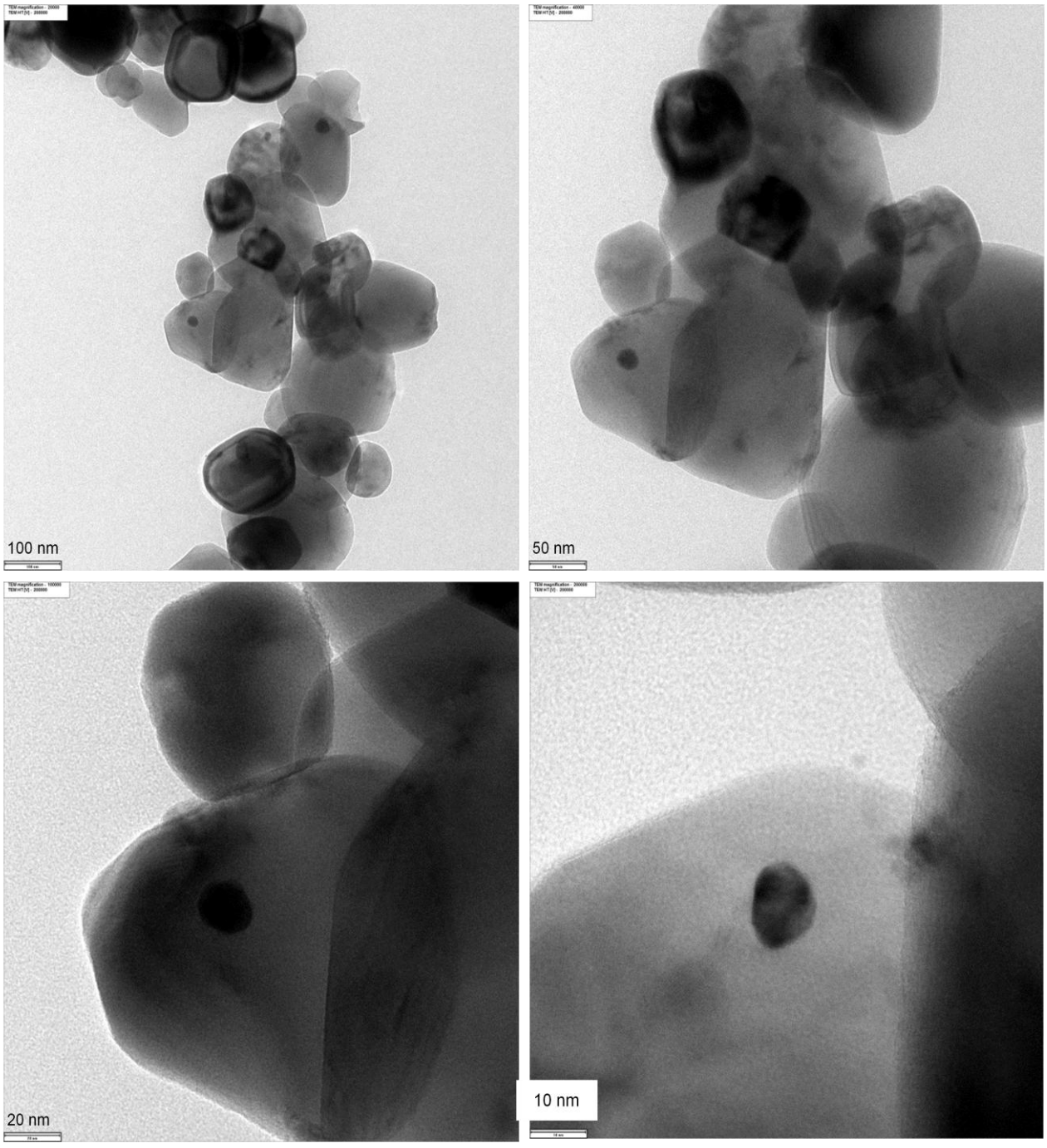

Figure 4.16 TEM micrographs of titanium dioxide activated in Pd/Sn solution

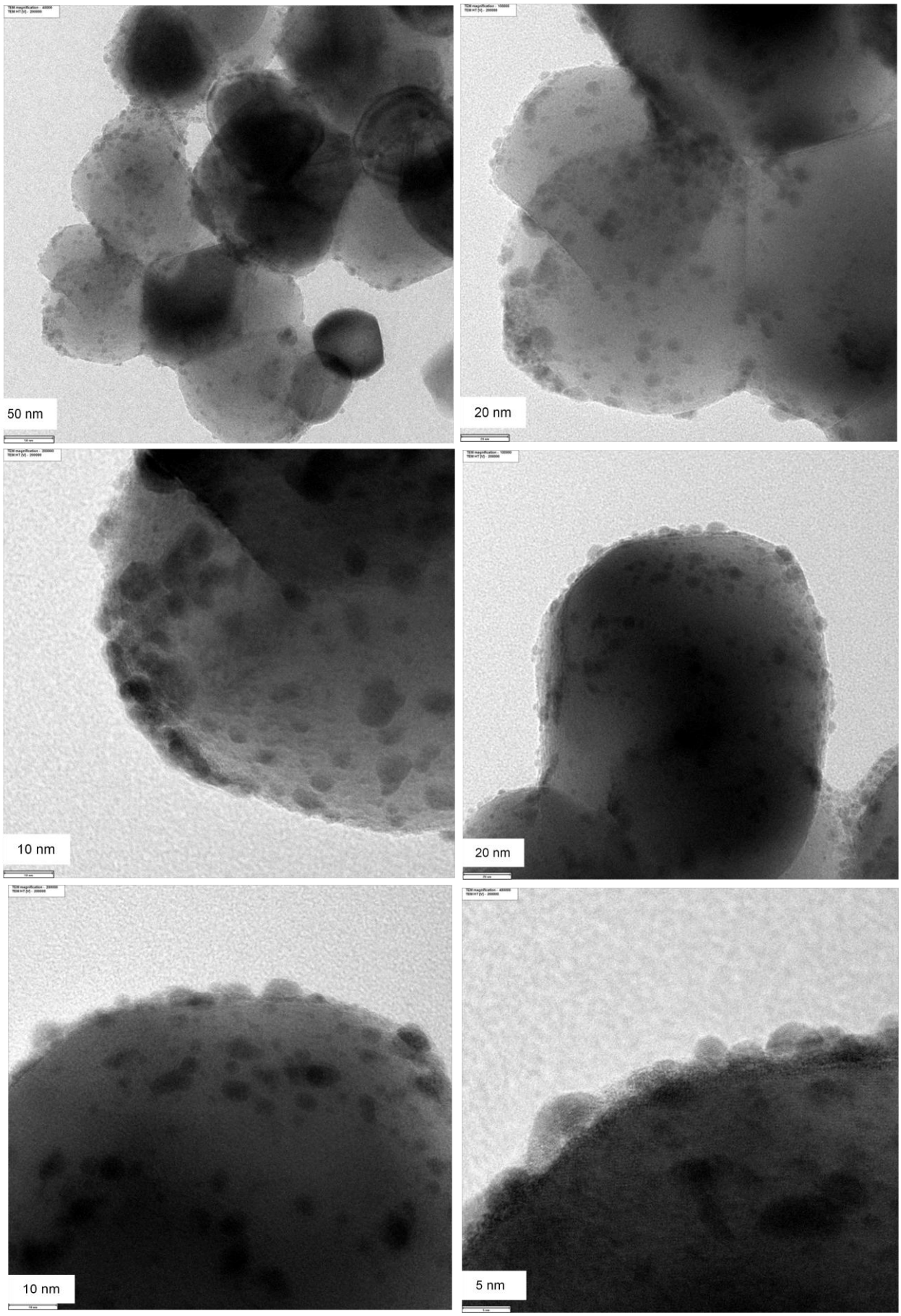

Figure 4.17 TEM micrographs of ED-Pd/TiO_2 Sn

Figure 4.18 shows the TEM micrographs of titania activated in Pd solution and reduced in sodium hypophosphite (non-Sn) followed by cleaning two times with distilled water, precipitated to remove excess distilled water, and then dried at 110 ^{o}C for 24 hr. From Figure 4.18, Pd metals in spherical shape with average size around 5-15 nm were observed.

From the Figure 4.16 and Figure 4.18, the average sizes of Pd metals between Pd/Sn activated and non-Sn activated for palladium electroless deposition were not significantly different.

Figure 4.19 shows the TEM micrographs of Pd/TiO_2 non-Sn activated prepared by electroless plating in palladium plating bath. Form Figure 4.19, the Pd particles of the ED-Pd/TiO_2 non-Sn show average sizes of 60-80 nm which were much larger than the Pd particles in Figure 4.17 (Sn activated) and poor Pd dispersion was observed on the titania support.

From the TEM micrographs Figure 4.17 - Figure 4.19, it can be summarized that the particle size of Pd metals of the electroless Sn catalysts was smaller than the palladium electroless non-Sn catalysts. It may be due to the effect of Sn in the activated process where Sn was claimed to stabilize the palladium metal through a strong Sn^{4+} adsorption that generates a well-dispersed Pd/TiO_2 catalysts. The actual amounts of Pd on the TiO_2 support were determined using the inductive coupled plasma optical emission spectrometer (ICP-OES).

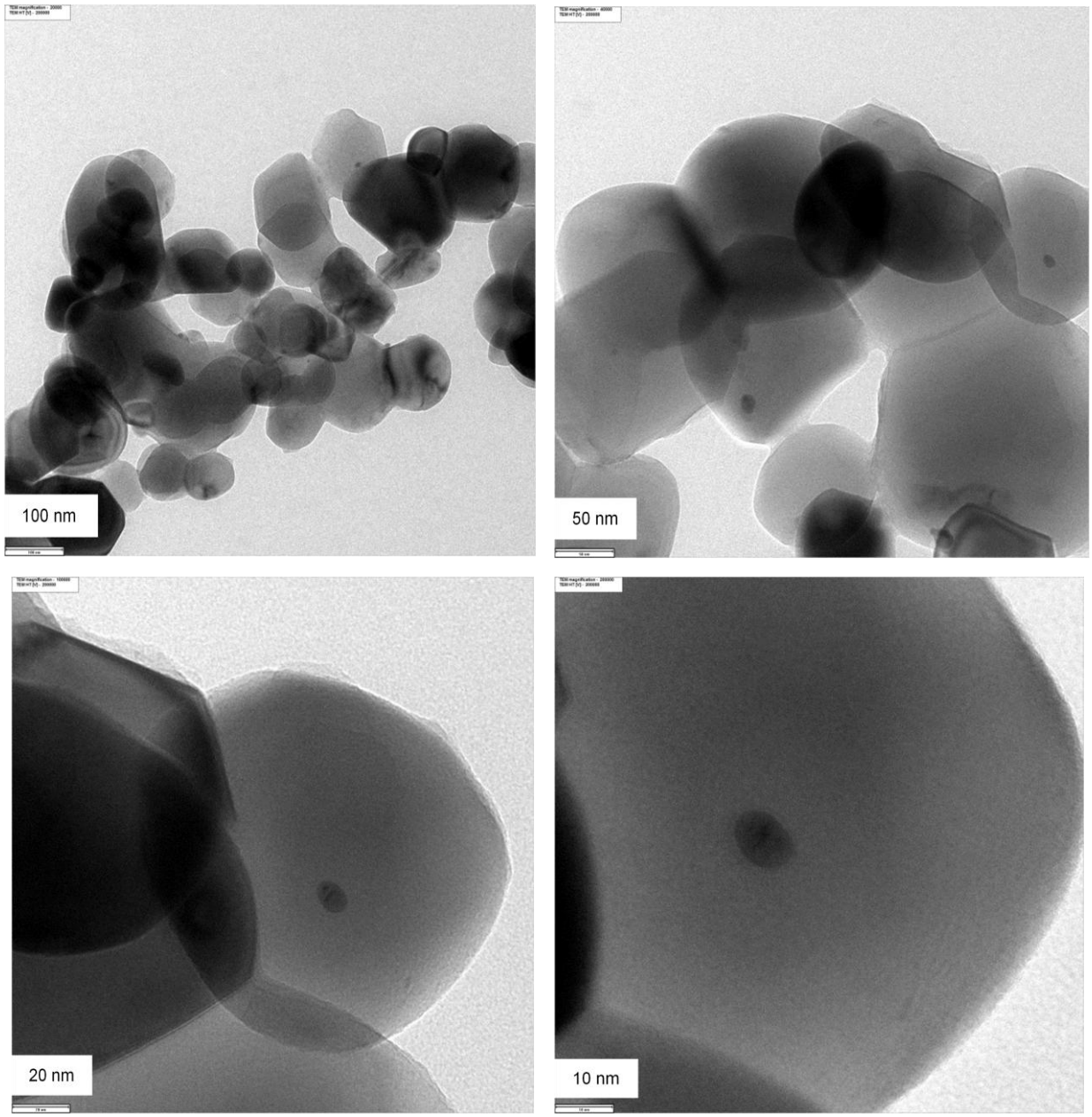

Figure 4.18 TEM micrographs of titanium dioxide activated in Pd/NaH_2PO_2 (non-Sn) solution

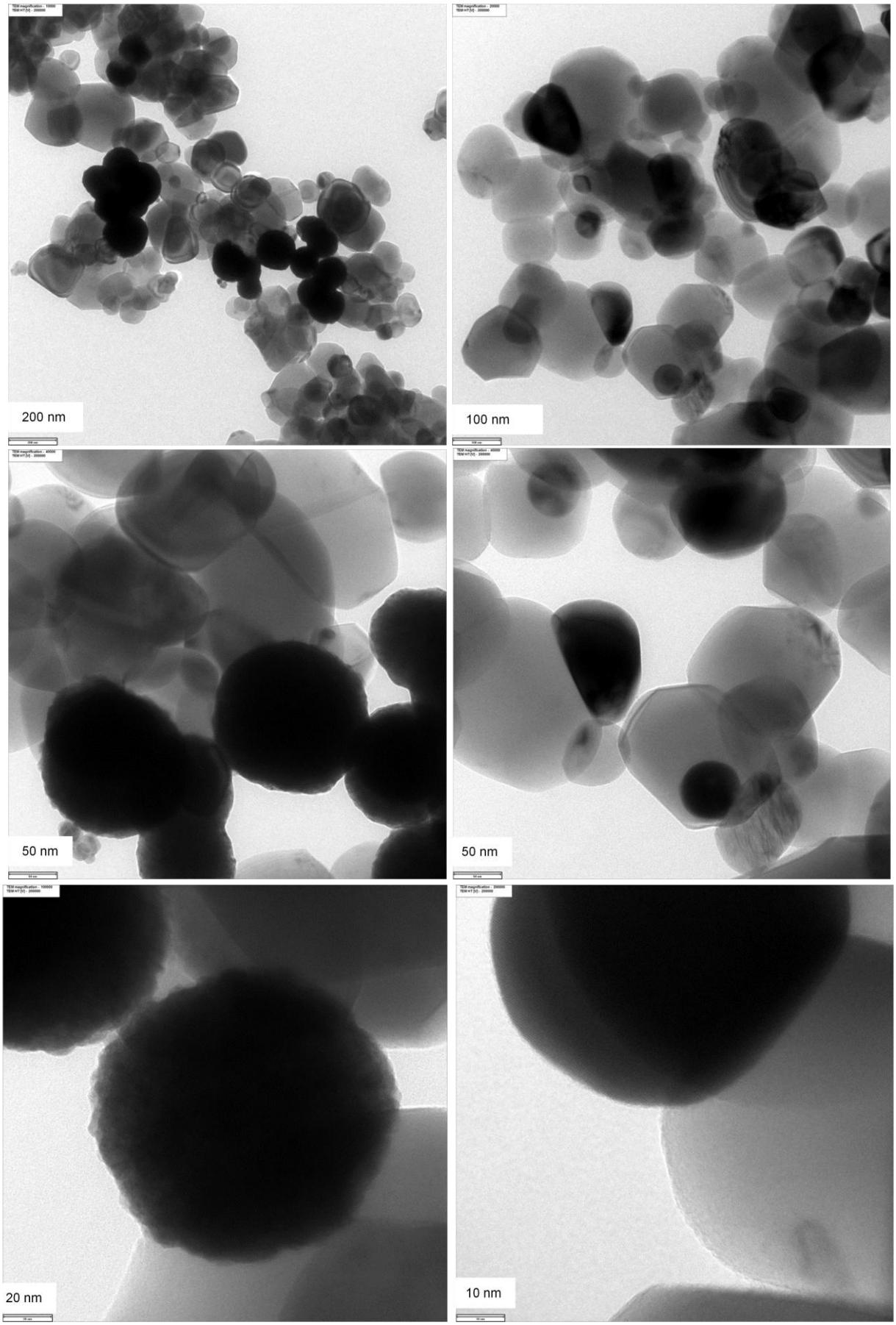

Figure 4.19 TEM micrographs of ED-Pd/TiO_2 non-Sn

4.2.5 Inductive coupled plasma optical emission spectrometer (ICP-OES)

In this study, the actual amounts of palladium loading before and after electroless deposition were determined by the inductive coupled plasma optical emission spectrometer and the results are given in Table 4.2. All the catalysts were prepared with Pd loading of 12 wt%. However, the actual amount of Pd on the Pd/TiO_2 catalysts after electroless was lower than the desired amount. The results form Table 4.2 indicated that some of Pd was leached during the electroless preparation process. The catalyst prepared using Sn in the activation process showed higher Pd content at 0.15 wt% after activated and Pd content at 5.41 wt% after palladium plating. The Pd content of the catalyst prepared with Sn in the activation process was about two times higher than those obtained from the catalyst prepared by non-Sn activation.

In the electroless deposition process, the surface has to be chemically roughened by acid or base to enhance mechanical cohesion between palladium and the substrate [4]. However, in this study Pd electroless deposition on titania by a non-Sn activated process has poor adhesion of Pd on the titania probably because the titania support is highly resistant to chemical attack. The catalysts prepared by electroless deposition non-Sn activation also show lower palladium content than the Sn activated due probably to the weak-interaction between palladium and titania support.

Table 4.2 Actual amounts of palladium in the catalysts before and after electroless deposition

Sample	palladium content (wt %)
TiO_2 activated Sn	0.16
TiO_2 activated non-Sn	0.08
ED-Pd/TiO_2 Sn	5.41
ED-Pd/TiO_2 non-Sn	2.75

The results form ICP-OES indicated that the actual amount of Pd on the titania support from non-Sn activated electroless deposition (2.75 wt%) were less than that prepared by Sn activated (5.41 wt%). In order to better compare their catalytic properties in the selective hydrogenation of 3-hexyne-1-ol, 1 wt% Pd/TiO2 were prepared by electroless deposition using Sn and non-Sn activated processes.

The use of centrifuge in cleaning and precipitation after electroless has shown to improve the amount of Pd deposited on the titania support. With this technique, the ED-1% Pd/TiO_2 Sn, ED-1% Pd/TiO_2 non-Sn, and IMP-1% Pd/TiO_2 were prepared and characterized by using several techniques such as SEM, EDX, XPS, and TEM. The catalytic performances were evaluated in the liquid-phase selective hydrogenation of 3-hexyne-1-ol at 40 ºC.

4.2.6 Scanning electron microscopy (SEM)

Figure 4.20 shows the SEM micrograph of ED-1% Pd/TiO_2 Sn. Figure 4.21 shows the SEM micrograph of ED-1% Pd/TiO_2 non-Sn and Figure 4.22 shows the SEM micrograph of the catalysts prepared by incipient wetness impregnation method (IMP-1% Pd/TiO_2).

From the SEM micrographs in Figure 4.20-4.22, there were no significantly differences in the particle sizes and morphology of the Pd/TiO_2 catalysts prepared by either impregnation or electroless deposition. The SEM micrograph shows the granule average sizes were about 0.2-0.6 µm with the spherical and polyhedral shapes. In addition, the granule particles of all Pd/TiO_2 catalyst were attached in form of small group with a size of 50-70 µm. It would appear that the shape and size of granule particle morphology of all the catalysts did not depend on the preparation methods.

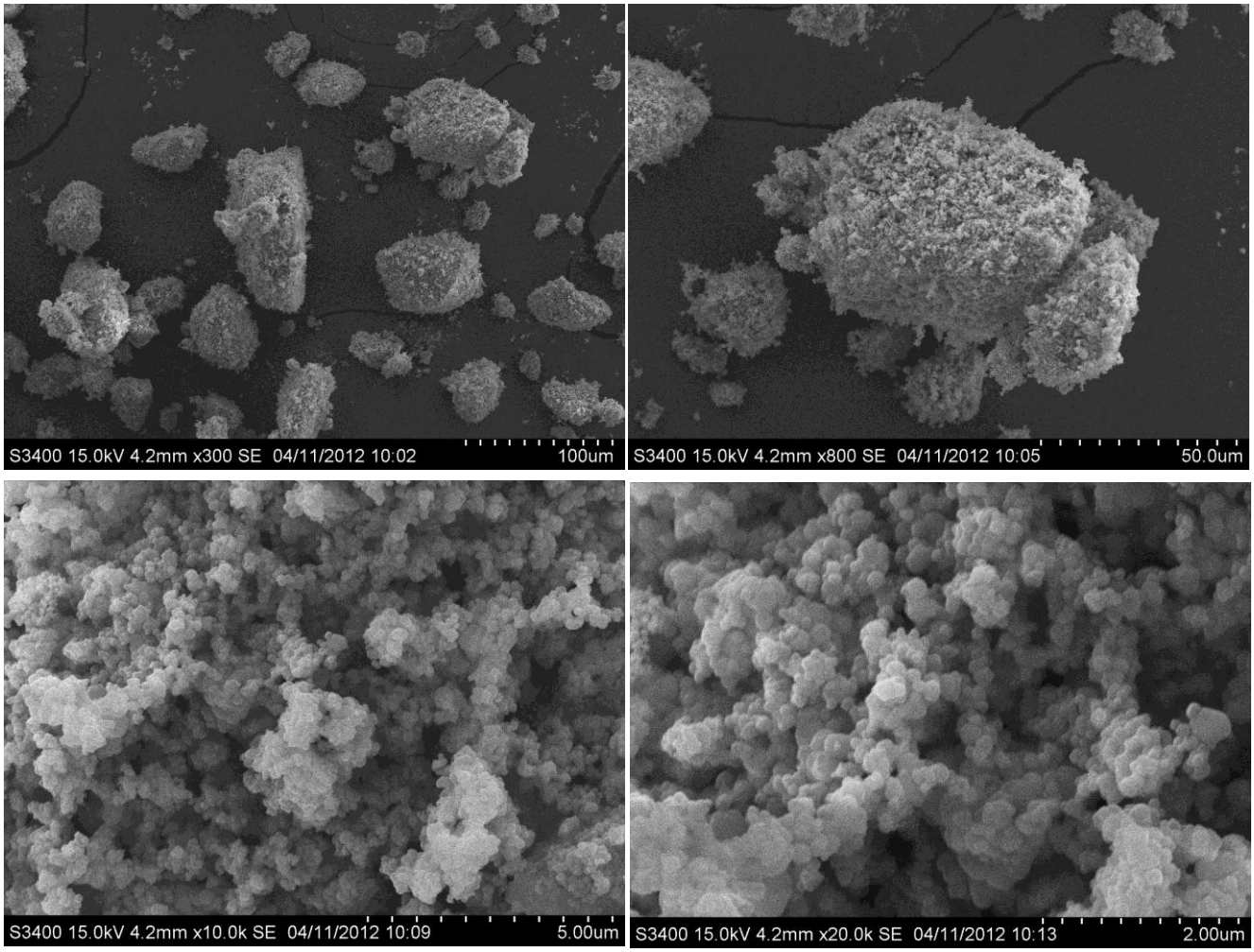

Figure 4.20 SEM Micrographs of ED-1% Pd/TiO_2 Sn

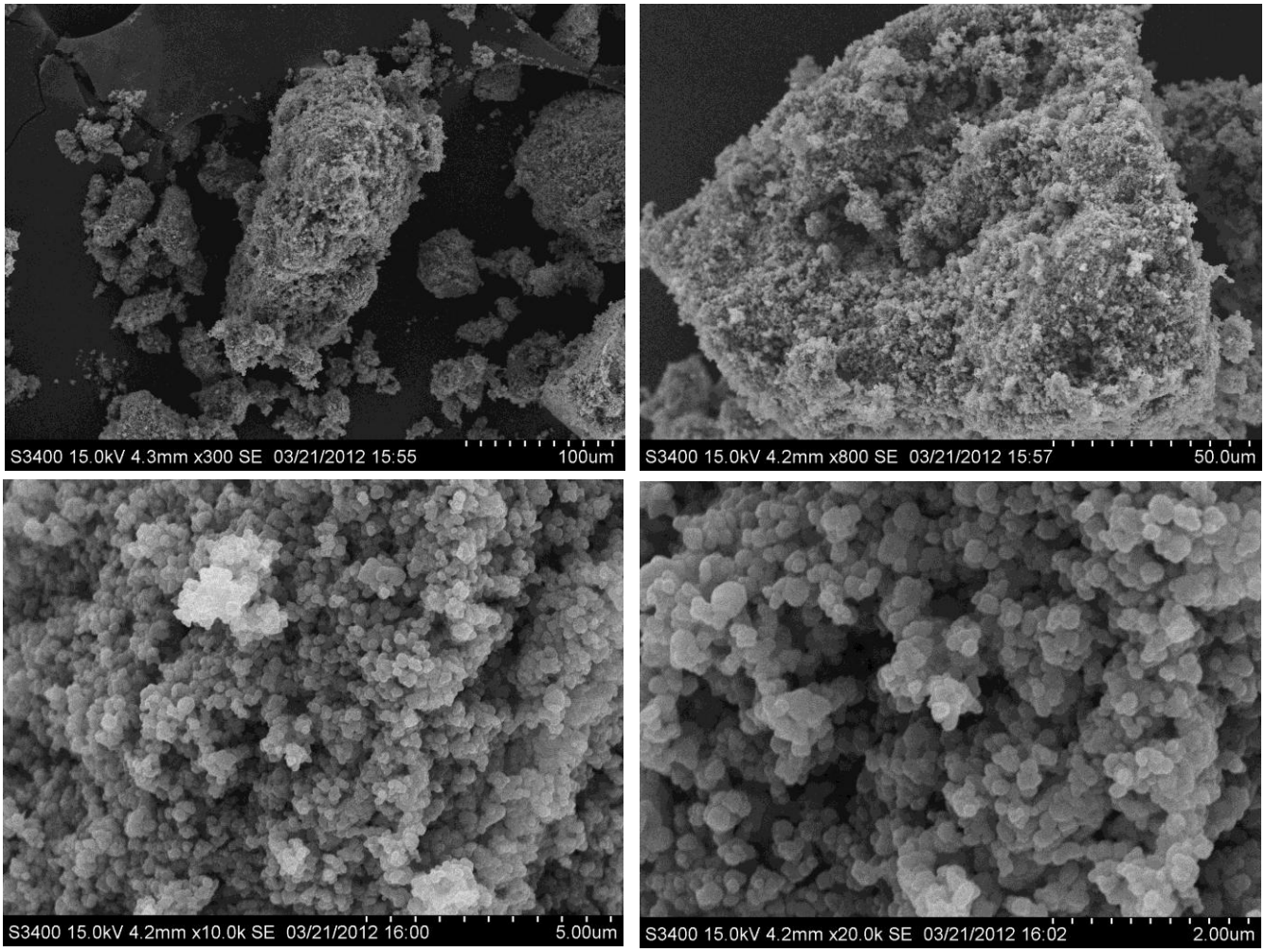

Figure 4.21 SEM Micrographs of ED-1% Pd/TiO_2 non-Sn

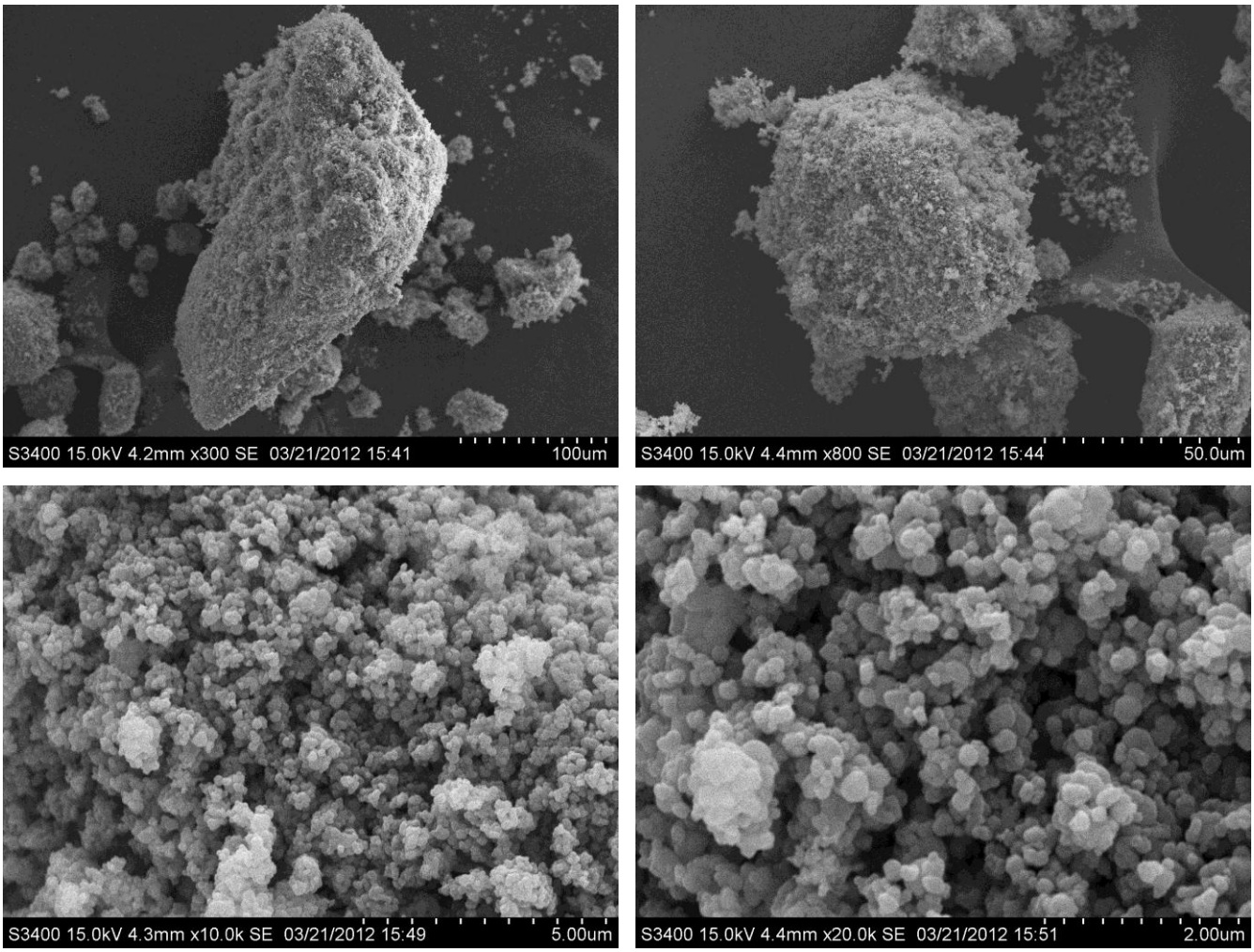

Figure 4.22 SEM Micrographs of IMP-1% Pd/TiO_2

4.2.7 EDX mappings

The EDX elemental mapping techniques are a graceful alternative to spotting experiment. The distributions of the palladium on the various Pd/TiO_2 catalysts from EDX mappings are shown in Figure 4.23 (a)-(c).

Figure 4.23 (a) shows the EDX elemental mapping of ED-1% Pd/TiO_2 Sn. Figure 4.23 (b) shows the EDX elemental mapping of ED-1% Pd/TiO_2 non-Sn and Figure 4.23 (c) shows the EDX elemental mapping of IMP-1% Pd/TiO_2 prepared by incipient wetness impregnation method.

The EDX palladium mapping of the catalysts in Figure 4.23 (a)-(c) shows a good distribution of Pd on the titania support. However, in Figure 4.23 (a) ED-1% Pd/TiO_2 Sn shows high intensity of Pd than the other catalysts, indicating higher amount of Pd on the TiO_2 support.

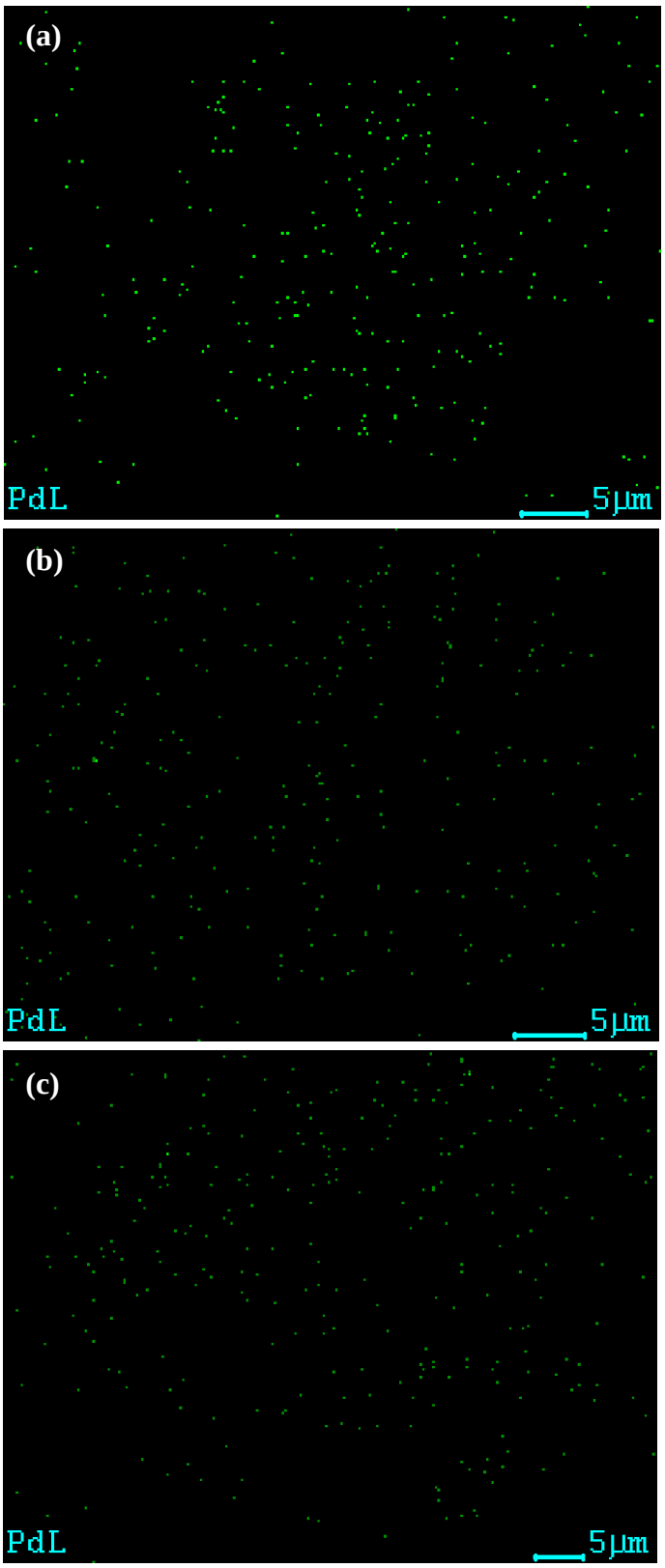

Figure 4.23 EDX elemental mapping of **(a)** ED-1% Pd/TiO_2 Sn, **(b)** ED-1% Pd/TiO_2 non-Sn and **(c)** IMP-1% Pd/TiO_2

4.2.8 X-Ray Diffraction (XRD)

The XRD patterns of ED-1% Pd/TiO_2 Sn, ED-1% Pd/TiO_2 non-Sn, and IMP-1% Pd/TiO_2 were measured at the 2θ degrees between 20º and 80º and the results are shown in Figure 4.24.All the catalyst samples did not exhibit the XRD characteristic peaks of Pd^0 or PdO due probably to the low amount of Pd present (1 wt%).

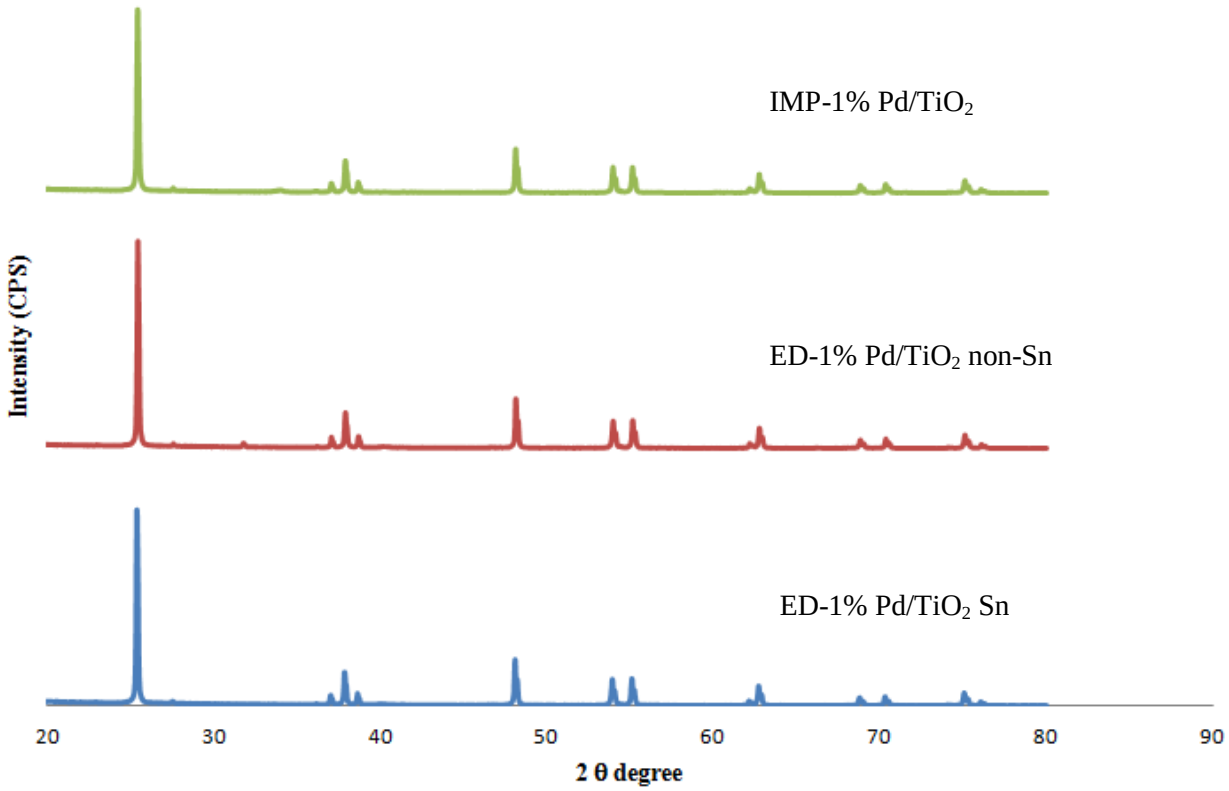

Figure 4.24 XRD patterns of ED-1% Pd/TiO_2 Sn, ED-1% Pd/TiO_2 non-Sn and IMP 1% Pd/TiO_2

4.2.9 Transmission Electron Microscopy (TEM)

TEM micrographs were also taken for the ED-1% Pd/TiO_2 Sn catalysts and compared to IMP 1% Pd/TiO_2 as shown in Figure 4.25 - Figure 4.26. Typically, higher amount of Pd loading on the support leads to larger metal particles and lower metal dispersion. However, comparing the electroless deposition catalysts with different amounts of Pd loading (Figure 4.17 and Figure 4.25), the Pd particle sizes were found to be similar at around 2-10 nm.

Figure 4.26 shows the TEM micrographs of 1% Pd/TiO_2 prepared incipient wetness impregnation method. In the most cases, Pd particle sizes of about 15-40 nm on the titania support were observed. From the TEM micrographs, the Pd metal particles size of the catalysts prepared by the electroless deposition Sn were smaller than the catalysts prepared by the incipient impregnation method.

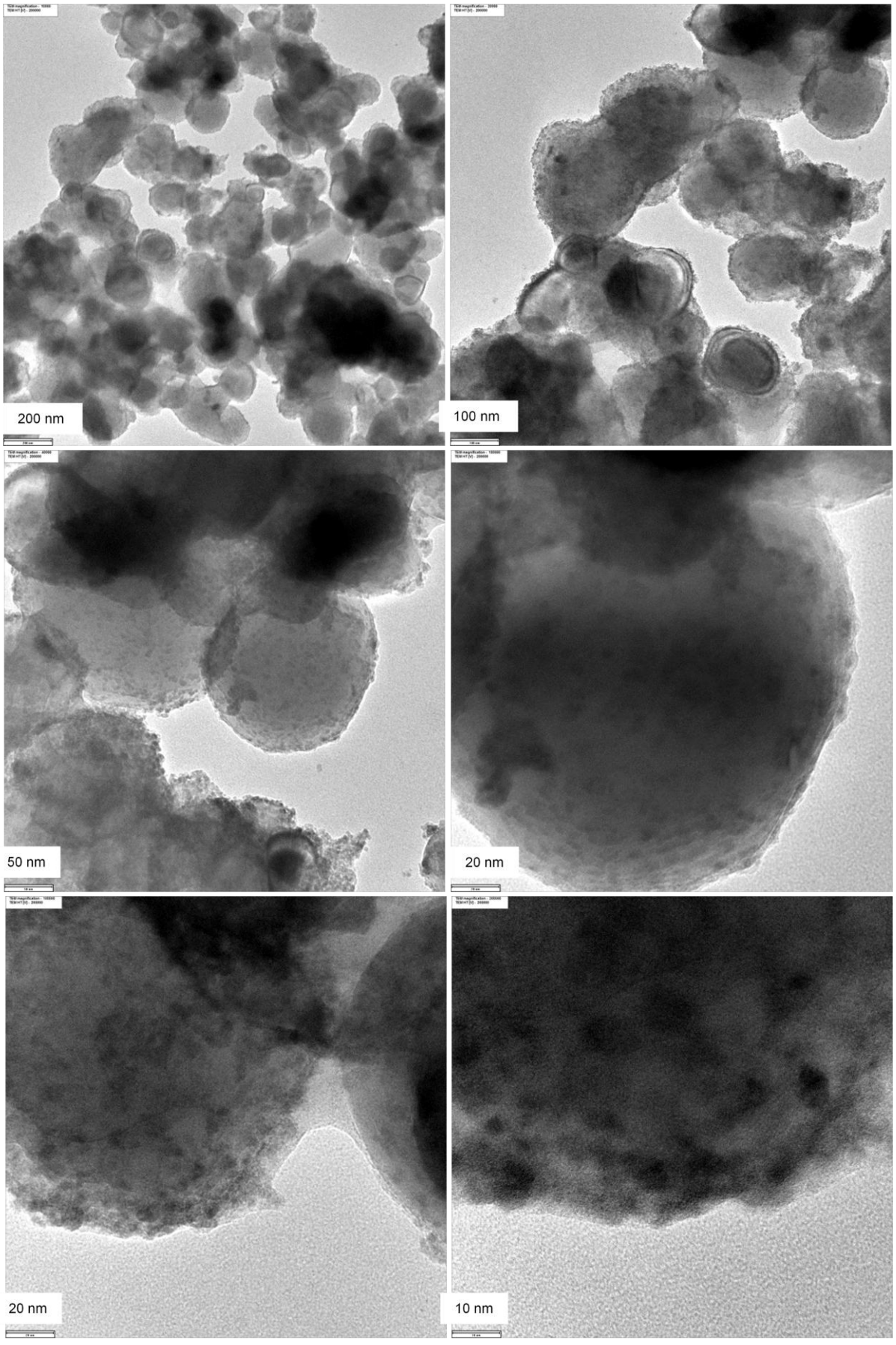

Figure 4.25 TEM micrographs of ED-1% Pd/TiO_2 Sn

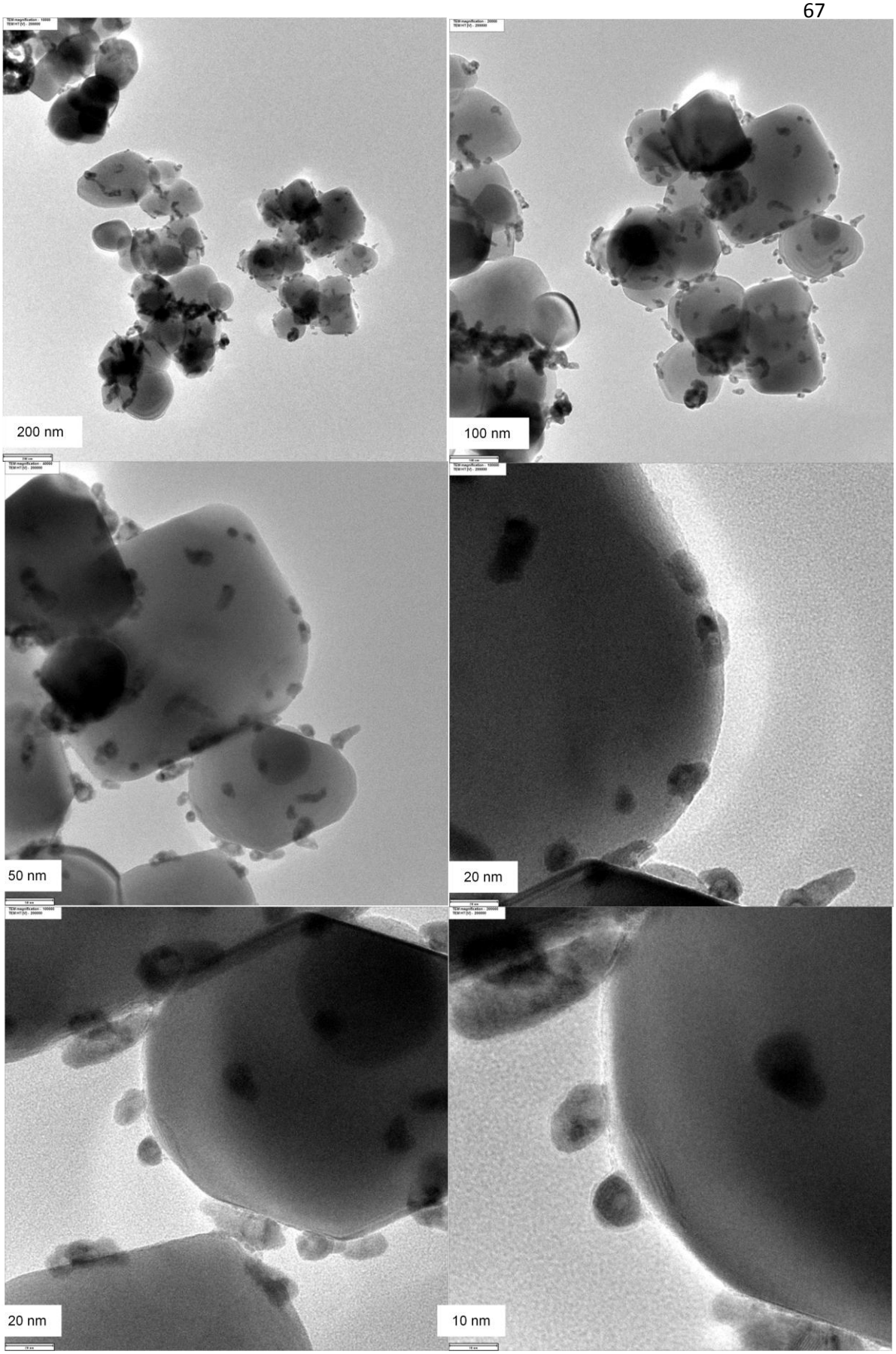

Figure 4.26 TEM micrographs of 1% Pd/TiO_2 incipient wetness impregnation method

4.2.10 CO-Pulse Chemisorptions

The amount of metal active sites Pd on the catalyst was measured by chemisorptions technique. All the catalysts were calcined at 450 ºC in air for 1 hr and reduced at 40 ºC for 2 hr. The calculation of Pd for CO chemisorptions has an assumption that one CO molecule adsorbs on the Pd site (CO/Pd is equal to 1) [59]. The results of Pd active sites are given in Table 4.3.

From the CO chemisorptions results, it was found that the Pd/TiO_2 electroless Sn (5.41 %wt) gave the highest CO chemisorptions about 4.19 x 10^{18} molecule CO/g.cat. The % Pd dispersion was 1.58 and the average particles size of Pd was calculated to be about 13.1 nm, which was in accordance to the TEM micrographs results. The active sites of ED-Pd/TiO_2 Sn catalysts decreased from 4.19 x 10^{18} to 0.65 x 10^{18} molecule CO/g.cat while %Pd dispersion increased from 1.58 to 3.76 % as the Pd contents decreased from 5.41 %wt to 1 %wt. It was clearly seen that the lower amount of Pd content gave the high values of %Pd dispersion on the support.

In addition, for a similar amount of Pd content (1 %wt) the dispersion of Pd on titania support varied in order of ED-Pd/TiO_2 Sn > IMP-Pd/TiO_2 > ED- Pd/TiO_2 non-Sn. The average particle sizes of ED-Pd/TiO_2 Sn (10-15 nm) were smaller than the particle size of Pd prepared impregnation and elecroless non-Sn. The calculated average particle sizes of Pd on the titania from the CO chemisorptions technique were in good agreement with the TEM analysis.

The results suggest that the catalysts prepared by electroless Sn achieve a good dispersion of Pd on the support and uniform of Pd particle sizes. It has been reported that Sn which was used in activated process was well-adsorbed onto most substrates. It was claimed to stabilize the Pd particles during the activation process so that a good dispersion of Pd on support was achieved [60-61].

Table 4.3 The amount of CO-chemisorptions of eleectroless deposition and impregnated catalysts with different Pd loading

Catalysts	**CO chemisorptions (x 10^{-18} molecule CO/g cat.)**	**Pd dispersion (%)**	**particle size d_p Pd^0 (nm)**
ED-5.41 % Pd/TiO_2 Sn	4.19	1.58	13.1
ED-2.75% Pd/TiO_2 non-Sn	2.21	1.25	32.5
IMP-1% Pd/TiO_2	1.67	3.11	36.1
ED-1% Pd/TiO_2 Sn	0.65	3.76	10.7
ED-1% Pd/TiO_2 non-Sn	0.46	2.39	43.7

4.2.11 Reaction study of liquid phase selective hydrogenation of 3-hexyne-1-ol

The catalytic performance of the Pd/TiO_2 catalysts was evaluated in the liquid-phase selective hydrogenation of 3-hexyne-1ol in ethanol at 40 ºC and H_2 pressures 2 bars for 10-60 minute in a batch-type 50 ml stainless steel reactor. The effect of mass transfer on the reaction rate was neglect by using the maximum speed (1000 rpm) of stirrer. The amount of catalyst was 10 milligram for all cases. The products were analyzed by gas chromatography with flame ionization (GC-FID).

The products of liquid phase hydrogenation of 3-hexyne-1-ol are shown in Scheme 1. The fragrance leaf alcohol (cis-3-hexene-1-ol) is the desired product which was produced via the cis- selective hydrogenation of 3-hexyne-1-ol. The other by-products from this reaction include tran-3-hexene-1-ol and hexanol.

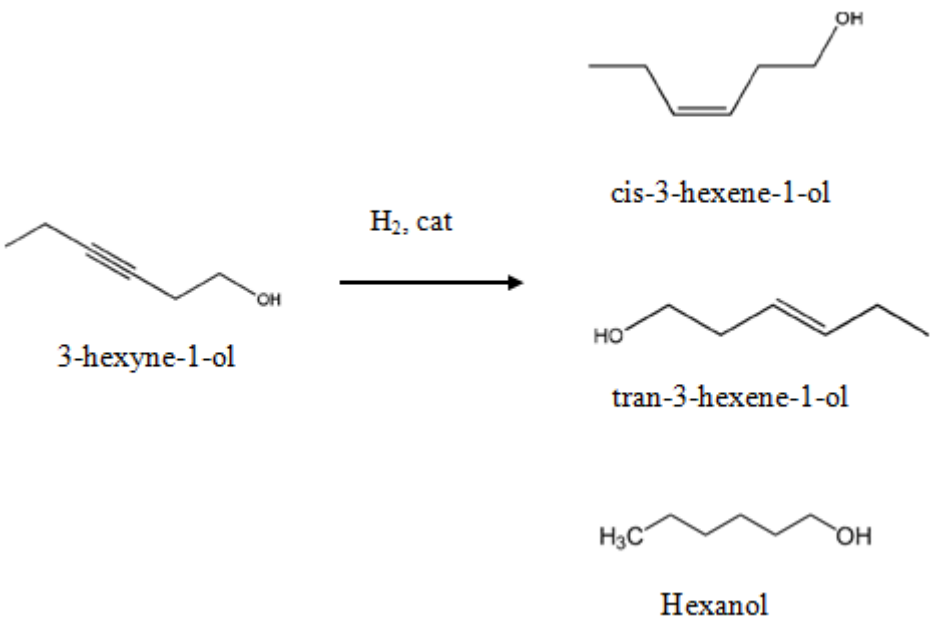

Scheme 1. Hydrogenation reaction of 3-hexyne-1-ol. [62]

The conversion of 3-hexyne-1-ol versus reaction time from 10-60 minutes by using different catalysts is shown in Figure 4.27. The X-axis shows the reaction time and Y-axis shows the % conversion of 3-hexyne-1-ol. Comparing the Pd/TiO_2 prepared by different methods, the ED-1% Pd/TiO_2 non-Sn and ED-Pd/TiO_2 non-Sn exhibited lower initial rates than IMP-1%Pd/TiO_2 due probably to the lower Pd metal active sites as shown by the results of CO chemisorption. For the electroless deposition catalysts with similar Pd loading, the hydrogenation rate of the ED-1% Pd/TiO_2 Sn was higher than the ED-1% Pd/TiO_2 non-Sn.

However, all the prepared catalysts exhibited % conversion of 3-hexyne-1-ol ≥80% after 30 minutes of reaction time. Concerning the selectivity to the desired product, cis-3-hexene-1-ol, IMP-1% Pd/TiO_2 catalyst with the highest hydrogenation rate showed very poor selectivity of cis-3-hexene-1-ol. The higher hydrogenation may cause an over-hydrogenation of cis-3-hexene-1-ol to hexanol.

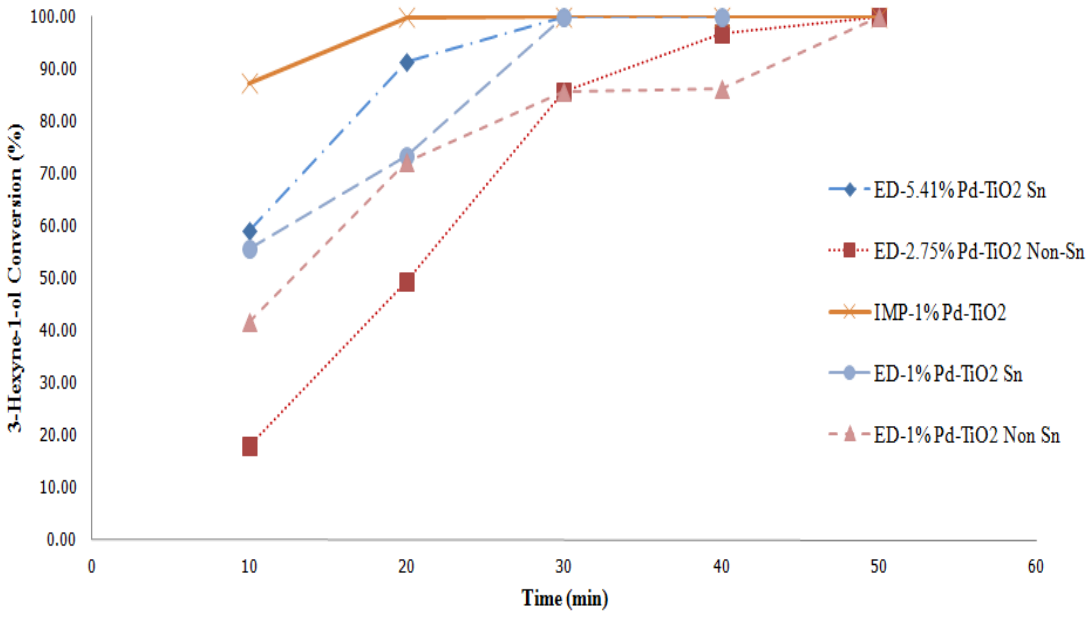

Figure 4.27 Conversion of Pd/TiO_2 catalysts in liquid phase selective hydrogenation of 3-hexyne-1-ol at 40 ºC, H_2 pressure 2 bars

The selectivity of cis-3-hexene-1-ol as a function of reaction time of the electroless made catalysts (Sn activated and non-Sn activated) and the impregnation catalyst are shown in Figure 4.28. From the Figure 4.27, it is shown that the hydrogenation rate of 3-hexyne-1-ol of the impregnated made was greater than the electroless Sn and electroless non-Sn made catalysts. However, the selectivity of cis-3-hexene-1-ol as shown in Figure 4.28 of the impregnated made dropped rapidly after the conversion reached 100 % after 20 minutes reaction time. The selectivity profiles were different for the electroless made catalysts in which the selectivity of cis-3-hexene-1-ol remained $\geq$ 60% at complete conversion of 3-hexyn-1-ol. It has been often been reported that Pd metal particle size and metal dispersion affect the hydrogenation activity in alkyne hydrogenation. For example, Mastalir et al. [63] reported that the catalytic activity of Pd/MCM-41 in the liquid phase semihydrogenation of various alkynes (phenylacetylene, 3-butyne-1-ol, 4-octyne, and 1-phenyl-1-butyne) was dependent on the Pd particle size in which larger Pd particle showed higher activity. In contrast, the selectivity of alkene formation was irrespective of the particle diameter for most reactants. The substantial cis-stereoselectivities and the limited over hydrogenation observed for the Pd-MCMs were attributed to the predominance of high-coordination terrace sites as the active species. For the low-coordination sites, the residence time of alkyne tends to be longer and the concentration of surface hydrogen is higher, resulting in low alkene selectivity [64].

For the semihydrogenation of 3-hexyne-1-ol, Roelofs et al. [62] reported 91% selectivity of cis-hexene-1-ol at > 95% conversion of 3-hexyne-1-ol over poly(N-vinyl-2-pyrrolidone)-stabilized Pd-nanoclusters supported on hydrotalcite. The remarkable catalytic performance in the selective hydrogenation of 3-hexyn-1-ol was ascribed to both the influence of the protecting polymer PVP as well as the nature of the support. Bonnemann et al. [65] also reported the use of surfactant for Pd colloidal stabilization for the semihydrogenation of 3-hexyne-1-ol. Poor selectivity of cis-alkene was observed on the catalysts with short-chained surfactant due to weak stabilization giving rise to the agglomeration of large Pd-particles.

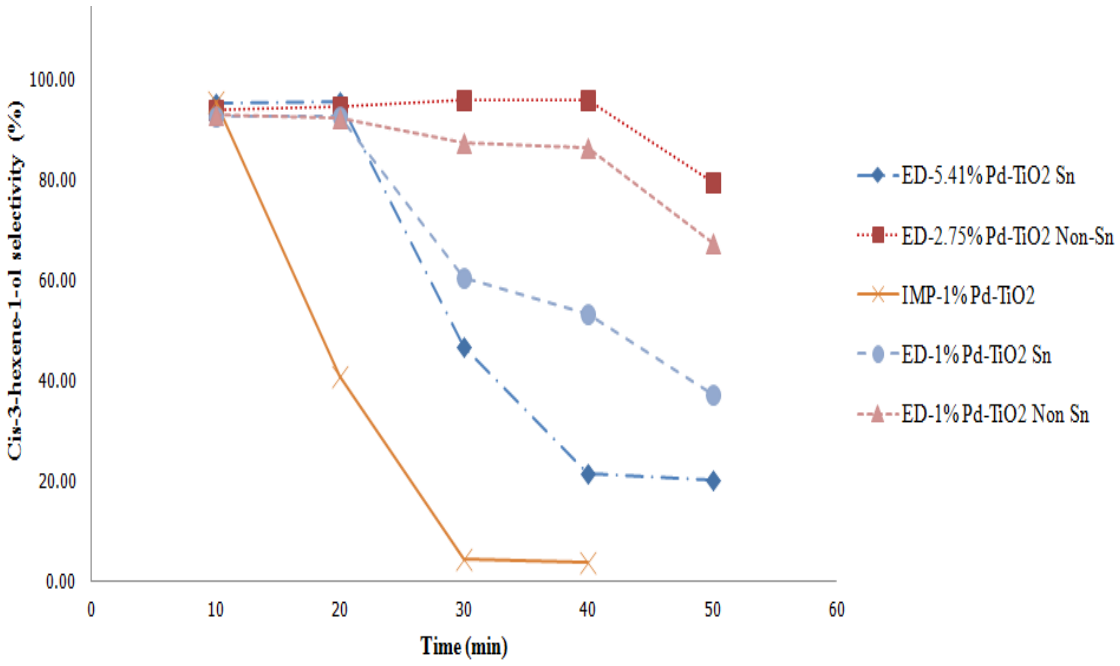

Figure 4.28 Selectivity of Pd/TiO_2 catalysts in liquid phase selective hydrogenation of 3-hexyne-1-ol at 40 ºC, H_2 pressure 2 bars

Figure 4.29 shows the performance of Pd/TiO_2 catalysts in the liquid phase selective hydrogenation of 3-hexyne-1-ol. Although, the 1% Pd/TiO_2 impregnation showed the highest initial conversion of 3-hexyne-1-ol but the selectivity of the desired product cis-3-hexen-1-ol was very poor. The selectivity of cis-3-hexen-1-ol at complete 3-hexyne-1-ol conversion was found to be in the order: ED-2.75% Pd/TiO_2 non-Sn > ED-1% Pd/TiO_2 non-Sn > ED-1% Pd/TiO_2 Sn > ED-5.4% Pd/TiO_2 Sn > IMP-1% Pd/TiO_2. In the present work, large particle size (10-30 nm) and non-uniform distribution of Pd particles observed on IMP-1% Pd/TiO_2 led to very high hydrogenation activity but poor selectivity to cis-alkene. The Pd/TiO_2 catalysts prepared by electroless with non-Sn activation process also possessed very large Pd particle size (> 50 nm) but they exhibited low hydrogenation activity and high cis-selectivity can be obtained at complete conversion of 3-hexyne-1-ol (> 80%). The Pd/TiO_2 catalysts prepared by electroless with $SnCl_2$ showed high dispersion of small Pd particles (2-10 nm). They exhibited moderately high conversion and moderate cis-selectivity in the selective hydrogenation of 3-hexyne-1-ol to cis-hexene-1-ol. The

results reveal that the catalyst performance did not depend on solely the Pd particle size/dispersion. The different surface orientations/imperfection also played important role determining the activity and selectivity of the catalysts. The rate of cis-alkene hydrogenation decreased with decreasing the frequency of surface imperfections [66-67].

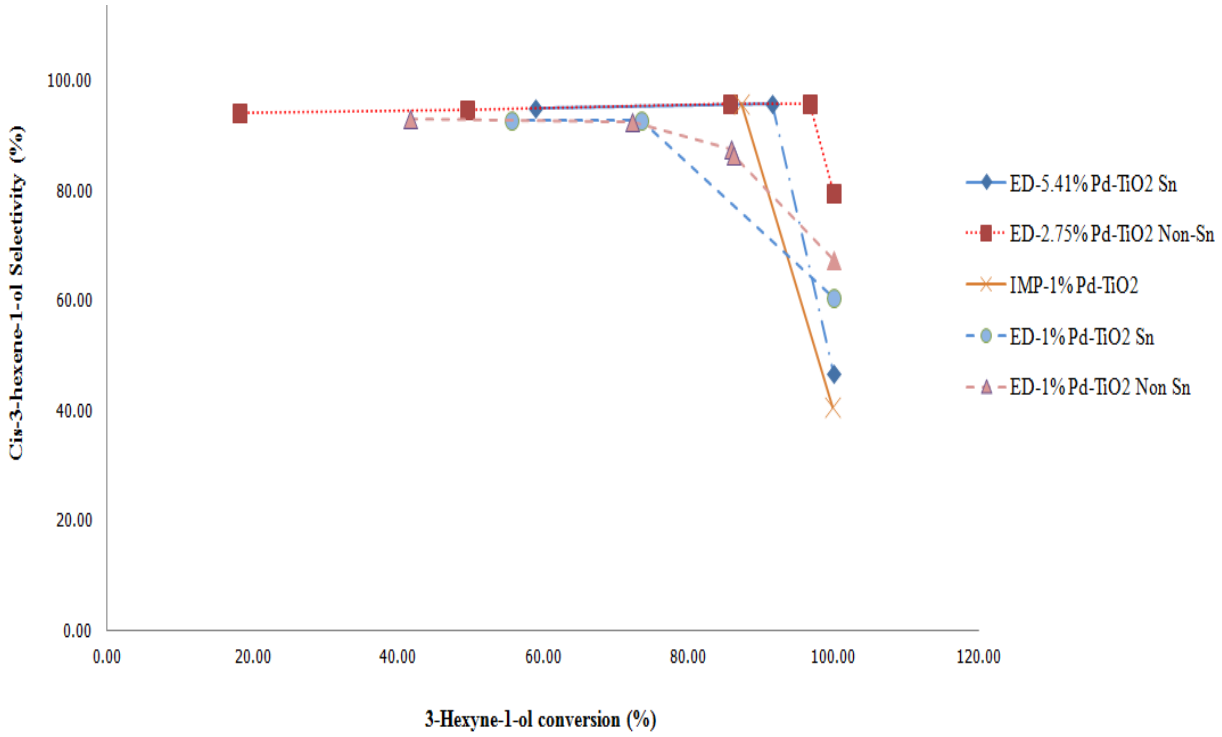

Figure 4.29 Selectivity and conversion of Pd/TiO_2 catalysts in liquid phase selective hydrogenation of 3-hexyne-1-ol at 40 ºC, H_2 pressure 2 bars

In this research**,** it is likely that preparation of Pd/TiO_2 catalysts by electroless deposition produced lower surface imperfections than the ones prepared by the conventional impregnation so that high cis-selectivity was obtained at relatively high conversion of 3-hexyne-1-ol.

CHAPTER V

CONCLUSIONS AND RECOMMENDATION

In this chapter is consisted of two sections, Section 6.1 shows the conclusions obtained from the experimental results and Section 6.2 is the recommendation for further study.

6.1 Conclusions

1. A tin-free activation process was developed for the preparation of Ni/PU foam and Pd/TiO_2 catalysts.
2. For the preparation of Ni/PU foam, the rate of deposition and the amount of Ni deposit were significantly increased with increasing amount of $PdCl_2$ during activation. The optimum conditions were determined to be (i) etching with 4M HCl for 1 hr (ii) activation with $PdCl_2$ solution 1.8 g/l, and (ii) plating time 60 min with sodium hypophosphite as a reducing agent. In addition, the nickel electroless bath did not decompose and can be reused by adding the nickel source components.
3. The morphology and mechanical properties of the Ni/PU foam prepared by electroless deposition with or without $SnCl_2$ activation were similar. In contrast, particle size and morphology of the Pd particles dispersed on TiO_2 powder were significantly dependent on the activation process. The non-Sn activation resulted in much larger Pd particle/cluster size than those of the electroless Sn.
4. The catalyst performances in the liquid-phase semihydrogenation of 3-hexyne-1-ol to cis-hexene-1-ol were improved in the order: ED-Pd/TiO_2 non-Sn > ED-Pd/TiO_2 Sn > Pd/TiO_2 impregnation. It is suggested that electroless deposition resulted in lower surface imperfections of the Pd/TiO_2 catalysts than the conventional impregnation technique.

6.2 Recommendations

1. Different support of electroless plating may be tried in order to confirm performance of a novel activation process (non-Sn).

2. The ED-1% Pd/TiO_2 non-Sn should be investigated using TEM technique to confirm the palladium particle sizes and morphology of the Pd particles dispersed on TiO_2 powder.

3. The surface imperfection of catalysts should be investigated using HRTEM technique.

REFERENCES

[1] B. Tian, and others. Modified electroless plating technique for preparation of palladium composite membranes. Master of science in engineering (2005) : 47–150.

[2] JN Keuler. Preparation and characterization of palladium composite membranes. Master of Engineering Thesis (1997) : 1–120.

[3] M. Charbonnier, M. Romand, Y. Goepfert, D. Leonard, F. Bessueille, M. Bouadi. Palladium (+2) reduction: A key step for the electroless Ni metallization of insulating substrates by a tin-free process. Thin Solid Films 515 (2006) : 1623–1633.

[4] M. Williams, C.A. Pineda-Vargas, E.V. Khataibe, B.J. Bladergroen, A.N. Nechaev. Surface functionalization of porous ZrO_2-TiO_2 membranes using γ-aminopropyltrietoxysilane in palladium electroless deposition. Applied Surface Science 254 (2008) : 3211–3219.

[5] X. Tang, M. Cao, C. Bi, L. Yan, B. Zhang, *Research on a new surface activation process for electroless plating on ABS plastic,* Materials Letters, 62 (2008) : 1089-1091.

[6] M. Palaniappa, S.K. Seshadri. Structural and phase transformation behaviour of electroless Ni–P and Ni–W–P deposits. Materials Science and Engineering A 460 (2007) : 638-644.

[7] T. ang, L. Zhang, D. Li, J. Yin, S. Wu, Z. Mao. Mechanical properties of polyurethane foam prepared from liquefied corn stover with PAPI. Bioresource Technology 99 (2008) : 2265-2268.

[8] J Eugene. Electroless deposition [online]. 2011. Available from : http://electrochem.cwru.edu/encycl/art-d02-eless-dep.htm [2011, December 7]

[9] R. Robege. Electroless metal coating [online]. 1999. Available from : http://corrosion-doctors.org/MetalCoatingfaces/Electroless.htm [2011, December 7]

[10] J. Shu, BPA Grandjean, A. Van Neste, *Canadian Journal of Chemical Engineering*, 69 (1999) : 1036-1060.

[11] A. William. Surface preparation for electroless nickel plating [online]. 1990. Available from : http://www2.bren.ucsb.edu/~dturney/port/papers /Electroless/07.pdf [2011, December 21]

[12] N. Feldstein. Electrochemical Science and Technology. Journal Electrochemical Society 121 (1974) : 738-744.

[13] F. Bessueille, S. Gout, S. Cotte, M. Romand. Selective metal pattern fabrication through micro-contact or Ink-Jet printing and electroless plating onto polymer surfaces chemically modified by plasma treatments. The journal of adhesion 85 (2009) : 690-710.

[14] G.O. Mallory, J.B. Hajdu. Electroless plating fundamentals and applications. American Electroplaters and Surface Finishers Society 1990 : 1.

[15] I Neissa. Bright nickel electroplating part 2 [online]. 2012. Available from : http://neissaindustries.com/2011/02/bright-nickel-electroplating-part-2/ [2011, December 8]

[16] W. Yang, S. Luo, B. Zhang, Z. Huang, X. Tang. Electroless preparation and characterization of magnetic Ni-P plating on polyurethane foam. Applied Surface Science 254 (2008) : 7427-7430.

[17] R Muhammad. Mechanical and failure properties of rigid polyurethane foam under tension [online]. 2007. Available from : http://ari3f.files.wordpress.com/2009/11/2007_ridha_m.pdf [2011, December 22]

[18] A. Fujishima, K. Hashimoto, T. Watanabe. TiO_2 photocatalysis fundamental and applications. 1 St ed. Tokyo: BKC (1999).

[19] Y. Li, B. Xu, Y. Fan, N. Feng, A. Qiu. The effect of titania polymorph on the strong metal-support interaction of Pd/TiO_2 catalysts and their application in the liquid phase selective hydrogenation of long chain alkadienes. Journal of Molecular Catalysis A: Chemical 216 (2004) : 107-114.

[20] E.M. McKenna, A. James, Anderson. Selectivity enhancement in acetylene hydrogenation over diphenyl sulphide-modified Pd/TiO_2 catalysts. Journal of Catalysis 281 (2011) : 231-240.

[21] W. Jia, L. Su, Y. Ding, A. Schempf. Pd/TiO_2 Nanofibrous Membranes and Their Application in Hydrogen Sensing. J. Phys.Chem.C 113 (2009) : 16402-16407.

[22] L. Su, W. Jia, A. Schempf, Yu Lei. Palladium/titanium dioxide nanofibers for glycerol electrooxidation in alkaline medium. Electrochemistry Communications 11 (2009) : 2199-2202.

[23] G. A. Willem, I. M. Robert, J. C. Neil. The selective hydrogenation of acetylene on palladium-carbon nanostructured catalysts. Applied Catalysis A : General 388 (2010) : 1-6.

[24] J. Rebelli, A. A. Rodriguez, S. Ma, J. R. Monnier. Preparation and characterization of silica-supported, group IB-Pd bimetallic catalysts prepared by electroless deposition methods. Catalysis Today 6824 (2010) : 1-9.

[25] S. Zoladek**,** A. R. Iwona **,** J. K. Pawa. Enhancement of activity of platinum towards oxidation of ethanol by supporting on titanium dioxide containing phosphomolybdate-modified gold nanoparticles. Applied Surface Science 257 (2011) : 8205-8210.

[26] Y. Tsuru, K. Mochinaga, Y. Ooyagi, F. R. Foulkes. Application of vapor-deposited carbon and zinc as a substitute for palladium catalyst in the electroless plating of nickel. Surface and Coatings Technology 169 (2003) : 116–119.

[27] Q. Zhang, M. Wu, W. Zhao. Electroless nickel plating on hollow glass microspheres. Surface & Coatings Technology 192 (2005) : 213-219.

[28] L. Luo, Y. Wu, J. Li, Y. Zheng. Preparation of nickel-coated tungsten carbide powders by room temperature ultrasonic-assisted electroless plating. Surface & Coatings Technology 206 (2011) : 1091–1095.

[29] W. D. Chen, Y. Sung, Ch. P. Chang, Y.C. Chen, M. D. Ger. The preparation of thermo-responsive palladium catalyst with high activity for electroless nickel deposition. Surface & Coatings Technology 203 (2010) : 2130-2135.

[30] V. K. Bulasara, O. Chandrashekar, R. Uppaluri. Effect of surface roughness and mass transfer enhancement on the performance characteristics of nickel-hypophosphite electroless plating baths for metal–ceramic composite membrane fabrication. chemical engineering research and design 89 (2011) : 2485–2494.

[31] J. Jiang , H. Lu , L. Zhang , N. Xu. Preparation of monodisperse Ni/PS spheres and hollow nickel spheres by ultrasonic electroless plating. Surface & Coatings Technology 201 (2007) : 7174–7179.

[32] V. K. Bulasara, M. S. Abhimanyu, T. Pranav, R. Uppaluri, M. K. Purkait. Performance characteristics of hydrothermal and sonication assisted electroless plating baths for nickel–ceramic composite membrane fabrication. Desalination 284 (2012) : 77–85.

[33] Y. Lu, L. Xue, F. Li. Silver nanoparticle catalyst for electroless Ni deposition and the promotion of its adsorption onto PET substrate. Surface & Coating Technology 205 (2010) : 519-524.

[34] M. Charbonnier, M. Romand. Tin-free electroless metallization of glass substrates using different PACVD surface treatment processes. Surface and Coatings Technology 162 (2002) : 19–30.

[35] H. Dai, H. Li, F. Wang. Electroless Ni–P coating preparation of conductive mica powder by a modified activation process. Applied Surface Science 253 (2006) : 2474-2480.

[36] X. Tang, J. Wang, C. Wang, B. Shen. A novel surface activation method for Ni/Au electroless plating of acrylonitrile–butadiene–styrene. Surface & Coatings Technology 206 (2011) : 1382-1388.

[37] S.H. KO, T.C. Chou. Selective hydrogenation of 1-α-pinene over nickel catalysts prepared by electroless deposition. Ind. Eng. Chem 457 (1995) : 457-467.

[38] K.S. Hua, Chou, T. Chuan. Hydrogenation of 1-α-pinene over nickel-phosphorus/aluminum oxide catalysts prepared by electroless deposition. Canadian Journal of Chemical Engineering 72 (1994) : 862-873.

[39] N. Sriring, N. Tantavichet, K. Pruksathorn. Preparation of Pt/C catalysts by electroless deposition for proton exchange membrane fuel cells. Korean Journal of Chemical Engineering 27 (2010) : 439-445.

[40] W. E. Mustain, H. Kim, V. Narayanan, T. Osborn, P. A. Kohl. Electroless deposition and characterization of PtxRu 1-x catalyst on Pt/C nanoparticles for methanol oxidation. Journal of Fuel Cell Science and Technology 7 (2010) : 0410131-0410137.

[41] M. Shaal, C. Williams, J. Monnier, A. Pickerell, T. Hoang. Characterization and kinetic evaluation of silver-containing bimetallic catalysts prepared via electroless deposition. AIChE Annual Meeting, Conference Proceeding 2005 : 10326.

[42] M. T. Shaal, A. Y. Metcalf, J. H. Montoya, J. P. Wilkinson, C. C. Stork, C. T. Williams, J. R. Monnier. Hydrogenation of 3,4-epoxy-1-butene over Cu-Pd/SiO_2 catalysts prepared by electroless deposition. Catalystsis Today 123 (2007) : 142-150.

[43] M. T. Schaal, A. C. Pickerell, C. T. Williams, J. R. Monnier. Characterization and evaluation of Ag-Pt/SiO_2 catalysts prepared by electroless deposition. Journal of Catalysis 254 (2008) : 131-143.

[44] J. Rebelli, M. Detwiler, S. Ma, C. T. Williams, J. R. Monnier. Synthesis and characterization of Au-Pd/SiO_2 bimetallic catalysts prepared by electroless deposition. Journal of Catalysis 270 (2010) : 224-233.

[45] J. Rebelli, A. A. Rodriguez, S. Ma, C. T. Williams, J. R. Monnier. Preparation and characterization of silica-supported, group IB-Pd bimetallic catalysts prepared by electroless deposition methods. Catalysis Today 160 (2011) : 170-178.

[46] M. Rakap, E. E. Kalu, S. Özkar. Hydrogen generation from the hydrolysis of ammonia borane using cobalt-nickel-phosphorus (Co-Ni-P) catalyst supported on Pd-activated TiO_2 by electroless deposition. International Journal of Hydrogen Energy 36 (2011) : 254-261.

[47] C. A. Jules, A. Roelofs, P. H. Berben. First example of high loaded polymer stabilized nanoclusters immobilized on hydrotalcite: effects in alkyne hydrogenation. Chom Comm 2004.

[48] S.N. Paglieri, J.D. Way. Sep. Purif. Methods 31 (2002) : 1–169.

[49] Y.S. Cheng, K.L. Yeung. Effect of electroless plating chemistry on the synthesis of palladium membranes. Journal of Membrane Science 182 (2001) : 195-203.

[50] W.J. Cheong, Ben L. Luana, D.W. Shoesmith. The effects of stabilizers on the bath stability of electroless Ni deposition and the deposit. Applied Surface Science 229 (2004) : 282–300

[51] M.C. Biesinger, B.P. Payne, L.W.M. Lau, A. Gerson, R.S.C. Smart. X-ray photoelectron spectroscopic chemical state quantification of mixed

nickel metal. oxide and hydroxide systems Surf. Interface Anal 41 (2009) : 324.

[52] F. Logio, M. Innocenti, A. Jarek. Nickel sulfur thin films deposited by ECALE: Electrochemical, XPS and AFM characterization. Journal of Electro analytical Chemistry 638 (2010) : 15–20.

[53] A. Machet, A. Galtayries, S. Zana. XPS and STM study of the growth and structure of passive films in high temperature water on a nickel-base alloy. Electrochimica Acta 19 (2004) : 3957–3964.

[54] M. Mukaida, N.Takahashi, K. Hisamatsu, M. Ishitsuka. Preparation for defect-free self-supported Pd membranes by an electroless plating method. Journal of Membrane Science 365 (2010) : 378-381.

[55] J.-E. Park, S.-G Park, A. Koukitu, O.Hatozaki, N.Oyama. Effect of adding Pd nanoparticles to dimercaptan-polyaniline cathodes for lithium polymer battery. Synthetic Metals 141 (2004) : 121-126.

[56] J. Pollmann, R. Franke, J. Hormes, H. Bonnemann, W. Brijoux, A. S. Tilling. An X-ray photoelectron spectroscopy investigation of a novel Pd-Pt colloid catalyst. Journal of Electron Spectroscopy and Related Phenomena 94 (1998) : 219-227.

[57] X. Cui, D.A. Hutt, D.J. Scurr, P.P. Conway. The evolution of Pd/Sn catalytic surfaces in electroless copper deposition. Journal of The Electrochemical Society 158 (2011) : 172-177.

[58] R.L. Cohen, K. W. West. The chemistry of palladium-tin colloid sensitizing processes. Journal of The Electrochemical Society 120 (1973) : 502.

[59] J. Panpranot, K. Phandinthong, P. Praserthdam, M. Hasegawa, S.Fujita, M. Arai. A comparative study of liquid-phase hydrogenation on Pd/SiO2 in organic solvents and under pressurized carbon dioside: Activity change and metal leaching/sintering. Journal of Molecular Catalysis A 253 (2006) : 20-24.

[60] J. Zhu, Y. Su, F. Cheng, J. Chen. Improving the performance of PtRu/C catalysts for methanol oxidation by sensitization and activation treatment. J Power Sources 166 (2007) : 331–336.

[61] K. Lin, W. Tsai, J. Chang. Decorating carbon nanotubes with Ni particles using an electroless deposition technique for hydrogen storage applications. Int J Hydrogen Energy 35 (2010) : 7555–7562

[62] C.A. Jules, A. Roelofs, P.H. Berben. First example of high loaded polymer-stabilized nanoclusters immobilized on hydrotalcite: effects in alkyne hydrogenation. Chem Communication 2004 : 970-971

[63] A. Papp, A. Molnar. A. Mastalir, Catalytic investigation of Pd particles supported on MCM-41 for the selective hydrogenations of terminal and internal alkynes. Applied catalysis A 289 (2005) : 256-266.

[64] A. Sarkany, A. Beck, A. Horvth, Zs. Revay, L. Guczi. Acetylene hydrogenation on sol-derived Pd/SiO_2. Applied catalysis A 253 (2003) : 283.

[65] H. Bonnemann, W. Brijoux, A. S. Tilling, K. Siepen. Application of heterogeneous colloid catalysts for the preparation of fine chemicals. Topics in Catalysts 4 (1997) : 217-227.

[66] J.G. Ulan, Maier, D.A. Smith. Rational design of a heterogeneous Pd catalyst for the selective hydrogenation of alkynes. Journal of Organic Chemistry 52 (1987) : 3132.

[67] P. Albers, K. Seibold, G. Prescher, H. Muller. XPS and SIMS studies of carbon deposits on Pt/Al_2O_3 and Pd/SiO_2 catalysts applied in the synthesis of hydrogen cyanide and selective hydrogenation of acetylene. Applied Catalysis A 176 (1999) : 135.

APPENDICES

APPENDIX A

CALCULATION OF METERIAL PROPERTIES OF NI/PU FOAM

Modulus of Ni/PU foam

Example calculation for the Ni/PU foam at 30 min with sodium hypophosphite as reducing agent

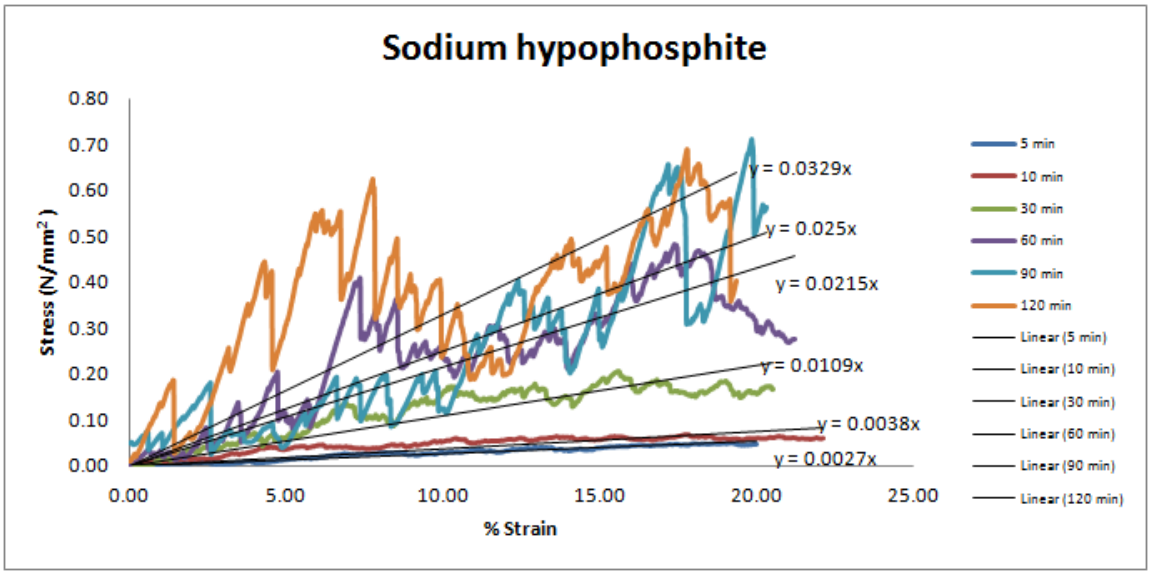

The results from instron machine are used to plot between Stress (N/mm^2) and % Strain in x-axis, which the slope of the graph is a modulus (Mpa). From the graph at 30 min the modulus of Ni/PU foam was 0.0109 Mpa.

APPENDIX B

CALCULATION OF CATALYST PREPARATION

B.1 Electroless palladium deposition method

Preparation of 1% Pd/TiO_2 electroless for Sn acitivated and non-Sn activated are shown as the follows:

Reagent: - Palladium (II) chloride (99.999%)

Molecular weight = 177.33 g

- Support: Titanium dioxide (TiO_2)

Based on 100 g of catalyst used, the composition of Pd and TiO_2 will be as the follows:

Palladium = 1 g

Titania = 100-1 = 99 g

For 2 g of TiO_2

Palladium required = 2 x (1/99) = 0.0202 g

The molecular weight of palladium is 106.42 then the Palladium (II) chloride is required:

$$\text{Palladium (II) chloride required} = \frac{\text{Mw of } PdCl_2 \text{ x palladium required}}{\text{Mw of Palladium}}$$

$$= (177.33/106.42) \text{ x } (0.0202) = 0.034 \text{ g}$$

The Palladium (II) chloride required 0.034 g was dip in a mixture of electroless palladium plating bath.

B.2 Incipient wetness impregnation method

Preparation of 1% Pd/TiO_2 incipient wetness impregnated is shown as the follows:

Reagent: - Palladium (II) chloride (99.999%)

Molecular weight = 177.33 g

- Support: Titanium dioxide (TiO_2)

Based on 100 g of catalyst used, the composition of Pd and TiO_2 will be as the follows:

Palladium = 1 g

Titania = 100-1 = 99 g

For 5 g of TiO_2

Palladium required = 5 x (1/99) = 0.0505 g

The molecular weight of palladium is 106.42 then the Palladium (II) chloride is required:

$$\text{Palladium (II) chloride required} = \frac{\text{Mw of } PdCl_2 \times \text{palladium required}}{\text{Mw of Palladium}}$$

$$= (177.33/106.42) \times (0.0505) = 0.084 \text{ g}$$

The Palladium (II) chloride required 0.084 g. Because of the pore volume of commercial titania support is 0.013 ml/g. then, the total de-ionized water required is 0.065 ml for incipient wetness impregnation method.

APPENDIX C

CALCULATION OF ACTUAL AMOUNTS OF PALLADIUM LOADING

The actual amounts of palladium loading of all catalysts were determined by inductive coupled plasma optical emission spectrometer (ICP-OES)

Example calculation for actual amounts of Pd on Pd/TiO_2 electroless

The 0.0125 g of Pd/TiO_2 electroless was dissolved in a solution containing 49% HF and 37% HCl with volume ratio 8:2 and heat at 40 ºC.

The result form ICP-OES analysis was 6.76 mg/l

$$\%\,Wt = \frac{concentration(ppm)}{weight(g) \times 100}$$

The actual % wt Pd = $\frac{6.767 \text{ mg/l}}{0.0125\text{g x}100}$ = 5.41 %

The actual amount of Pd on Pd/TiO_2 electroless with Sn activated was 5.41 %

APPENDIX D

CALCULATION FOR METAL ACTIVE SITES AND METAL DISPERSION

Calculation of the metal active sites, metal dispersion and average particles size of all the catalysts measured by CO chemisorptions as follows:

Calculation of metal active sites

The weight of catalyst used	=	W	g
Whole area of CO peak after adsorption	=	A	unit
Whole area of 80 µl of standard CO peak	=	B	unit
Amounts of CO adsorbed on catalyst	=	B-A	unit
Volume of CO adsorbed on catalyst	=	$80 \times \frac{(B-A)}{B}$	µl
Volume of 1 mole of CO at 30 ºC	=	24.86×10^6	µl
Mole of Co adsorbed on the catalyst	=	$\frac{80}{24.86 \times 10^6} \times \frac{(B-A)}{B}$	µmole

Molecule of CO adsorbed on the catalyst = $[3.22 \times 10^{-6}] \times [6.02 \times 10^{23}] x \frac{(B-A)}{B}$ molecules

Metal active sites $= 1.93 \times 10^{18} \times \left[\frac{(B-A)}{B}\right] \times \frac{1}{w}$ molecules of CO/g of catalyst

Calculation of % dispersion of metal

From the Operater's manual of Chemisorb 2750 used for determined the % dispersion of metal on the support shows as follow:

$$\%D = S_f \times \left[\frac{V_{ads}}{V_g}\right] \times \left[\frac{Mw}{\%M}\right] \times 100\% \times 100\%$$

Where

%D	=	% metal dispersion
S_f	=	stoichiometry factor, (CO on Pd =1)
V_g	=	molar volume of gas at STP = 22414 (cm^3/mol)
Mw	=	molecular weight of the metal (a.m.u.)
%M	=	% metal loading
V_{ads}	=	volume adsorbed (cm^3/g)

$$V_{ads}(cm^3) = \left[\frac{V_{inj}}{m}\right] \times \sum_{i=1}^{n}\left(1 - \frac{A_i}{A_f}\right)$$

Where

V_{inj}	=	volume injected (cm^3) = 0.080 cm^3
m	=	weight of sample (g)
A_i	=	area of initial peak
A_f	=	area of last peak

Example: % Dispersion of Pd/TiO_2 electroless Sn

$$V_{ads} = \left[\frac{0.080}{0.2042}\right] \times \left[\left(1 - \frac{0.24}{0.43}\right) + \left(1 - \frac{0.40}{0.43}\right) + \left(1 - \frac{0.42}{0.43}\right)\right]$$

$$= \quad 0.460 \text{ cm}^3$$

$$\% \text{ D} = 1 \times \left[\frac{0.460}{22414}\right] \times \left[\frac{106}{1}\right] \times 100\% \times 100\%$$

$$= \quad 1.58 \%$$

Then the % Pd dispersion is 1.58 %

Calculation of average metal particle size

The average particle size of palladium metal can be determined based on active metal surface

$$d_p^o = \left[\frac{F_g}{pxMSAm}\right] \times \left[\frac{m^3}{10^6 cm^3}\right] \times \left[\frac{10^9}{m} nm\right]$$

Where

$d_p^{\ 0}$ = average crystallite size of palladium metal

F_g = crystallite geometry factor (hemisphere = 6)

P = specific gravity of the active metal (palladium =12.0 g/cm^3)

MSAm= active metal surface area per gram of metal (m^2/g_{metal})

$$\text{MSAm} = S_f \times \left[\frac{V_{ads}}{V_g}\right] \times \left[\frac{100\%}{\%M}\right] \times N_A \times \sigma_m \times \left[\frac{m^2}{10^{18} nm^2}\right]$$

Where

N_A = Avogado number (6.02×10^{23}molecules/mol)

σ_m = cross-sectional area of active metal atom (palladium=0.0787 nm^2)

Example: Average particle sizes of Pd/TiO_2 electroless Sn

$$\text{MSAm} = 1 \times \left[\frac{0.460}{22414}\right] \times \left[\frac{100\%}{1\%}\right] \times 6.02 \times 10^{23} \times 0.0787 \times 10^{-18}$$

= 38.01 $m^2/g_{\text{ metal}}$

d_p^0 = 6000/ (12×38.01)

= 13.13 nm

The average crystallite size of palladium on support for Pd/TiO_2 electroless Sn was 13.13 nm

APPENDIX E

CALCULATION OF 3-HEXYNE-1-OL CONVERSION AND CIS-3-HEXENE-1-OL SELECTIVITY

The catalytic performance of all catalysts was calculated in terms of activity for 3-hexyne-1-ol conversion and cis-3-hexene-1-ol selectivity of liquid phase hydrogenation.

Activity of the catalyst achieved in term of 3-hexyne-1-ol conversion. 3-hexyne-1-ol conversion is defined as mole of 3-hexyne-1-ol converted with respect to 3-hexyne-1-ol in feed:

$$\text{3-hexyne-1-ol conversion (\%)} = \frac{\text{mole of 3-hexyne-1-ol in (feed-product)}}{\text{mole of 3-hexyne-1-ol in feed}} \times 100$$

Where mole of 3-hexyne-1-ol can be measured in form of Area of 3-hexyne-1-ol peak from GC-2014

Selectivity of product is defined as mole of cis-3-hexyne-1-ol formed with respect to mole of 3-hexyne-1-ol converted:

$$\text{cis-3-hexene-1-ol selectivity(\%)} = \frac{\text{mole of cis-3-hexene-1-ol formed}}{\text{mole of total product}} \times 100$$

Where mole of cis 3-hexyne-1-ol and other products can be measured in form of Area peak from GC-2014

APPENDIX F

LIST OF PUBLICATION

1. Jaratpon Sitthikun, Joongjai Panpranot and Yuttanant Boonyongmaneerat. A study of tin-free activation process for electroless nickel plating on polyurethane foam. *Proceeding of The 21st Thailand Chemical Engineering and Applied Chemistry Conference (TiChe) 2011 conference,* Songkhla, Thailand, November 10 – 11, 2011.

VITA

Mr. Jaratpon Sitthikun was born in March 19th, 1987 in Suratthani, Thailand. He finished high school from Suratthani School, Suratthani in 2005. After that, he received bachelor's degree in the department of Chemical Technology form Faculty of Science, Chulalongkorn University in 2009.